CR-171 768
c.1

AgRISTARS

SR-P3-04399
NAS9-16528

A Joint Program for Agriculture and Resources Inventory Surveys Through Aerospace Remote Sensing

Supporting Research

February 1983

Remote Sensing of Agricultural Crops and Soils

Annual Technical Summary, Contract NAS9-16528

by M.E. Bauer and Staff

Purdue University
Laboratory for Applications of Remote Sensing
West Lafayette, Indiana 47907

(E84-10107) REMOTE SENSING OF AGRICULTURAL CROPS AND SOILS Final Report (Purdue Univ.) 173 p HC A08/MF A01 CSCL 02C
N84-21925
Unclas
G3/43 00107

NASA

Star Information Form

1 Report No	2 Government Accession No	3 Recipient's Catalog No
SR-P3-04399		

4 Title and Subtitle	5 Report Date
Remote Sensing of Agricultural Crops and Soils	February 1983
	6 Performing Organization Code

7. Author(s)	8 Performing Organization Report No
M.E. Bauer and Staff	LARS 022183

9 Performing Organization Name and Address	10 Work Unit No
Laboratory for Applications of Remote Sensing Purdue University 1220 Potter Drive West Lafayette, IN 47906	11. Contract or Grant No. NAS9-16528

12. Sponsoring Agency Name and Address	13 Type of Report and Period Covered
NASA Johnson Space Center Earth Resources Research Division Houston, TX 77058	Final
	14 Sponsoring Agency Code

15 Supplementary Notes

Forrest G. Hall, Technical Monitor
Marvin E. Bauer, Principal Investigator

16 Abstract

This report presents a summary of the research results and accomplishments for contract NAS9-16528, Remote Sensing of Agriculture and Earth Resources, to Purdue University for the period December 1981 to November 1982. Results of nine tasks in the following areas are described:

- Scene radiation research
- Soil moisture research
- Preprocessing and registration research
- Computer and data base services

17. Key Words (Suggested by Author(s))	18 Distribution Statement

19 Security Classif (of this report)	20 Security Classif (of this page)	21 No of Pages	22 Price
Unclassified	Unclassified		

*For sale by the National Technical Information Service, Springfield, Virginia 22161

NASA - JSC

TABLE OF CONTENTS

Page

I. INTRODUCTION..... 1

II. SCENE RADIATION RESEARCH..... 7

1. Corn and Soybean Landsat MSS Classification Performance as a Function of Scene Characteristics. By B.T. Batista, M.M. Hixson, and M.E. Bauer..... 9

2. Estimating Crop Development Stages From Multispectral Data. By James C. Tilton and Steven E. Hollinger..... 23

3. Crop Condition Assessment..... 35

A. Interception of Photosynthetically Active Radiation in Corn Canopies. By K.P. Gallo and C.S.T. Daughtry..... 35

B. Interception of Photosynthetically Active Radiation in Soybean Canopies. By C.C. Brooks, C.S.T. Daughtry, and M.E. Bauer..... 44

C. Costs of Measuring Leaf Area Index of Corn. By C.S.T. Daughtry, S.E. Hollinger, G. Drape, and E.M. Luke..... 49

4. Landsat Spectral Inputs to Crop Models..... 59

A. Use of Greenness Index to Assess Crop Stress. By S.E. Hollinger..... 59

B. Evaluation of Landsat MSS Data for Estimating Corn and Soybean Development Stages. By S.E. Hollinger..... 69

5. Field Research-Experiment Design Data Acquisition and Preprocessing. By L.L. Biehl..... 79

6. Sun-View Angles Studies of Corn and Soybean Canopies in Support of Vegetation Canopy Reflection Modeling. By K.J. Ranson, L.L. Biehl, and M.E. Bauer..... 95

III. SOIL MOISTURE RESEARCH.....117

7. Spectral Estimation of Corn Canopy Phytomass and Water Content. By S.E. Hollinger.....119

IV. REGISTRATION RESEARCH.....137

8. Correlative and Noncorrelative Approaches to Image Registration. By P.E. Anuta.....139

I. Introduction

INTRODUCTION

This report presents a summary of the research results and accomplishments for Contract NAS9-16528, Research in Remote Sensing of Agricultural Crops and Soils, at Purdue University, West Lafayette, IN for 1982.

Research was conducted in three major areas: Scene radiation, soil moisture, and image registration. Significant accomplishments during the contract year include:

- Soil, crop, and weather variables affecting Landsat classification accuracy were identified and quantitatively described.
- A model for early to mid-season prediction of corn development stages from spectral data was developed.
- Direct measurements of the amount of light intercepted by corn and soybean canopies, along with leaf area index and spectral reflectance measurements, were made. Spectral estimates of leaf area index and canopy light interception are potential key inputs to crop growth and yield models.
- Landsat spectral variables as inputs to crop stress and development stage models were evaluated.
- In support of the scene radiation research objectives, spectral and agronomic data were acquired for corn, soybean, sunflower, and sorghum cultural practices experiments.
- A tower- and sensor-mount was constructed to facilitate acquisition of canopy reflectance measurements at multiple sun and view angles.
- An angle transformation of greenness-brightness was developed for estimation of crop phytomass.
- Research was conducted on noncorrelative methods for temporal registratiion of dissimilar scenes.

Additional detailed information describing the various tasks, experiments, and results are available from scientific papers and technical reports published during the past year (see Table I.1, pp. 4-6).

PAGE 2 INTENTIONALLY BLANK PRECEDING PAGE BLANK NOT FILMED

Table I.1. Papers, Technical Reports, and Other Publications Prepared for Contract NAS9-16528. Numbers in parentheses are AgRISTARS and LARS technical report numbers, respectively.

Papers in Scientific Journals

Published

1. Daughtry, C.S.T., V.C. Vanderbilt, and V.J. Pollara. 1982. Variability of reflectance measurements with sensor altitude and canopy type. Agronomy Journal 74:744-751. (SR-P1-04191; LARS 111481).

2. Hixson, M.M., M.E. Bauer, and D.K. Scholz. 1982. An assessment of Landsat acquisition history on identification and area estimation of corn and soybeans. Remote Sensing of Environment 12:123-128. (SR-P0-00494; LARS 060480)

3. Kollenkark, J.C., V.C. Vanderbilt, C.S.T. Daughtry, and M.E. Bauer. 1982. Influence of solar illumination angle on soybean canopy reflectance. Applied Optics 21:1179-1184. (SR-P1-04039; LARS 021681)

4. Kollenkark, J.C., C.S.T. Daughtry, M.E. Bauer, and T.L. Housley. 1982. Effects of cultural practices on agronomic and reflectance characteristics of soybean canopies. Agronomy Journal 74:751-758. (SR-P1-04038; LARS 021781)

5. Vanderbilt, V.C., L. Grant, L.L. Biehl, and B.F. Robinson. Specular, diffuse, and polarized light scattering by two wheat canopies. Applied Optics (in press). (SR-P1-04139; LARS 090981 revised)

6. Walburg, G., M.E. Bauer, C.S.T. Daughtry, and T.L. Housley. 1982. Effects of nitrogen nutrition on the growth and reflectance characteristics of corn canopies. Agronomy Journal 74:677-683. (SR-P1-04044; LARS 030381)

Submitted

1. Daughtry, C.S.T., and S.E. Hollinger. Costs of measuring leaf area index of corn. AES Journal Paper 9655. (Submitted to Agronomy Journal.)

2. Paw U, K.T., and C.S.T. Daughtry. A new method of the estimation of diffusive resistance of leaves. AES Journal Paper 9828. (Submitted to Agricultural Meteorology.)

3. Seubert, C.E., C.S.T. Daughtry, D.A. Holt, and M.F. Baumgardner. Aggregating of available soil water holding capacity for crop yield models. AES Journal Paper 9287. (Submitted to Agronomy Journal.)

4. Vanderbilt, V.C. Measuring plant canopy structure. (Submitted to Photogrammetric Engineering and Remote Sensing.) (SR-P1-04141; LARS 060881 revised)

(Table I.1. (continued)

Conference Papers and Abstracts

1. Anuta, P.E., and F. Davallou. 1982. Resolution matching for registration of dissimilar images. Proc. of IEEE Computer Soc. Conf. on Pattern Recognition and Image Processing, Las Vegas, NE. (LARS 061682)

2. Batista, G.T., M.M. Hixson, and M.E. Bauer. 1982. Corn and soybean Landsat MSS performance as a function of scene characteristics. Proc. 8th Intl. Symp. on Machine Processing of Remotely Sensed Data, Purdue University, West Lafayette, IN, July 7-9, 1982, pp. 178-188. (LARS 071182)

3. Biehl, L.L., M.E. Bauer, B.F. Robinson, C.S.T. Daughtry, L.S. Silva, and D.E. Pitts. 1982. A crops and soils data base for scene radiation research. Proc. 8th Intl. Symp. on Machine Processing of Remotely Sensed Data, Purdue University, West Lafayette, IN, July 7-9, 1982, pp.169-177. (SR-P2-04263; LARS 070782)

4. Biehl, L.L, and B.F. Robinson. 1982. Data acquisition and preprocessig techniques for remote sensing field Research. Soc. of Photo-Optical Instrumentation Engineers, SPIE, Vol. 356, Box 10, Bellingham, WA. (LARS 082182)

5. Daughtry, C.S.T., S.E. Hollinger, and J.C. Cochran. 1982. Estimating silking and maturity dates of corn. Agronomy Abstracts 74:12.

6. Daughtry, C.S.T., and S.E. Hollinger. 1983 . Costs of measuring leaf area index of corn. Agronomy Abstracts 75:11.

7. Gallo, K.P., C.C. Brooks, C.S.T. Daughtry, M.E. Bauer, and V.C. Vanderbilt. 1982. Spectral estimates of intercepted solar radiation by corn and soybean canopies. Proc. 8th Intl. Sym. on Machine Processing of Remotely Sensed Data, Purdue University, West Lafayette, IN, July 7-9, 1982, pp. 190-198. (LARS 071682)

8. Gallo, K.P., C.S.T. Daughtry, M.E. Bauer, and B.F. Robinson. 1982. Measurement of photosynthetically active radiation intercepted by corn canopies. Agronomy Abstracts 74:13.

9. Gallo, K.P., C.S.T. Daughtry, and M.E. Bauer. 1983. Effect of LAI and solar angle on interception of PAR in corn canopies. Agronomy Abstracts 75:12.

10. Grant, L., V.C. Vanderbilt, and C.S.T. Daughtry. 1983. Measurements of specularly reflected radiation from individual leaves. Agronomy Abstracts 75:12. (LARS 081583)

Table I.1 (concluded)

11. Hollinger, S.E., C.S.T. Daughtry, M.E. Bauer, and V.C. Vanderbilt. 1982. Remote sensing of canopy water content and phytomass. Agronomy Abstracts 74:15.

12. Holt, D.A., S.E. Hollinger, C.S.T. Daughtry, and H.F. Reetz. 1982. A theoretical and practical approach to large area production forecasting. Biological Systems Simulation Group, Fourth Workshop on Crop Simulation, Auburn University, Auburn, AL, Mar. 16-18, 1982.

13. Robinson, B.F., and L.L. Biehl. 1982. Overview of remote sensing field research: requirements and status. Soc. of Photo-Optical Instrumentation Engineers, SPIE, Vol. 356, Box 10, Bellingham, WA. (LARS 082082).

14. Robinson, B.F., R.E. Buckley, and J.A. Burgess. 1982. Performance evaluation and calibration of a modular multiband radiometer for remote sensing field research. SPIE, Vol. 308, Box 10, Bellingham, WA. (SR-P2-04318; LARS 061182)

Technical Reports

1. Bauer, M.E., and Staff. 1982. Remote sensing of agricultural crops and soils. NAS9-15466 Annual Technical Summary for Dec. 1980-May 1982. 209p. (SR-P2-04266; LARS Contract Report 113081)

2. Bauer, M.E., and Staff. 1983. Remote sensing of agricultural crops and soils. NAS9-16528 Annual Technical Summary for Dec. 1981-Nov. 1982. (SR-P3-04399; LARS Contract Report 022183)

3. Biehl, L.L. 1982. LARSPEC spectroradiometer-multiband radiometer data formats. Laboratory for Applications of Remote Sensing (LARS), Purdue University, West Lafayette, IN. (SR-P2-04277; LARS 050182)

Theses

1. Pollara, V.J. 1982. An inquiry into the use of spectral data for assessing crop development stage. M.S. thesis. Dept. of Agronomy, Purdue University, West Lafayette, IN.

2. Marshall, D.S. 1982. Epidiemology and multispectral sensing of leaf rust of wheat. Ph.D. thesis. Dept. of Botany and Plant Pathology, Purdue University, West Lafayette, In.

3. Ward, J.P. 1982. Effects of management practices on the reflectance of corn and soybean canopies. M.S. thesis. Dept. of Agronomy, Purdue University, West Lafayette, IN.

II. Scene Radiation Research

1. CORN AND SOYBEAN LANDSAT MSS CLASSIFICATION PERFORMANCE AS A FUNCTION OF SCENE CHARACTERISTICS

G.T. Batista, M.M. Hixson, and M.E. Bauer

Introduction

Previous research has demonstrated that satellite remote sensing has the potential to provide accurate, timely crop production information (MacDonald and Hall, 1978) or when combined with conventional survey data to improve the accuracy and efficiency of area estimates (Hanuschak et al., 1980). But, to fully develop and utilize Landsat data to inventory crop production, it is important to identify and understand the factors that affect Landsat crop classification accuracy.

Classification accuracy of Landsat MSS data depends on a number of variables including scene characteristics; procedures for training, classification, and area estimation; and the general quality of the data. The variability in accuracy found using the same classification procedure and the similar distributions of Landsat data acquisition dates, at different locations is due primarily to scene variability. Understanding the way scene characteristics affect classifier performance is an important step in determining not only the accuracy that can be expected for a particular area, but also the amount of effort required for training, classification, and area estimation procedures to achieve an optimal accuracy and efficiency.

The primary objective of this research was to investigate the accuracy of Landsat MSS data classifications of corn and soybeans as a function of scene characteristics in the U.S. Corn Belt. The scene characteristics involved several aspects of crop, soil, and weather variables. A second objective was to examine the interrelationships among the scene characteristics.

The study has an immediate potential application in the design of a crop inventory system using remote sensing. For example, areas with high expected classification accuracy could be sampled with lower frequency than areas where local characteristics are known to induce poorer classification results.

Review of Previous Findings

Many remote sensing researchers have found that a difference exists among the Landsat classification and area estimation accuracies in different sites. Bizzell et al. (1975), reporting on the results of CITARS project, found two site characteristics, field size and proportion of corn and soybeans, to be correlated with proportion estimation accuracy. They

PAGE 8 INTENTIONALLY BLANK PRECEDING PAGE BLANK NOT FILMED

attributed the effect of field size to the decreasing percentage of mixed pixels as field size increases. Further, areas with predominantly larger fields tended to be more uniform and have fewer cover types, thus decreasing the amount of spectral variation. Field size effects have also been noted by Bauer et al. (1978), Hixson et al. (1980) and Pitts et al. (1980).

The LACIE project, involving large-area production estimates, dealt with a wider source of errors. Pitts et al. (1978) identified sampling and classification errors as the two major components of area estimation errors. Classification error, which is the subject of our study, was viewed by LACIE as composed of analyst-labeling error sources and machine-classification error sources. The magnitude of the labeling error was affected by Landsat acquisition date, crop development stage, and a number of confusion crops, while classification error was associated with field size, training statistics, and classification algorithm selected. Both labeling and classification were affected by the general quality of the data, such as registration accuracy and atmospheric effects. In addition to these scene characteristics, soil and weather variability were noted as contributing factors to classification accuracy by Bizzell et al. (1975) and Bauer et al., (1979).

In summary, the literature on remote sensing applications has extensively demonstrated the feasibility of using Landsat data and computer-aided analysis for crop identification and area estimation. Although several studies have indicated that scene characteristics, including weather variations, affect classification performance, no work, to our knowledge, has been carried out with sufficient supporting data to define satisfactory functional relationships between specific scene characteristics and performance of a classification system for crop inventory.

Approach

Description of Study Area and Landsat Data

Multitemporally registered Landsat-2 and -3 MSS data acquired over the U.S. Corn Belt during the summer of 1978 were analyzed. The data set consisted of 23 sample segments, each 5 x 6 n. miles in size. The locations (Figure 1-1) of the test sites were selected to represent a broad range of conditions in terms of climate, soil, topography, field sizes, cropping practices of corn and soybeans, and confusion classes (e.g. oats, sorghum, sunflowers, and trees).

Aerial photography and a subsequent wall-to-wall inventory of crop types was digitized and registered to the Landsat data to provide a digital map of each site for evaluation of the classification results. Two data acquisition windows of the corn development stages, based on the investigations by Hixson et al. (1982), were selected for analysis: (1) preplant to 12 leaves, and (2) tassel to dent.

Color composites of Landsat imagery for all segments and all acquisitions, along with full-frame Landsat color imagery were used to select cloud-free dates of Landsat data and for visual assessment of the contextual aspect of a segment in relation to the county where the segment was located.

ORIGINAL PAGE IS
OF POOR QUALITY

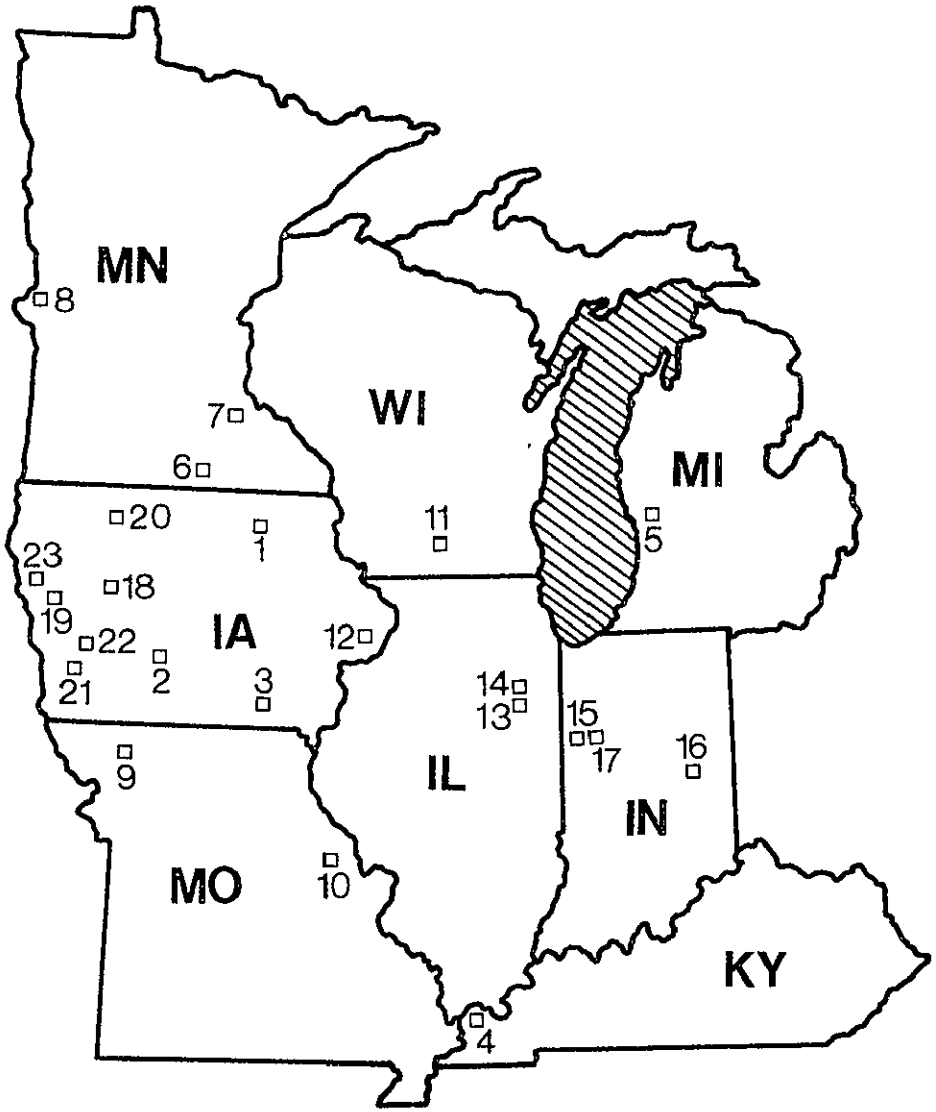

1	Chicksaw, IA	(135)
2	Madison, IA	(141)
3	Wapello, IA	(144)
4	Ballard, KY	(146)
5	Kent, MI	(180)
6	Freeborn, MN	(183)
7	Goodhue, MN	(184)
8	Traverse, MN	(185)
9	Gentry, MO	(209)
10	Lincoln, MO	(215)
11	Dane, WI	(246)
12	Clinton, IA	(800)
13	Iroquois, IL	(824)
14	Kankakee, IL	(828)
15	Benton, IN	(837)
16	Henry, IN	(843)
17	Tippicanoe, IN	(854)
18	Calhoun, IA	(862)
19	Monona, IA	(881)
20	Palo Alto, IA	(883)
21	Pottawatomie, IA	(886)
22	Shelby, IA	(892)
23	Woodbury, IA	(895)

Figure 1-1. Location of test sites in Corn Belt region (AgRISTARS segment number).

Training and Classification

A systematic sample of the data was used for training and testing the classifier. The pixel at every tenth line and column of the Landsat data was examined. If that pixel fell in a field, the cover type in the field was identified from the ground inventory. Only field center pixels were selected.

From the fields selected by this procedure were randomly assigned for either training the classifier or testing classification accuracy. From those fields selected for training, three sets of data were clustered: all fields of corn, all fields of soybeans, and all fields of other cover types. This procedure insures "pure" cluster classes (i.e., clusters containing pixels from only one cover type). After refinement of the statistics was complete, the entire segment was classified using a per point Gaussian maximum likelihood classifier from LARSYS (Phillips, 1973).

Measures of Classification Performance

Classification performance was evaluated for corn, soybeans and overall by three categories of performance measures: (1) wall-to-wall accuracy, obtained by comparing Landsat classifications of all pixels of a segment to the ground inventory identification; (2) test field accuracy, obtained by comparing test field classifications to the ground inventory; and (3) proportion estimate error, obtained by comparing the ground inventory proportions with the Landsat proportions. The latter measure used RMS error for corn and soybeans to represent an overall error. Corn and soybean proportion estimate errors were defined as the absolute relative difference between the Landsat proportion and cover type proportion of corn.

Scene Characteristics

Twenty-nine variables were defined to describe the scene characteristics. They were grouped into four categories: (1) soil variables, (2) cover type variables, (3) productivity variables, and (4) seasonal variables.

Soil variables were defined and estimated from available publications.

SLOPE - Average slope: 0-nearly level to moderately sloping (0-12%), 1-strongly sloping to very steep (12-25%).

DRAIN - Natural drainage: 1-poor to somewhat poor, 2-moderately well, 3-well.

PARM - Parent material: 0-not loess or not loess on till, 1-loess or loess on till.

ORDER - Taxonomic order: 0-not Mollisol, 1-Mollisols.

VARI - Soil variability: 1-low, 2-medium, 3-high, 4-very high.

VAXOR - Interaction of VARI and ORDER.

DRXOR - Interaction of DRAIN and ORDER.

DRXVG - Interaction of DRAIN and original vegetation.

Cover type variables characterizing the proportions of cover types present were obtained from the ground inventory data.

CORN - Proportion of corn.

SOYB - Proportion of soybeans.

PAST - Proportion of pasture, alfalfa, grass, hay and clover.

TREE - Proportion of trees and orchards.

ELSE - Proportion of homesteads, water bodies, non-agriculture, and idle fields.

ALL - Proportion of all field crops together.

ALLAC - Coded field size for all field crops: 1-small, 2-medium, 3-large, 4-very large.

MIX - Proportion of mixed pixels.

ALXMI - Interaction of ALL and MIX.

SWI - Shannon-Wiener diversity index, using 22 cover types:

$$SWI = e^{H} \text{ and } H = -\Sigma P_i \log_e P_i$$

where P_i is the proportion (0.0 to 1.0) of cover type i. A scaling was used to make this index vary from 0 (least diverse) to 1 (most diverse).

Productivity variables related to crop yields were:

MAX - 1978 soybean "maximum yield" (range 40.0 to 73.1 u/ac). Maximum yield as proposed by Holt et al. (1979) is the yield that would have been obtained if weather was not limiting throughout the growing season. Maximum yield values were computed on a county basis.

CYLDAVE - Long-term (approximately 20 years) average corn yield for the counties where the segments were located (range 56.1 to 100.4 bu/ac).

SYLDAVE - Long-term (approximately 20 years) average soybean yield for the counties where the segments were located (range 18.1 to 35.5 bu/ac).

BELT - A qualitative variable that reflects the relative position of the segment in the Corn Belt. Two levels were defined: 0=Corn Belt fringe area (9 observations) and 1=inside the Corn Belt (14 observations).

Seasonal variables used to characterize the 1978 growing season were:

WF - 1978 "weather factor" for representing the environmental limitations on soybean yield prevailing during the growing season (Holt et al., 1979). Low values of WF correspond to severe limitations on yield.

CPER1 - Corn development stage at first Landsat acquisition.

SPER1 - Soybean development stage at first Landsat acquisition.

CPER3 - Corn development stage at second Landsat acquisition.

SPER3 - Soybean development stage at second Landsat acquisition.

CYLD - 1978 county average corn yield (USDA data).

SYLD - 1978 county average soybean yield (USDA data).

Statistical Analyses

The Statistical Analysis System (SAS Institute, 1979) was extensively used in this study. Initially, plots of each independent variable versus the dependent variables were obtained to examine the form of the relationships and, secondly, simple correlations of all possible combinations of variables were run. Plots and correlations were also used to examine the interrelationships among the independent variables.

A separate multifactor analysis was performed for each dependent variable. Several regression models using the STEPWISE procedure of SAS with the MAXR option were run. Initially only the cover type variables were allowed to enter the model. After the selection of a subset of the cover type variables based on the ability to explain the variability in the dependent variables, a subset of the soil variables was selected. Following the same procedure, productivity variables were entered, and finally a subset of the seasonal variables was selected after the cover type, soil, and productivity variables, previously selected, were already in the model.

An additional analysis consisted of all possible regressions of subsets of 4 to 14 of the 29 independent variables. The output of this program lists subsets of independent variables for each subset size in order of amount of variation explained in the dependent variable.

ORIGINAL PAGE IS
OF POOR QUALITY

Results and Discussion

Classification Results

Results show that Landsat proportion estimates were strongly related to ground inventory proportions with R^2 greater than 0.90. Figure 1-2 indicates that the regression lines are close to the 1:1 line between Landsat proportions and cover type proportions with no major departures from the regression lines in any of the segments analyzed.

Wall-to-wall classification accuracy was linearly related to test field accuracy for corn, soybean, and overall classifications with correlation coefficients around 0.70. Since the computation of wall-to-wall accuracies takes into account all pixels of a segment, including mixed pixels, as opposed to only pure pixels of the test field, it was expected that test field accuracies would be higher than wall-to-wall accuracies. In fact, the average test field accuracies were 14, 15 and 12% higher, respectively, for corn, soybean and overall.

Table 1-1 presents the overall test field performance for all segments together. Omission error was smaller for corn than for both soybean and "other" classes. More soybean and "other" were classified as corn than vice versa in most of the segments. This was associated with the predominance of corn in the study area rather than with analyst bias.

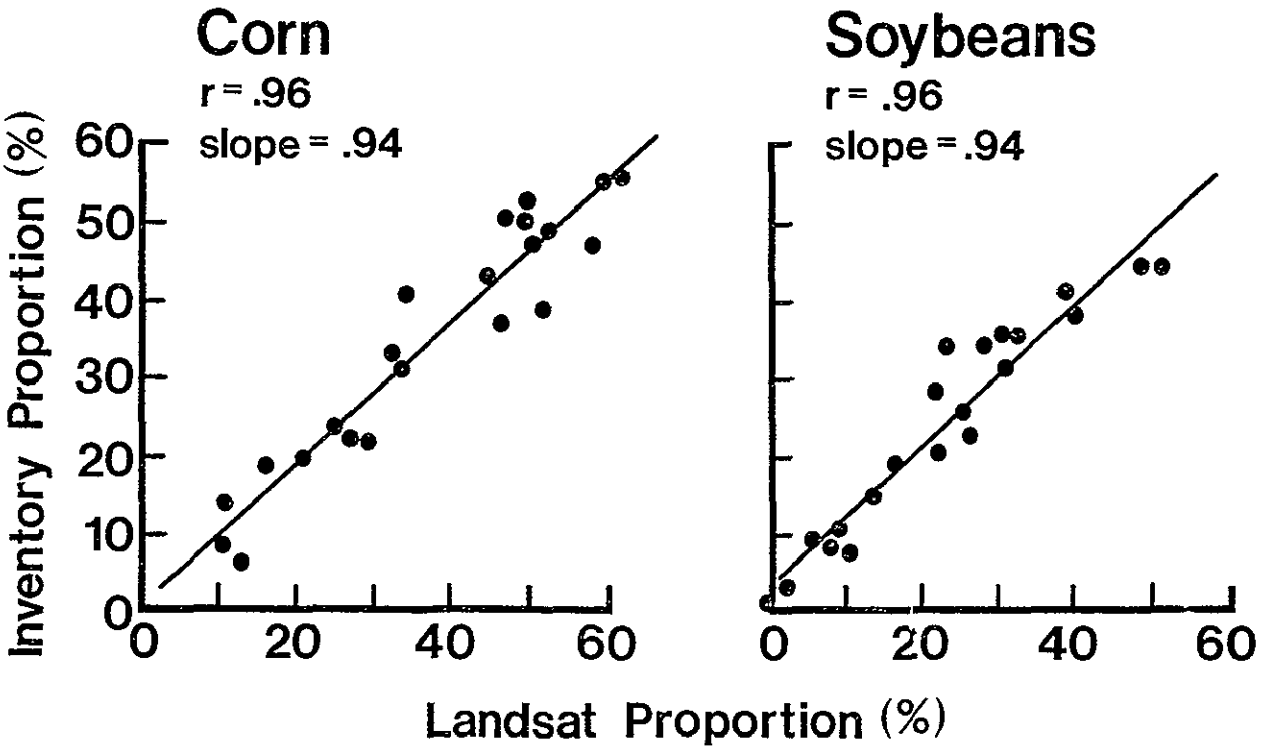

Figure 1-2. Relationship of Landsat estimates and ground inventory of corn and soybean proportions.

ORIGINAL PAGE IS
OF POOR QUALITY

Table 1-1. Mean classification accuracy of 22 segments (segment 883 was not included).

Class	No. of Pixels	Pct. Classified as Corn	Soybean	Other
Corn	13727	85.9	6.6	7.4
Soybean	8534	12.0	81.8	6.2
Other	11872	11.2	5.8	83.0
Total	34133			

Overall Accuracy = 83.9%

Single Factor Analysis

This analysis involved the study of the relationship between each dependent variable and each independent variable. Plots of all possible pairs of variables were examined, and only linear relationships appeared to be present. Correlation coefficients were computed for all possible pairs of variables (Table 1-2). Both productivity and cover type variables were linearly related to more dependent variables than either soil or seasonal variables.

Corn accuracy measures were related to more independent variables than either overall or soybean accuracies. Proportion error for soybeans (ARSD) did not have a significant relationship with any independent variable. Test field accuracies for both overall and soybeans were related to more independent variables than wall-to-wall accuracies.

The effect of field size on classification accuracy was investigated using the test fields previously selected for test field accuracy assessment. The advantage of using test field size in addition to average field size (ALLAC) as previously presented was that test fields were composed of only pure pixels, therefore the effects of mixed pixels and of small fields, which are otherwise confounded, could be separated. Another advantage was the considerable increase in the number of observations.

Figure 1-3 presents the relationship between average classification accuracy and average test field size where each observation corresponds to the average of all individual test fields for each classification class, i.e., corn, soybean, and others for each segment. Although a wide range of average accuracies was observed for small field sizes, the average accuracies were usually higher and less variable for larger test fields. The effect of small fields was associated not only with an increase in the proportion of mixed pixels, but also with the intrinsically large spectral variability of small fields.

ORIGINAL PAGE IS
OF POOR QUALITY

Table 1-2. Correlation of scene characteristics and several measures of classification performance (for clarity, only the coefficients that were significant at $\alpha = 0.15$ are presented). All coefficients are based on 23 observations, except for MAX which had 22 observations.

	Measures of Classification Performance								
	Corn			Soybeans			Overall		
Scene Characteristics	CO	CT	ARCD	SO	ST	ARSD	OV	OVT	RMS
Soil									
SLOPE	-.52	-	-	-	-.33	-	-	-	-.41
DRAIN	-	-	-	-	-	-	-	-	-.34
PARM	-	-	-	-	-	-	-	-	-.46
ORDER	.35	.49	-	-	-	-	-	.43	-
VARI	-.39	-	-	-	-	-	-	-	-.33
VAXOR	-	-	-	-	-	-	.37	-	-
DRXVG	.35	.60	-	-	-	-	-	.63	-
DRXOR	-	.51	-	-	.35	-	-	.59	-
Ground Truth									
CORN	.84	.59	-.56	-	.36	-	-	.34	-
SOYB	.39	-	-.38	.57	.36	-	-	-	-
PAST	-.53	-	-	-	-	-	-	-	-
TREE	-.71	-.43	-	-	-	-	-	-.33	-
ELSE	-	-	-	-.54	-	-	-	-	-
ALL	.74	.36	-	-	-	-	-	-	-
ALLAC	.73	.60	-	-	-	-	-	.32	-
MIX	-.54	-.48	-	-	-	-	-	-	-
SWI	-.72	-.58	.60	-	-.33	-	-	-	-
ALXMI	.57	-	-.35	-	-	-	-	-	-
Productivity									
MAX	-	.47	-.53	-	.37	-	.35	.47	-.33
CYLDAVE	.63	.53	-.57	-	.47	-	-	-	-
SYLDAVE	.67	.63	-.77	.36	.49	-	-	.40	-
BELT	.57	.67	-.51	-	-	-	-	.52	-
Seasonal									
WF	-	-	-	-.41	-	-	-	-	-
CPER1	.37	-	-	-	-	-	-	-	-
CPER3	-	-	-	.44	.40	-	-	-	-
SPER1	.50	.43	-	-	-	-	-	-	-
SPER3	-	-	-	-	-	-	-	-	-
CYLD	.64	.65	-.69	-	.44	-	-	.34	-
SYLD	.75	.70	-.59	-	.48	-	-	.54	-

ORIGINAL PAGE IS
OF POOR QUALITY

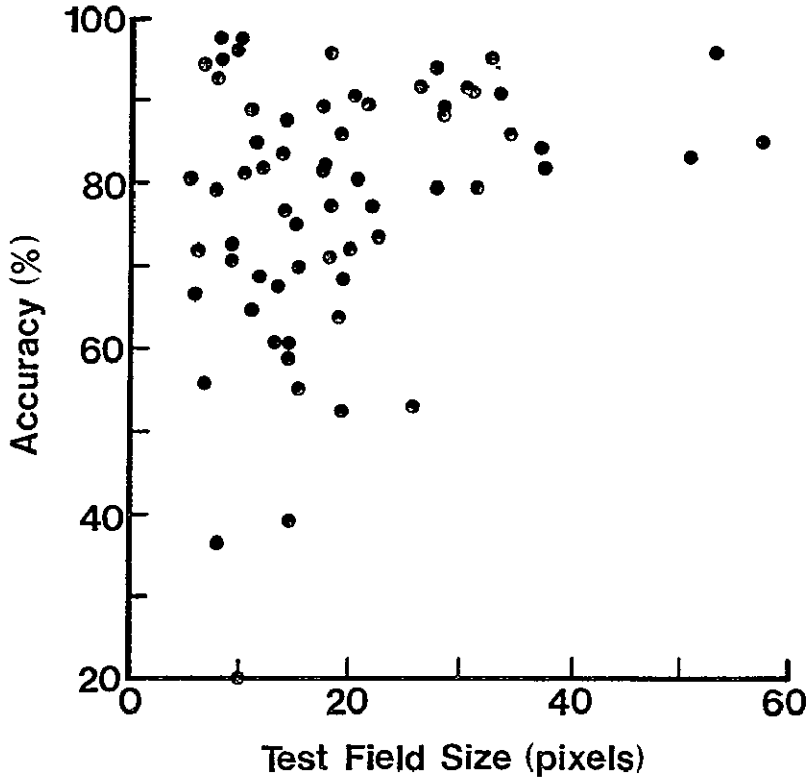

Figure 1-3. Relationship between average classification accuracy of corn, soybeans, and else and average test field size expressed in number of pixels (66 observations corresponding to 22 segments and 3 classification classes).

Multifactor Analysis

To investigate the interrelationships between the independent variables and to understand the nature of the independent variables better, a multicollinearity analysis was performed. Table 1-3 shows the significant correlations between all possible pairs of independent variables. The correlation between variables of the same group was generally strong except for some of the seasonal variables. Although soil variables were not correlated with many productivity or seasonal variables, they were significantly correlated with cover type variables. Cover type variables were also strongly correlated with the productivity variables, with the exception of the maximum yield (MAX) variable. Productivity variables, as expected, were strongly related to both 1978 corn and soybean yields (CYLD and SYLD). Field size (ALLAC), proportion of all field crops (ALL), crop diversity index (SWI), proportion of trees, slope, and proportion of corn were significantly correlated with many other independent variables. In addition, proportion of mixed pixels (MIX), proportion of soybeans, long-term average soybean yield (SYLDAVE), soil order and relative position of the segment in the Corn Belt (BELT) were also significantly correlated with several other independent variables.

ORIGINAL PAGE IS
OF POOR QUALITY

Table 1-3. Simple correlation coefficients between pairs of scene characteristics. For clarity, only the coefficients that were significant at $\alpha = 0.05$ are presented (29 independent variables and 23 observations).

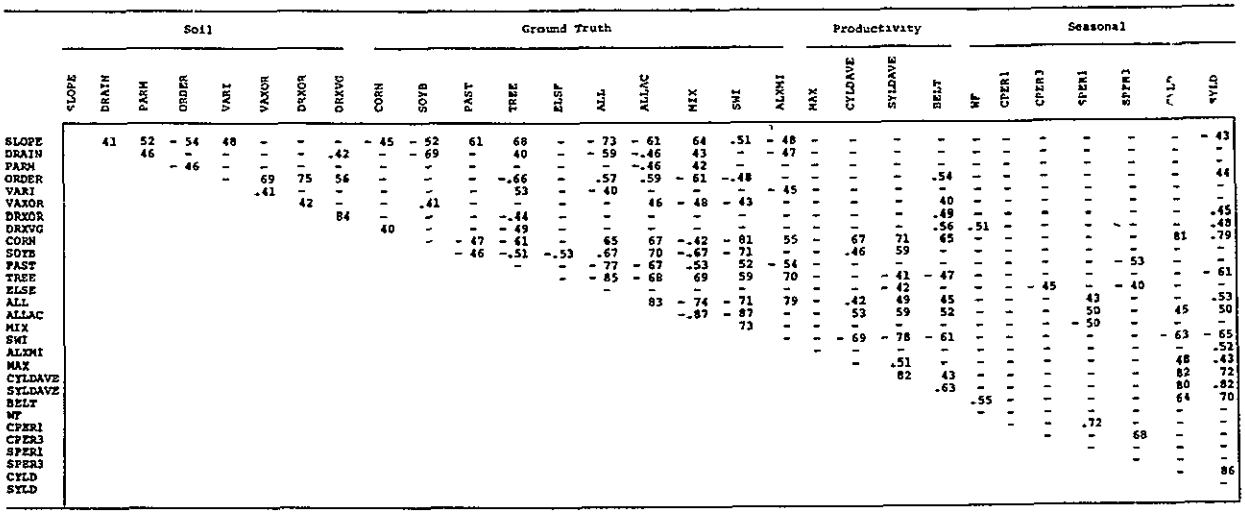

Table 1-4. Variables selected and coefficients of determination as a result of adding a group of scene characteristics given that the selected variables of previous group(s) were already in the model.

Dependent Variables	Ground Truth Variables Entered (R^2)	Soil Variables given Ground Truth Variables (R^2)	Prod Variables given Ground Truth + Soil Variables (R^2)	Seasonal Variables given Ground Truth + Soil + Prod. Variables (R^2)
Corn				
Wall (CO)	CORN,ELSE,ALL (.77)	DRAIN (78)	SYLDAVE (81)	SPER1 (86)
Test (CT)	CORN,SOYB,PAST, ALLAC (61)	DRAIN,PARM (68)	SYLDAVE (79)	SYLD (85)
Prop (ARCD)	CORN,SOYB,ELSE, ALL (89)	PARM (92)	SYLDAVE (95)	
Soybeans				
Wall (SO)	SOYB,ELSE,ALL (49)	SLOPE (.51)	BELT MAX (58)	WF (65)
Test (ST)	CORN,SOYB,PAST, SWI (.47)	DRAIN,DRXOR,DRXVG (~69)	BELT (76)	WF (84)
Prop.(ARSD)	PAST,ALLAC,SWI (10)	SLOPE,ORDER,VARI, DRAIN,DRXVG (39)	MAX,CYLDAVE (.49)	WF,SPER3,CYLD (99)
Overall				
Wall (OV)	CORN,SOYB,ELSE, ALLAC (23)	ORDER,DRAIN,VAXOR, DRXOR (68)	BELT,MAX (73)	WF (.85)
Test (OVT)	SOYB,PAST,ELSE, ALLAC (45)	SLOPE,ORDER,DRAIN DRXOR (63)	SYLDAVE (.71)	CPER3,SPER3 (90)
Prop (RMS)	ELSE,ALL,ALLAC, ALAMI (.16)	SLOPE,ORDER,VARI, DRXOR (63)	CYLDAVE (67)	WF,SPER3 (.79)

To investigate the amount of variability in the dependent variables that could be explained by a group of scene characteristics, several multilinear regression analyses were run. In building the regression models, cover type variables were the first variables to be acquired, followed by soil variables, then productivity variables, and finally the seasonal variables. Thus, models for each independent variable were run initially using only the cover type variables. Then soil, productivity and seasonal variables were entered in order. The results of these analyses are presented in Table 1-4.

Cover type variables alone explained much of the variability of corn accuracy measures, especially of corn proportion error (ARCD) where only four cover type variables gave an R^2 of .89 (Table 1-4). However, they did not explain much of the variability of soybean proportion error (ARSD), overall proportion error (RMS), and overall accuracy (OV). Corn, soybean, and other proportions and field size (ALLAC) were among the most frequently selected cover type variables. Proportion of all field crops (ALL) and proportion of pasture were also frequently selected. The cover type variables selected less frequently (SWI and ALXMI) or never selected (MIX and TREE) were strongly correlated with other cover type variables.

Soil variables added considerable information to the cover type variables already in the model, particularly for the overall accuracy measures and for soybean test field accuracy. Drainage, slope, order, and interactions between drainage and order (DRXOR) were the most frequently selected soil variables given that the previously selected cover type variables were already in the model. Drainage (DRAIN) and parent material (PARM) were important in explaining corn accuracies while slope, order, and interaction variables (DRXOR, DRXVG, VAXOR) contributed more to explaining soybean and overall accuracies.

After cover type and soil variables were in the model, productivity variables were entered. Although only one or two productivity variables were selected, their contribution to explaining the variability in the dependent variables was large. Long-term average soybean yield (SYLDAVE) and maximum yield were the most frequently selected variables.

Seasonal variables explained a significant portion of the variability of the dependent variables even after the selected variables of all three previous groups were already in the model. They were particularly effective in explaining the variability in the overall and soybean accuracies. The weather factor (WF) was the most frequently selected seasonal variable, followed by soybean development stage at the second acquisition date (SPER3).

Table 1-5 shows R^2 values obtained by the regression of each dependent variable on an increasing number of independent variables. In these analyses, all 29 independent variables were allowed to enter the model as candidate variables and the best combinations of four to 14 independent variables were selected based on R^2 values. Only four variables were required to explain the variability of corn accuracies compared to six to nine variables for soybean and overall accuracies, except for overall test field accuracy for which only four independent variables explained 81% of

ORIGINAL PAGE IS
OF POOR QUALITY

Table 1-5. Coefficients of determination of the regressions of the measures of classification on the best combinations of the scene variables. Total of 29 candidate variables and 4 to 14 variables entering the model (22 observations).

	Corn			Soybeans			Overall		
Number of Var.	CO	CT	ARCD	SO	ST	ARSD	OV	OVT	RMS
4	.84	.82	.87	.70	.62	.32	.49	.81	.57
5	.86	.84	.90	.75	.75	.56	.63	.88	.63
6	.87	.86	.91	.77	.80	.70	.66	.91	.67
7	.88	.86	.92	.81	.83	.78	.72	.92	.81
8	.89	.87	.93	.84	.85	.81	.80	.94	.85
9	.93	.88	.94	.90	.90	.87	.82	.95	.87
10	.97	.89	.95	.92	.91	.88	.84	.97	.89
11	.98	.93	.96	.94	.95	.94	.86	.97	.96
12	.99	.94	1.00	.97	.96	.96	.89	.99	.96
13	.99	.97	1.00	.97	.96	.98	.97	.99	.97
14	1.00	.98	1.00	.99	.98	.99	.98	.99	.99

its variability. Similarly, it was observed in the single factor analysis previously presented that corn accuracy measures and overall test field accuracy were more strongly related to individual independent variables than either soybean accuracies, overall proportion error (RMS) or overall wall-to-wall accuracy.

Summary and Conclusions

In summary, this study clearly indicated that several scene characteristics significantly affect classification accuracy. Further investigations should be directed toward modeling classification performance as a function of scene characteristics. Future studies should also include areas with more confusion crops and greater soil variability. Training and classification procedures are the two most controllable sources of variation in classification accuracy after the variability due to scene characteristics has been accounted for. Therefore, after the construction and testing of the model, an investigation of how specific training and classification procedures modify the predicted accuracy based on scene characteristics should be performed.

References

1. Bauer, M.E., J.E. Cipra, P.E. Anuta, and J.B. Etheridge. 1979. Identification and area estimation of agricultural crops by computer classification of Landsat MSS data. Remote Sensing Envir. 88:77-92.

2. Bauer, M.E., M.M. Hixson, B.J. Davis, and J.B. Etheridge. 1978. Area estimation of crops by digital analysis of Landsat data. Photo. Engr. and Remote Sensing 44:1033-1043.

3. Bizzell, R.M., F.G. Hall, A.H. Feiveson, M.E. Bauer, B.J. Davis, W.A. Malila, and D.P. Rice. 1975. Results from the crop identification technology assessment for remote sensing (CITARS) project. Proc. Tenth Symp. Remote Sensing of Environment, ERIM, pp. 1189-1198, Ann Arbor, MI.

4. Hanuschak, G., R. Sigman, M. Craig, M. Ozga, R. Luebbe, P. Cook, D. Kleweno and C. Miller. 1980. Crop area estimates from Landsat - Transition from research and development to timely results. IEEE Geoscience and Remote Sensing 18:160-167.

5. Hixson, M.M., M.E. Bauer, and D.K. Scholz. 1982. An assessment of data acquisition history on identification and area estimation of corn and soybeans. Remote Sensing Envir. 12:(in press).

6. Hixson, M.M., D.K. Scholz, N.C. Fuhs, and T. Akiyama. 1980. Evaluation of several schemes for classification of remotely sensed data. Photo. Engr. and Remote Sensing 46:1547-1553.

7. Holt, D.A., C.S.T. Daughtry, H.F. Reetz, and S.E. Hollinger. 1979. Separating soil and water effects in large area yield prediction. Agron. Abstracts 71:12.

8. MacDonald, R.B. and F.G. Hall. 1980. Global crop forecasting. Science 208:670-679.

9. Phillips, T.L. 1973. LARSYS User's Manual. Lab. Applic. Remote Sensing, Purdue Univ., W. Lafayette, IN.

10. Pitts, D.E. and G. Badhwar. 1980. Field size, length, and width distributions based on LACIE cover type data. Remote Sensing Envir. 10:201-213.

11. Pitts, D.E., A.G. Houston, G. Badhwar, M.J. Bender, M.L. Rader, W.G. Eppler, C.W. Ahler, W.P. White, R.R. Vela, E.M. Hsu, J.F. Potter, and N.J. Clinton. 1978. Accuracy assessment system and operation. Proc. LACIE Symp., JSC-16015:265-280, NASA Johnson Space Center, Houston, TX.

12. SAS Institute. 1979. SAS user's guide. SAS Institute, Inc., Raleigh, NC.

ORIGINAL PAGE IS
OF POOR QUALITY

2. ESTIMATING CROP DEVELOPMENT STAGES FROM MULTISPECTRAL DATA

James C. Tilton and Steven E. Hollinger

Introduction

If the calendar day a crop reaches a certain development stage is known, the stress a crop is experiencing can be assessed fairly accurately from weather information. Crop yields can then be predicted from this knowledge of the level and type of stresses a crop experiences during its development.

Accurate prediction of crop yields requires knowledge of the crop's development stage at critical times during the growing season. Development stage as defined here describes where the crop is in its life cycle. The Hanway scale(1) (Table 2-1) is commonly used to describe corn development and the Fehr-Caviness scheme(2) to describe soybean development. There are several other scales which are used to describe other crops.

Various meteorological models have been developed to estimate the calendar day a crop reaches a particular development stage. The most common methods involve the calculation of a thermal unit or a photothermal unit. The thermal unit or growing degree unit is calculated by summing the

Table 2-1. Corn development stages as defined by Hanway (1).

Stage Number	Stage Name
-1.00	Preplant
0.00	Planted
0.10	Emerged
0.25	1 leaf
1.00	4 leaves
2.00	8 leaves
3.00	12 leaves
4.00	16 leaves
4.50	Tasseled
5.00	Silked
6.00	Blister
6.50	Milk
7.00	Dough
8.00	Begin dent
9.00	Full dent
10.00	Physiologic maturity
10.50	Harvest maturity
11.00	Harvested

difference between the daily mean temperature and some threshold temperature. The modified growing degree unit developed by Gilmore and Rogers(3) is the most commonly used method to estimate corn development stages in the United States.

The thermal unit method of estimating crop development stages requires the planting date of a field and the temperature experienced by that field as inputs. The planting date for any given field in a large area is usually not known, so the average planting date for a state, crop reporting district (CRD), or county is often used. Temperature data for a given area is available from only one or at best three stations per county. Therefore, the mean temperature for a CRD is often used to describe the temperature regime for the entire area. This practice of using one planting date and temperature value gives an estimate of the mean development stage within a large area, but fails to fully describe the range and variation of development stages within the area. If remotely sensed spectral data from satellite can provide an estimate of the spatial variation of planting dates and/or development stages over large areas, it would be possible to make a more accurate estimate of the yield variation within a given region.

Considerable effort has been devoted to developing methods of estimating development stage using remote sensing. A spectral-temporal profile model using spectral data to describe development stage throughout the season has been developed recently by Badhwar and Henderson(4). The model has shown promise in accurately estimating development stages of corn and soybeans. However, the model requires a minimum of five acquisitions spread throughout the growing season to depict development. This becomes a problem because development stage cannot be described until after the end of the growing season and the value of the information is greatly reduced as far as assessing yield potential during the growing season is concerned. Because of this limitation, we have pursued the development of a model to give a spectral estimate of development stage early in the growing season. This model can also be used to estimate development stages late in the crop season. The model has its biggest advantage in early season development stage estimation in that observations are only required through mid-season rather than through the entire crop season. Another advantage of our model is that it does not require the computationally-intensive curve-fitting required by the Badhwar and Henderson model.

Multispectral Crop Modeling

The spectral response of a crop canopy, as measured by Landsat-type multispectral scanners (MSS), changes in a typical manner throughout the growing season, depending on the crop type. The greenness component of the Kauth and Thomas tasseled-cap transformation(5) exhibits these changes particularly well. The greenness and brightness components of the tasseled-cap transformation are the two largest components obtained from a principle components analysis of four channel Landsat MSS data. The greenness component correlates with the amount of green vegetation present while the brightness component correlates with the overall brightness of the scene (often the brightness of the underlying soil). In this investigation we

ORIGINAL PAGE IS
OF POOR QUALITY

considered the behavior of the greenness component of the tasseled-cap transformation for individual pixels or for field averages, which we will refer to as the green number for that particular pixel or field.

A typical plot for corn of green number versus calendar date is shown in Figure 2-1. Prior to planting the green number stays essentially constant at a level we call the "soil green number." After planting the green number stays at the soil green number until sufficient vegetative matter appears above the soil, usually when two or three leaves emerge from the corn plant (Hanway stage 0.50 or 0.75). Then the green number increases with calendar date relatively quickly until the "maximum canopy green number" value is reached, usually at about tasseling or silking (Hanway stage 4.50 or 5.00). The green number then holds fairly constant or falls slightly as subsequent development stages occur through the beginning of denting (Hanway stage 8.00). It then falls rapidly as the corn matures until it approaches the soil green number again at harvest. Many other crops have similar green number curves with time, where the green number rises or falls rapidly over relatively short time intervals.

The crop development stage estimation technique described here basically notes the calendar days when the green number rises and falls to values half-way between the soil green number and the maximum canopy green number. These calendar days are then correlated with particular crop development stages through the use of training data. Since the green number changes most rapidly with both time and crop development stage at these half-way rise and fall points, the development stage can be estimated most accurately at these points. Of particular interest is the crop development stage estimate for the calendar day when the green number first rises to

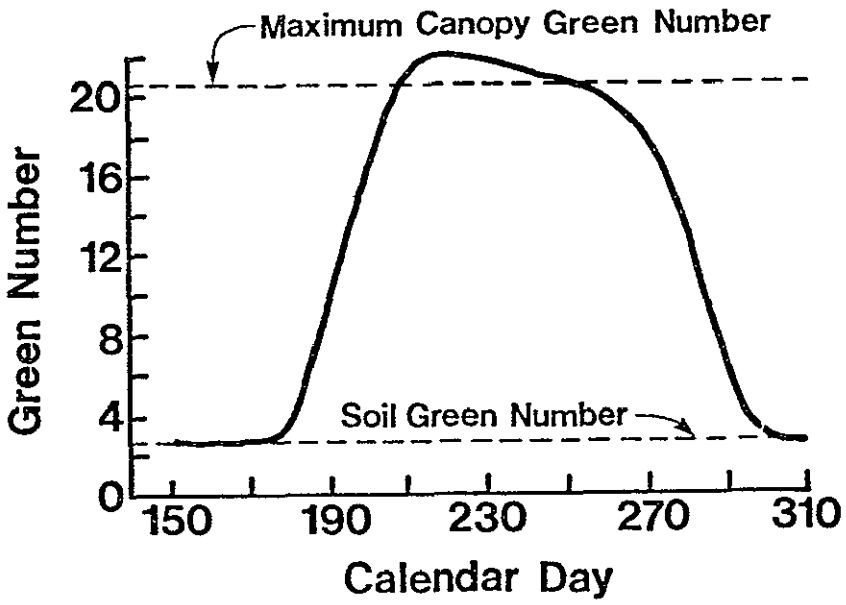

Figure 2-1. Typical plot of Landsat green numbers versus calendar day for a midwestern corn field.

ORIGINAL PAGE IS
OF POOR QUALITY

cross the value half-way between the soil green number and maximum canopy green number. All that is required to make this estimate are MSS observations through enough of the growing season to make an estimate of the maximum canopy green number, or roughly half of the growing season. At least one observation at or prior to planting is required for the soil green number estimate. In order for good estimates to be made, the MSS observations should be made at intervals of 36 days or less.

Crop Development Stage Estimation Technique

Agronomy Farm Data

Spectral data acquired over experimental plots at the Purdue University Agronomy Farm near West Lafayette, Indiana were used in the early development work on our crop development stage estimation technique. The data were collected using a truck-mounted Exotech-100 radiometer which has the same wavelength bands as the Landsat MSS. The data were calibrated and corrected for sun-angle effects. Various agronomic measures, including crop development stage, were recorded simultaneously with each radiometric observation. For a complete description of the data see Bauer, et al(6). The Kauth-Thomas greenness component of the Exotech-100 wavelength bands (B1, B2, B3 and B4) is given by the following transformation(7):

$$\text{Green number} = -0.4894*B1 - 0.6126*B2 + 0.1729*B3 + 0.5854*B4.$$

A key step in estimating crop development stages from the green number values is a process through which the soil green number and the maximum canopy green number are estimated from the data. This estimation process requires green number estimates at regular time intervals throughout the growing season. This regular interval was chosen to be nine days to make the Agronomy Farm data look more like Landsat MSS data. The shortest time interval over which repeat Landsat MSS data may be available is generally nine days. Since the MSS observations are generally available at irregular time intervals, interpolation must be used to obtain green number estimates for every nine days. The interpolator employed should be conservative (not prone to wide oscillations) since we do not expect green number variations due to crop development to have wide oscillations. Such an interpolator is the quasi-Hermite spline interpolator contained in the IMSL mathematical and statistical subroutine software package (8). This interpolator is designed to approximate a curve drawn manually through the data points.

As noted above, Landsat MSS data are generally available no more frequently than every nine days. Data from controlled experiments may be available more frequently. Data at intervals less than about nine days may contain misleading short-term fluctuations due to such things as changes in illumination level and soil moisture level (e.g. it rained between observations). Where such short-term fluctuations occur, even the conservative quasi-Hermite spline interpolator produces green number estimates with unrealistic oscillations. (Data at widely spaced intervals also contain fluctuations due to short-term events, but these fluctuations are about a long-term trend and are not interpreted as high frequency oscillations by an interpolator.)

Because of the problems with short-term fluctuations in the data, the calculated green number values are smoothed (or filtered) to dampen out the high frequency variations suggested by the short-term fluctuations in the data. This smoothing also serves to make the Agronomy Farm data look more like Landsat MSS data, since Landsat MSS data generally cannot contain fluctuations of shorter term than nine days. This smoothing is accomplished by a time-domain convolution of the data with a sinc**2 function ((sin(pi*x)/pi*x)**2). Since such a convolution makes sense only for stationary data and since the green number values for the entire growing season cannot be considered stationary, the convolution is only performed over an eighteen day window. The data can be considered to be approximately stationary over a time span of about eighteen days or less. A sinc**2 function with zeros nine days before and nine days after its peak has been found to perform well. The function is in effect set to zero by the eighteen day window for times earlier than nine days before the central peak and for times later than nine days after the central peak. Convolving with such a function does not affect green number values calculated from observations which are nine days or more apart.

The soil green number and the maximum canopy green number are estimated from the smoothed and interpolated green number estimates. These estimates are first normalized so that the minimum green number value is zero and the maximum green number value is twenty. These minimum and maximum values are arbitrary, but they are roughly the minimum and maximum values typically found in the Agronomy Farm data.

The soil green number is estimated as follows: the normalized green numbers are ordered from smallest to largest. Initially, the smallest green number is considered to be the soil green number estimate. The next largest green number is tested against the current soil green number estimate using a one-sided chi-square test with one degree of freedom. This test gives the probability that the tested green number is not an observation of the soil green number. We will refer to this as the probability that the tested green number is "above" the current soil green number estimate. If the tested green number has a probability of 50% or less of being above the soil green number estimate, the tested green number is considered to be an additional observation of the soil green number and averaged with the other soil green number observations to produce a new soil green number estimate. The above process is repeated for the next largest green number. If the tested green number has a probability of more than 50% of being above the current soil green number estimate, the current soil green number estimate is considered to be the final soil green number estimate.

The maximum canopy green number is estimated in a similar way to the method for estimating the soil green value. Here, however, the normalized soil green numbers are ordered from maximum to minimum, and the next smallest green number is tested against the current maximum canopy green number estimate for being "below" the maximum canopy estimate. The threshold probability here is taken to be 90% rather than 50% since the maximum canopy green number observations tend to be more variable than the soil green number observations. We should note that if the green number

ORIGINAL PAGE IS
OF POOR QUALITY

observations were not normalized, or if they were normalized differently, we would obtain different estimates for the soil green number and the maximum canopy green number because of the nature of the chi-square test, unless we would adjust our threshold probabilities appropriately.

The soil green number and maximum canopy green number estimation process assumes that each green number observation is of equal importance. This assumption is satisfied if green number estimates are taken at equal time intervals. If the green number observations are left at irregular time intervals, the estimation process would require weighting each observation according to its relative importance. The relative importance or weight of each observation could be determined by the time interval between the observation and the previous and following observations. (If the observation is the first or last observation, we would have to make some reasonable assumption.) These relative weights should be used when these green number observations are averaged together to give estimates of the soil green number or maximum canopy green number. In addition, the relative weight of each observation being tested in the chi-square test would have to be incorporated into the test. It is much easier to interpolate green number estimates at regular time intervals (as we have done) than to resort to such observation weighting.

Now that we have estimates of the soil and maximum canopy green numbers, we can make estimates of the time certain growth stages occur. A fairly typical graph of the processed green numbers is shown in Figure 2-2. This graph is for a plot of corn that was planted later than most other corn

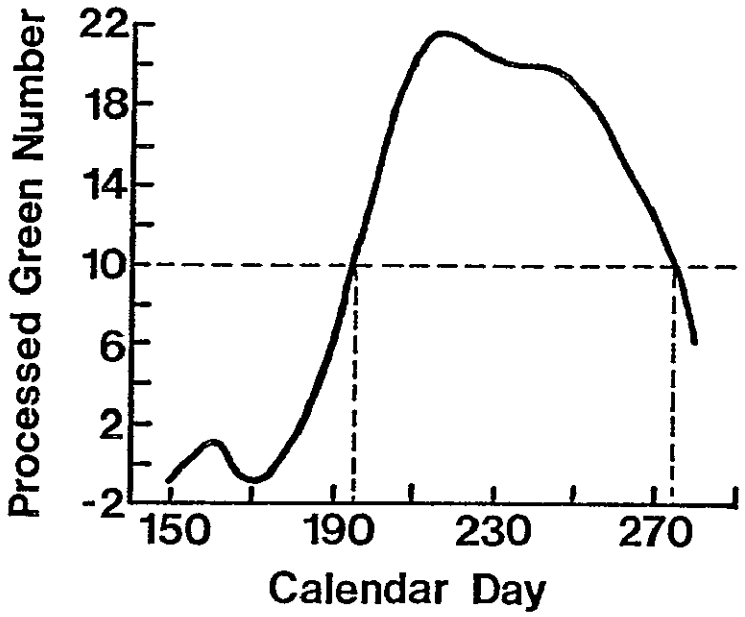

Figure 2-2. A fairly typical plot of processed green numbers exhibiting early non-crop "green-up." In this case ten is the green number value half-way between the soil green number and maximum canopy green number. The calendar dates where the processed green numbers cross this half-way value are indicated.

on the Purdue Agronomy Farm. Such late plantings typically exhibit a non-crop "green-up" such as shown here at about calendar date 160. The field was then tilled and planted on calendar date 163. For this corn plot, the calendar dates that the processed green values crossed the half-way rise and fall value between the soil green number and maximum canopy green number were day 196 and day 276. The Hanway stage at day 196 was about 1.75 (7 leaves) and the Hanway growth stage at day 276 was about 9.00 (full dent).

Landsat MSS Data

The crop development stage estimation technique was also tested on three 9.3 by 11.1 km Landsat data segments, two from 1978 and one from 1979. Field observations of crop development stages were made for selected fields in the segments at several times during the growing season. The Landsat-2 and -3 observations were calibrated to each other and corrected for sun angle. The Kauth-Thomas greenness component of the calibrated Landsat wavelength bands (B1, B2, B3 and B4) is given by(5):

$$\text{Green number} = -0.283*B1 - 0.660*B2 + 0.577*B3 + 0.3884*B4.$$

It is reasonable to assume that the crop observed in each pixel of a particular field should have approximately the same development stage. For this reason, field averages are taken for each Landsat spectal band. Also, estimating crop development stages for field averages rather than for each individual pixel is much more cost effective. Sample standard deviations are also calculated for each field for each Landsat channel as an indication of the variability of the crop within the field. The field green number standard deviation is calculated from the individual Landsat wavelength band standard deviations (SD1, SD2, SD3 and SD4) as follows:

$$\text{Green number standard deviation} = [(0.283*SD1)^2 + (0.660*SD2)^2 + (0.577*SD3)^2 + (0.3884*SD4)^2]^{.5}.$$

Occasionally two sets of Landsat MSS observations are available which are separated by only one day where adjacent orbital paths give overlapping coverage. These observations from adjacent orbital paths may sometimes give noticeably different green number values due to factors other than crop development stage such as atmospheric changes, changes in crop moisture level, a different sun angle, and different sensor look angle. Because of this, the Landsat MSS green numbers need to be filtered (smoothed) in the same manner that the Agronomy Farm green numbers were smoothed to dampen out misleading high frequency variations suggested by the short-term fluctuations. As noted in the Agronomy Farm data discussion, this filtering does not affect observations taken nine or more days apart. The green number standard deviations are filtered in the same way the green number field averages are.

After smoothing, green number estimates are interpolated every nine days with the same quasi-Hermite spline interpolator used with the Agronomy Farm data. Interpolated standard deviation estimates are obtained by running the interpolator directly on the green number standard deviations calculated from the observations (after smoothing). This is a reasonable approach if we consider the green number standard deviation to be an inherent characteristic of a field which may increase or decrease throughout the season depending on several factors including crop development stage.

In the Landsat MSS data case, where the field averages and standard deviations of green numbers are estimated, the soil green number is estimated in a manner similar to that described above for the Agronomy Farm data. The only difference is that instead of a chi-square test, a test is employed that exploits the standard deviation information. This is a test designed to solve the problem of testing two samples of normal populations with unequal variances (or standard deviations) against each other for having identical means. Besides the field mean and standard deviation estimates of the green number, this test also requires knowledge of the number of pixels used to estimate the mean and standard deviation of the green number in the field in question. In this case, appropriate one-sided probability thresholds are 75% for both the soil green number estimate and the maximum canopy number estimate. Two different thresholds are not required, because this test already takes into account the variability of the green number estimates through the standard deviation information. Since standard deviation information is exploited by the test for soil green number and maximum canopy green number, the test will give the same results whether or not the green number estimates are normalized as is done in the Agronomy Farm data case.

As we shall see in the results section below, fields in particular geographic areas tend to have processed green number values that cross the half-way rise and fall value at characteristic development stages early and late in the growing season. We will call these estimates of development stages, respectively, early and late season estimates of the crop development stage. The characteristic development stage estimates vary somewhat from one geographic area to another and from one year to the next, so training data for a particular geographic area and/or year is needed to establish these characteristic development stages for the geographic area and/or year in question.

Evaluation of Results

Agronomy Farm Data

The method for estimating crop development stages was first tested on Purdue Agronomy Farm data. The method gives the calendar day when the normalized green number value rises and falls to cross the half-way value. To get crop development stage estimates, we would have to use training fields to correlate the half-way rise and fall calendar days with crop development stages. Since we did not have enough reference data to divide it into an adequate number of mutually exclusive test and training fields, we chose to use a test of the potential of this method rather than a direct test.

Our test for the potential of our method is as follows: First we use our method to find the calendar day the normalized green number rises to cross the half-way value and the calendar day it falls to cross the half-way value for each plot. Then we estimate from the reference data the actual crop development stage the crop was at for the indicated calendar days. (We generally have to estimate the crop development stage by interpolation because in most cases the indicated calendar day did not happen to fall on a day a ground observation was made.) Then we calculate the mean and standard deviation of the early season crop development stage estimates and the mean

and standard deviation of the late season development stage estimates. A small standard deviation for both cases would indicate that this method has good potential for making accurate estimates of crop development stage early and late in the growing season, given adequate training data. We can compare the mean values of the estimated development stages for data sets from different years and locations to get an indication of how sensitive the training is to changes in years and geographic location.

We tested Purdue Agronomy Farm corn plot data from both 1979 and 1980 in this way. The experiments included several planting dates, three plant populations and two soil types (dark and light). With 36 test plots in 1979 we found the observed average Hanway crop development stage was 2.04 for the early season estimate, with a standard deviation of 0.36. (For convenience we write this result 2.04±0.36.) The observed Hanway stage for the late season estimate was 9.51±0.40. (Complete reference and spectral data sets were available for the late season estimate for 27 out of the 36 plots.) With 52 corn test plots in 1980 we found observed Hanway stages of 2.02±0.26 and 8.99±0.08. (Complete data were available for the late season estimate for 40 out of the 52 plots.) See Figure 2-3 for a histogram of these results. For both the 1979 and 1980 Agronomy Farm data, we find standard deviations of less than 0.50, which is close to the commonly accepted error bound for observing development stages in the field. This indicates that the method does have potential for making reasonably accurate estimates of crop development stages. The closeness of the mean values for the two years may indicate that the training may not be very critical for different years at the same location.

Landsat MSS Data

Thus far we have completed a limited test with Landsat MSS data on selected fields in only three segments. We tested 10 fields each in two segments of 1978 data. For segment 127 (located in Montgomery Co., Indiana) we found the late season estimate of the Hanway stage to be 9.28±0.78. Ground observations were not taken early enough in the growing season to make an early season test. For segment 862 (located in Calhoun Co., Iowa) we found Hanway stage early season estimate of 4.58±0.37 and late season estimate of 9.62±0.32. (Only 4 fields were used in the late seaon estimate due to insufficient data.) We tested 15 fields in one segment of 1979 data. In 1979 a different development stage scale was used for ground observations of development stage (see Table 2-2). For segment 892 (located in Shelby Co., Iowa) we found development stages of 3.44±0.19 (using 6 fields) and 6.20±0.31 (using all 15 fields) for the early and late season estimates. These development stages correspond roughly to the Hanway stages 3.00 and 10.00, respectively. As with the Agronomy Farm results, the standard deviations for these estimates are below 0.50 (except for one case), indicating that the method has good potential for making accurate crop development stage estimates from Landsat MSS data. The fairly wide differences in early and late season estimates for the segments tested indicate separate training may be necessary for data sets from different geographic areas and different years.

ORIGINAL PAGE IS
OF POOR QUALITY

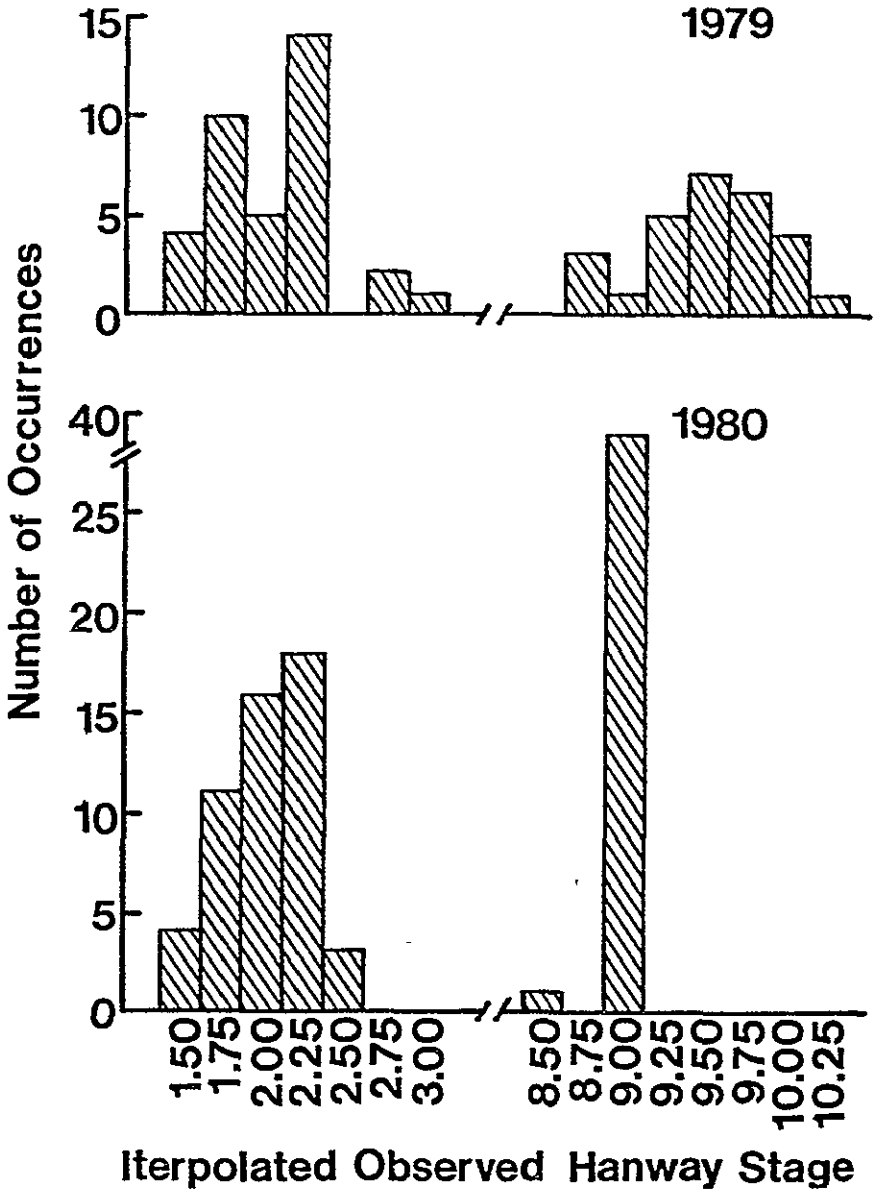

Figure 2-3. Histograms of the interpolated observed Hanway stages at the early and late season estimates (calendar days that the green number rose and fell to cross the half-way value) for the 1979 and 1980 Agronomy Farm data.

Conclusions

The preliminary tests indicate that, given sufficient training data, our method should be able to make accurate estimates of the calendar date a crop reaches a particular early season crop development stage using Landsat MSS observations from the first half of a growing season with minimal computation cost. An estimate of the calendar date a crop reaches a particular late season crop development stage can be made using Landsat MSS observations from the last half (or all) of a growing season. The method is insensitive to varying plant population.

The method can be used to initialize a meteorological development stage model to provide estimates of the calendar day a particular field reaches any given development stage. The meteorological model could be run forward in time from the development stage provided by our method to the critical development stages for yield estimation. The meteorological model could even be run backwards to give estimates of planting dates (possibly for comparison with other methods).

The examples cited and the experimental results given were for corn only; however, this method should be applicable for other crops that exhibits a similar peaking of green numbers towards the middle of the growing season.

References

1. Hanway, J.J. 1966. How a corn plant develops. Iowa State University Cooperative Extension Service Special Report #48. Ames, Iowa.

2. Fehr, W.R. and C. E. Cavines. 1977. Stages of Soybean Development. Iowa State University Cooperative Extension Service Special Report #80, Ames, Iowa.

3. Gilmore, E.C., Jr. and J. S. Rogers. 1958. Heat Units as a Method of Measuring Maturity in Corn. Agron. J. 50:611-615.

4. Badhwar, G.D. and K.E. Henderson. 1981. Estimating Development Stages of Corn from Spectral Data: An Initial Model. Agron. J. 73:748-755.

5. Kauth, R.J. and G.S. Thomas. 1976. The Tasselled Cap - A Graphic Description of the Spectral-Temporal Development of Agricultural Crops as Seen by Landsat. Proc. 1976 Machine Processing of Remotely Sensed Data Symposium, June 1976.

6. Bauer, M.E., L.L. Biehl, C.S.T. Daughtry, B.F. Robinson and E.R. Stoner. 1979. Agricultural Scene Understanding and Supporting Field Research. Laboratory for Applications of Remote Sensing (LARS), Purdue University, West Lafayette, Indiana. NASA Contract NAS9-15466.

7. Malila, W.A. and J.M. Gleason. 1977. Investigations of Spectral Separability of Small Grains, Early Season Wheat Detection, and Multicrop Inventory Planning. Environmental Research Institute of Michigan (ERIM), Ann Arbor, Michigan. ERIM Report 122400-34-E.

8. Bickel, P.J. and K.A. Doksum. 1977. Mathematical Statistics: Basic Ideas and Selected Topics. Holden-Day, Inc., San Francisco, pp. 218-219.

Table 2-2. Corn development stage coding used for 1979 Landsat reference data.

Stage Number	Stage Name
1.0	Planting
2.0	Emerged
3.0	Six leaves
4.0	Tassels emerged
5.0	Blister
6.0	Physiologic maturity
7.0	Harvest

3. CROP CONDITION ASSESSMENT

The overall objective of this research is to develop approaches for using spectral data as a source of information for crop yield models. Under this general objective three tasks are being pursued. The first two address issues related to the interception of solar radiation, particularly photosynthetically active radiation (PAR), by corn and soybean canopies. The third section addresses problems associated with methods of directly measuring leaf area index of crops. These sections are progress reports which present analysis plans and preliminary results. A series of technical reports will be prepared as each major phase of data analysis is completed.

A. Interception of Photosynthetically Active Radiation in Corn Canopies

K.P. Gallo and C.S.T. Daughtry

Introduction

Recent research indicates that remotely sensed data may be used to estimate agronomic variables associated with yields of corn. The proportion of solar radiation intercepted (SRI) by the crop canopy is one important predictor of dry matter production and grain yield. SRI has been estimated as a function of canopy leaf area index (LAI) using the following equation:

$$SRI = 1 - \exp(-0.79\ LAI). \qquad (1)$$

This is an application of Bouger's Law using measured LAI and an extinction coefficient of 0.79 (Linvill et al., 1978). When LAI is 0, no energy is intercepted by the canopy. When LAI is 2.8, approximately 90% of the incoming solar radiation is intercepted by the canopy and is potentially useful to the crop. When daily values of SRI were accumulated from planting to maturity, the total SRI was associated with 65 percent of the variation in corn yields over two years (Daughtry et al., 1983). In the same experiment SRI was also estimated using multispectral data and explained 62 percent of the variance in corn yields.

Additional factors also influence corn yields and are included in an energy-crop growth (ECG) model (Coehlo and Dale, 1980). The ECG model includes the incoming solar radiation (SR), the latent energy (LE) of water, the ratio of daily evapotranspiration to potential evapotranspiration (WF), and the relative growth rate of corn as a function of temperature (FT).

$$ECG = \sum_{\text{plant}}^{\text{mature}} (SR_i/LE)\ (SRI_i)\ (WF_i)\ (FT_i) \qquad (2)$$

The ECG variable, summed daily from planting to maturity, accounted for more of the variance in corn grain yields than SRI alone (Daughtry et al.,

1983). A portion of the variance in crop yields unexplained by Eq.'s 1 and 2 may be attributed to the estimation, as opposed to the direct measurement, of SRI. Another source of variance may be due to the use of total incoming SR (0.3 to 3.0 μm) rather than the portion of SR actually used by plants during photosynthesis. The wavelengths of photosynthetically active radiation (PAR) range from 0.4 to 0.7 μm of the electromagnetic spectrum.

Direct measurements of PAR intercepted (IPAR) by the plant crop should explain more of the variance in crop yields than SRI. IPAR also should be useful information to the ECG (Eq. 2) model or similar crop growth and yield models. IPAR should be predictable from remotely sensed spectral variables and should provide a valuable input to large area crop condition and yield models.

The overall objective of this study is to develop approaches (models) for using spectral data as a source of information for crop yield models. The specific objectives are:

1. Develop and evaluate techniques for measuring IPAR in corn canopies.

2. Determine the effects of planting date and planting density on IPAR, agronomic (e.g. LAI, percent soil cover, and dry matter production), and spectral characteristics of corn canopies throughout the growing season,

3. Develop and evaluate models relating spectral reflectance to the biophysical characteristics of corn canopies,

4. Develop and evaluate methods for combining spectral and meteorological data in crop yield models.

Those methods that best estimate yields at agricultural experiment stations will be extended to large areas using Landsat MSS and TM data. Finally the results of estimating yields with and without the input of spectral data will be compared. Multispectral data from satellites could form the basis for estimating crop yields over regions where ground observations may be difficult or impossible to obtain.

Materials and Methods

Experimental Design

Corn (Zea mays L., 'Adler 30X') was planted in N-S rows, with 76 cm spacing between rows, on two planting dates (14 May and 24 June 1982) at two planting densities (thinned to 50,000 and 100,000 plants/ha) in a randomized complete block design with two blocks. Plot size was 15.2 by 15.2 m allowed sufficient borders for measurements of IPAR components at low solar elevation angles (AM measurements). Tillers were removed from all plants to assure as uniformly structured a canopy as possible. The soil type was a Chalmers silt loam (Typic Argiaquoll), with a dark (10 YR 4/1) surface. Prior to planting 250, 53, and 100 kg/ha of N, P, and K respectively, were applied to maintain high fertility.

IPAR Data Collection

The portion of incoming PAR that is intercepted by the canopy may be computed by measuring the four PAR components (Hipps et al., 1982) shown in Figure 3-1. The measured amount of IPAR is dependent on canopy geometry and the incoming PAR. Incoming PAR fluctuates throughout the day due to changes in solar azimuth and zenith angles as well as changes in atmospheric conditions including clouds, gases, and particulates. Thus IPAR is expressed as a proportion of incoming PAR to account for these variations.

$$IPAR = [(PAR + RPARs) - (TPAR + RPARcs)]/PAR \quad (3)$$

RPARs is the amount of incoming PAR reflected from the soil surface under the canopy. TPAR is the amount of PAR (direct and diffuse) transmitted through the canopy to a sensor located on the soil surface, and RPARcs is the amount of PAR reflected from the canopy and soil surface.

Frequently IPAR (or SRI) is measured only within a specified time interval of solar noon (Adams and Arkin, 1977; Fakorede and Mock, 1977; Hatfield and Carlson, 1979; Hipps et al., 1982; and Loomis et al., 1968). This time interval when solar elevation is at its maximum generally minimizes the extinction coefficient. However, other work (Warren Wilson, 1960; Anderson, 1966) suggests that at a solar elevation angle of 32.5° the extinction coefficient (Eq. 1) is least affected by foliage inclination. The four components of IPAR (Eq. 3) were measured at two time intervals during the day: in the morning between solar elevation angles of 30 to 35° (AM measurements) and within $\pm$ 0.5 hr of solar noon (SN). Additional measurements of IPAR were acquired in conjunction with radiometric measurements of spectral reflectance. In each case all measurements were acquired under clear sky ($\leq$10% cloud cover) conditions.

A line quantum sensor (LICOR 191SB) and a data logger (Omnidata Polycorder Model 516) were used for all IPAR measurements. PAR and TPAR were measured at approximately weekly intervals for all times of observations. The reflected PAR components (i.e., RPARs and RPARcs) were measured less frequently due to their relatively small contributions to IPAR. Table 3-1 summarizes the frequency of measurements of the IPAR components for 1982. Incoming PAR was measured within 30 seconds of the IPAR components listed in Table 3-1.

Agronomic Data Collection

Agronomic data included plant height, stage of development, percent soil cover, leaf area index, total fresh and dry biomass, and dry biomass of leaves, stems, ears, and grain. These data were acquired at weekly intervals from a random sample of five plants per plot. Leaf area (one side of leaf) of two plants per plot was measured using a LI-COR model LI-3100 area meter. Total leaf area for the five plants was computed using the total dry weight of leaves and the mean leaf area to leaf dry weight ratio. Leaf area index was computed by dividing total leaf area by the soil area represented by the five plants. Grain yields were measured after physiological maturity (as indicated by black layer formation) and corrected to 15.5 percent moisture.

ORIGINAL PAGE IS
OF POOR QUALITY

$$IPAR = \left[\underbrace{(PAR + RPARs)}_{\text{ENTERING CANOPY}} - \underbrace{(TPAR + RPARcs)}_{\text{LEAVING CANOPY}} \right] / PAR$$

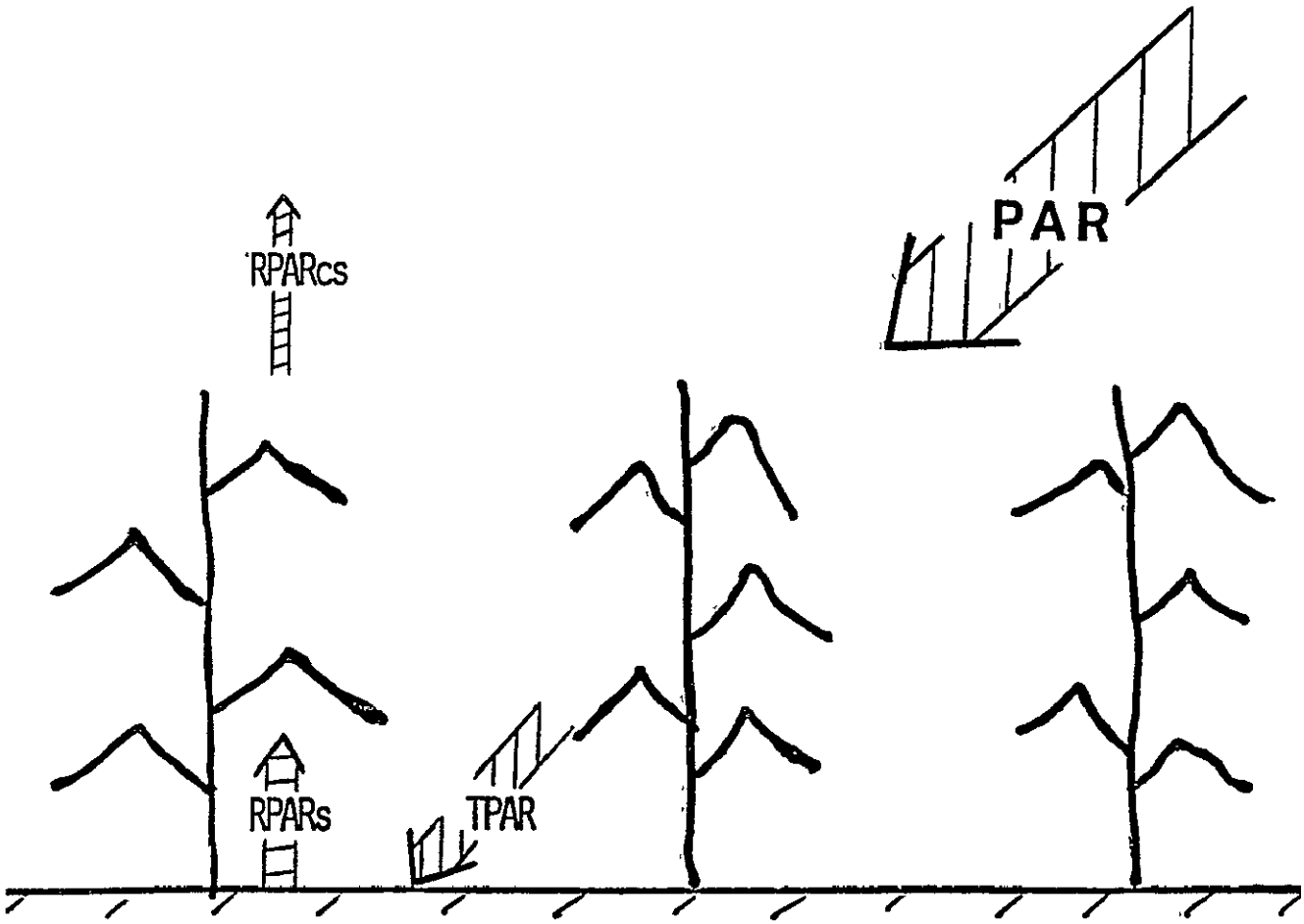

Figure 3-1. Components of intercepted photosynthetically active radiation (IPAR).

Table 3-1. Summary of number of data sets acquired for the corn IPAR experiment in 1982.

Measurement	Planting Date		
Type/Time	14 May	24 June	Total
	------number of data sets-----		
TPAR[†]			
- 30 to 35° elevation	17	12	29
- solar noon +/- 0.5 hr.	21	13	34
- with RF measurements[§]	24	14	38
RPARs, RPARcs[¶]			
- throughout the day	9	21	30

[†]Transmitted PAR.

[§]TPAR measured in conjunction with reflectance factor measured by Exotech 100 and Barnes 12-1000 radiometers.

[¶]Reflected PAR from soil (RPARs) and canopy (including soil) surface (RPARcs).

Spectral Data Collection

Spectral reflectances were measured using Exotech 100 (Landsat bands) and Barnes 12-1000 (TM bands) radiometers. The frequency of spectral data acquisition are described by L. Biehl in this report. Three independent sets of on- and off-row measurements were acquired for each plot.

Results and Discussion

These IPAR data span the entire growing season and will allow analysis of the variation in IPAR components with crop development. Figure 3-2 shows the percent of incoming PAR that is transmitted through the canopy (TPAR) as a function of crop development stage (Hanway, 1963) for the AM and SN observation intervals. The low planting density of corn had a significantly greater TPAR compared to the high density for both observation intervals.

ORIGINAL PAGE IS
OF POOR QUALITY

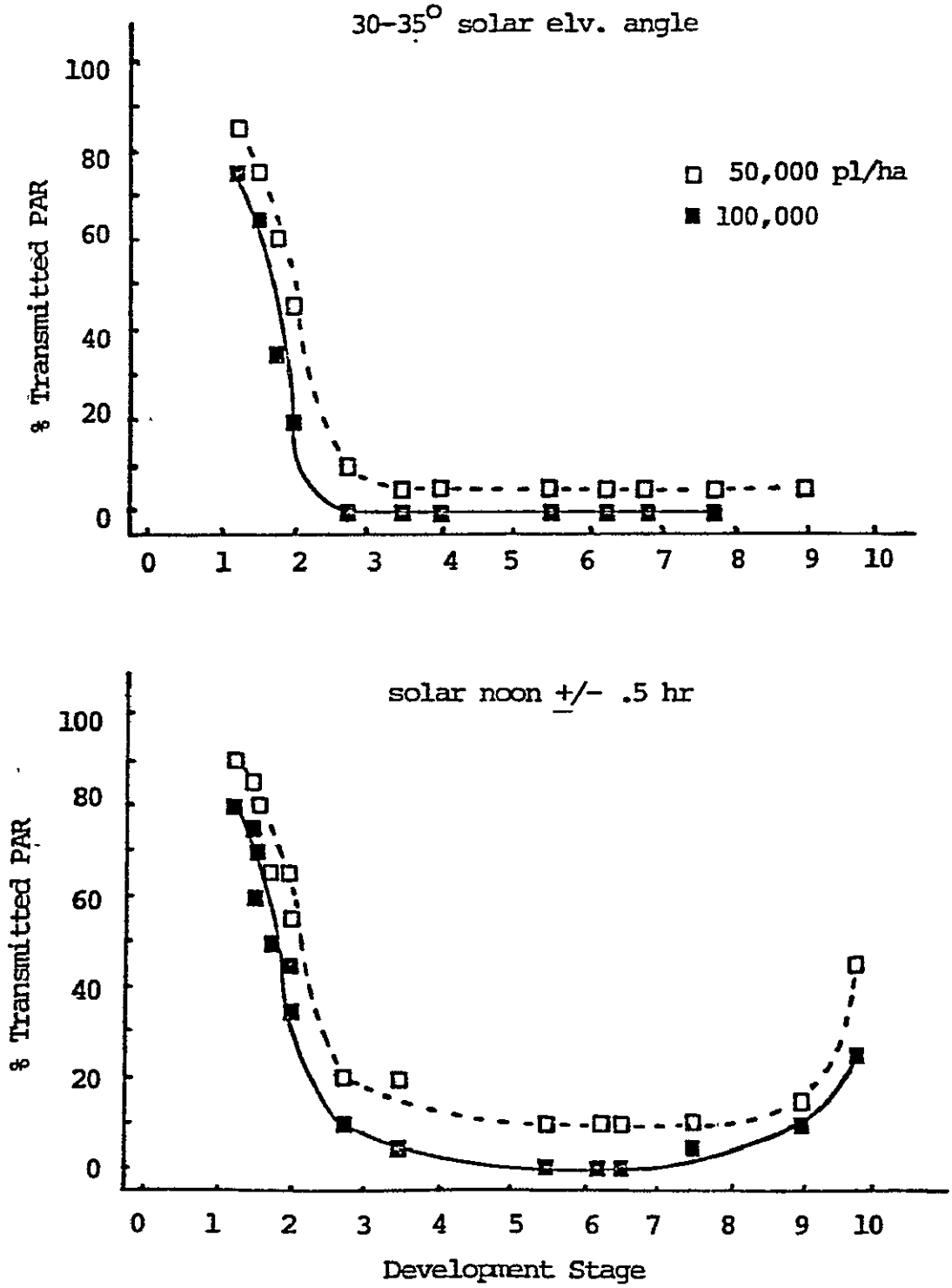

Figure 3-2. Mean values of %TPAR measured as a function of solar elevation, planting density, and crop development stage for the 14 May planting date. For the means presented, $s_{\bar{x}}$ is usually less than 3.0%.

ORIGINAL PAGE IS
OF POOR QUALITY

More radiation reaches the soil during the SN observation interval compared to the AM interval.

Less than 10 percent of the incoming PAR is reflected by the canopy and soil (RPARcs) (Figure 3-3). Prior to stage 2 soil reflectance (RPARs) is the major contributor to RPARcs. No significant differences were found in RPARcs between the two planting densities from stage 2 (8 leaves) to stage 6 (milk stage) of development (Figure 3-3).

SRI computed using measured LAI values (Eq. 1), was compared to IPAR as a function of crop development stage for the low and high planting densities (Figure 3-4). SRI predicts that more energy was intercepted by both plant densities throughout the season than was measured by IPAR. The general shape of the two curves is similar which suggests that a constant may account for the difference.

There are two possible explanations for the observed differences between SRI and IPAR. First, SRI, as defined by Linvill et al. (1978) and Daughtry et al. (1983), does not include the reflected radiation components (e.g. RPARs and RPARcs). Thus SRI fundamentally differs from IPAR. Second, the extinction coefficient in Eq. 1 is not a constant as solar elevation angles change unless the foliage is horizontal (Anderson, 1966; Norman, 1980). A variable extinction coefficient dependent on plant density and solar angle should be considered.

In summary, data were collected in 1982 which will permit us to address many of the concerns discussed in this report. Models for predicting intercepted PAR using remotely sensed data will be developed and evaluated.

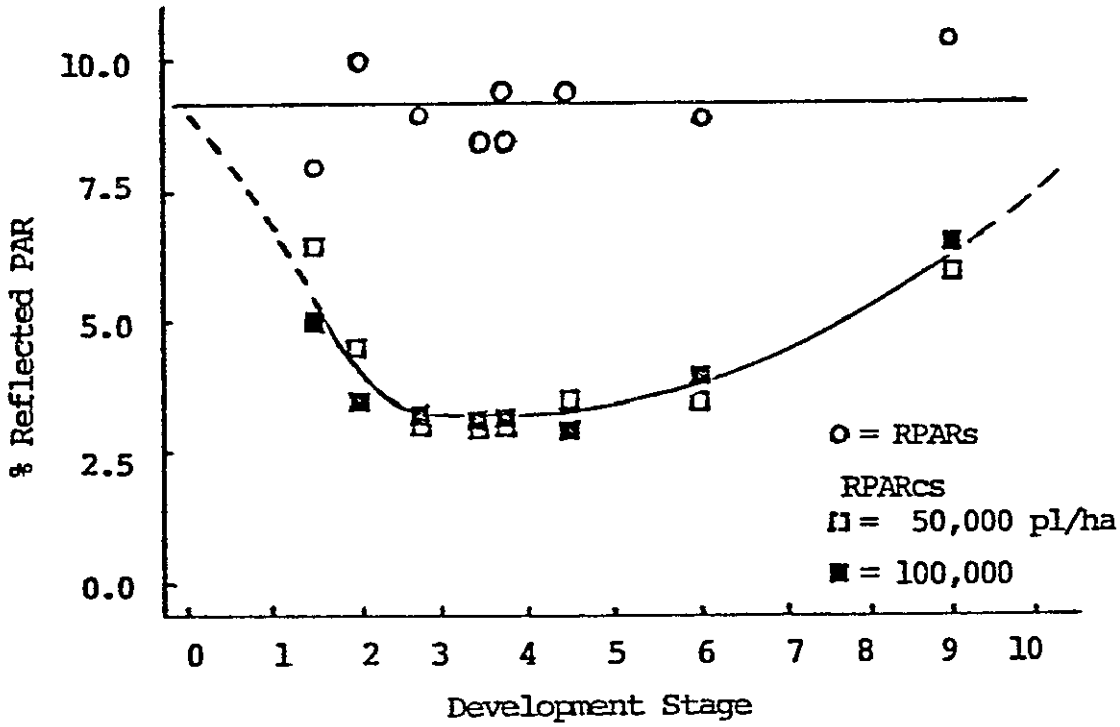

Figure 3-3. Means of % reflected PAR from bare soil (RPARs) and canopy including soil surface (RPARcs), as a function of planting density and crop development stage. Data are presented for the 14 May planting and projections are plotted for the seasonal values of reflected PAR. For all means presented, $s_{\bar{x}}$ is less than 0.18.

ORIGINAL PAGE IS
OF POOR QUALITY

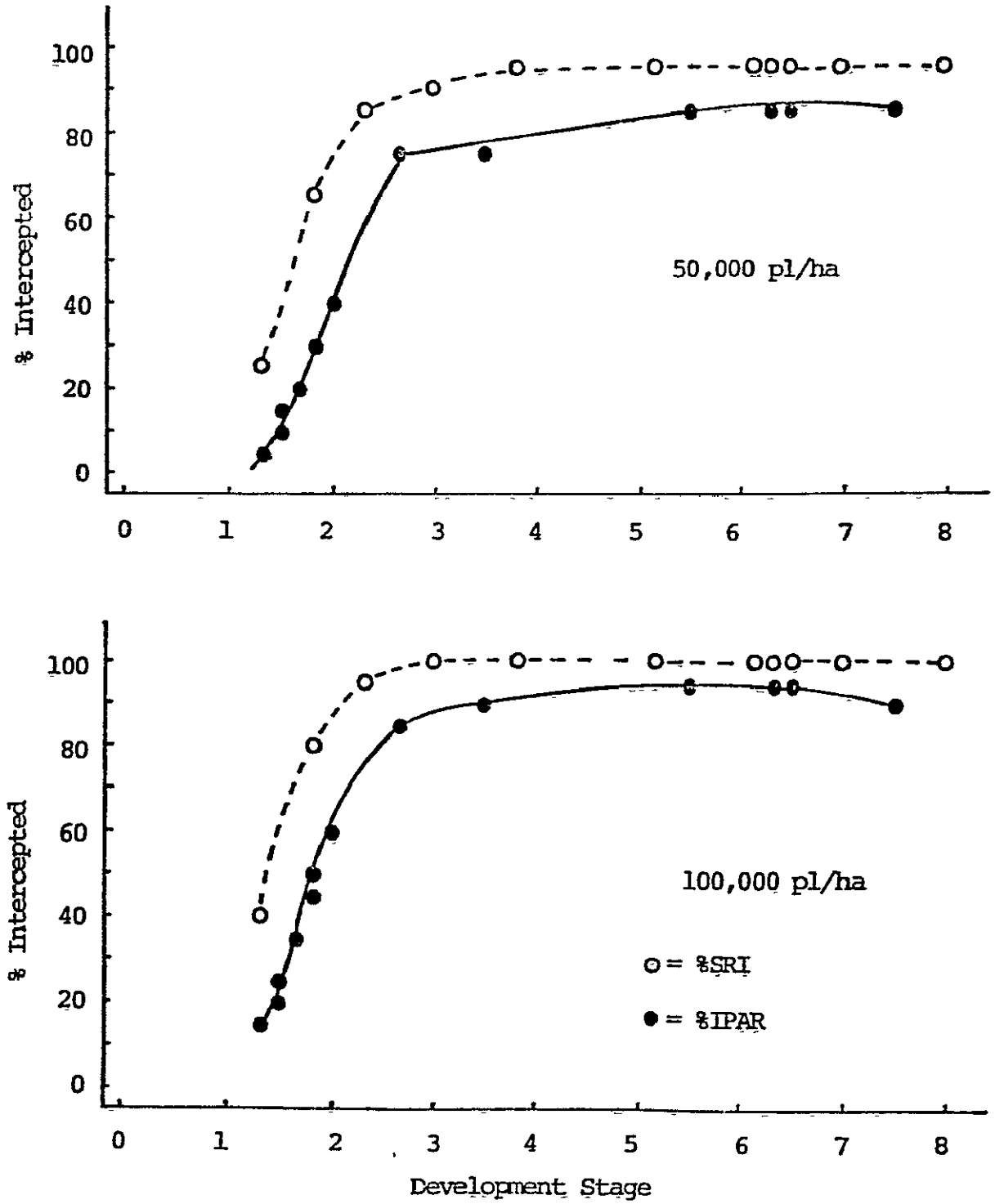

Figure 3-4. %SRI computed as a function of LAI, and %IPAR measured as a function of planting density and crop development stage. Measurements were made on the 14 May planting date plots at solar noon ± 0.5 hr.

References

1. Adams, J.E. and G.F. Arkin. 1977. A light interception method for measuring row crop ground cover. Soil Sci. Soc. Am. J. 41:789-792.

2. Anderson, M.C. 1966. Stand structure and light penetration. II. A Theoretical Analysis. J. Appl. Ecology 3:41-54.

3. Coelho, D.T. and R.F. Dale. 1980. An energy-crop growth variable and temperature function for predicting corn growth and development: planting to silking. Agron. J. 72:503-510.

4. Daughtry, C.S.T, K.P. Gallo, and M.E. Bauer. 1983. Spectral estimates of solar radiation intercepted by corn canopies. Agry. J. 75:(In press).

5. Fakorede, M.A.B. and J.J. Mock. 1977. Leaf orientation and efficient utilization of solar energy by maize (Zea mays L.). pp. 207-230. Proc. of the Symp. on Agrometeorology of the Maize (Corn) Crop. Ames, Iowa, USA. 5-9 July 1976.

6. Hanway, J.J. 1963. Growth stages of corn (Zea mays L.). Agron. J. 55:487-491.

7. Hatfield, J.L. and R.E. Carlson. 1979. Light quality distribution and spectral albedo of three maize canopies. Agr. Meteorol. 20:215-226.

8. Hipps, L.E., G. Asrar, and E.T. Kanemasu. 1982. Assessing the interception of photosynthetically active radiation in winter wheat. AgRISTARS Supporting Research Tech. Rep. SR-M2-04270. NASA/JSC Earth Resource Research Division, Houston, TX.

9. Linvill, D.E., R.F. Dale, and H.F. Hodges. 1978. Solar radiation weighting for weather and corn growth models. Agron. J. 70:257-263.

10. Loomis, R.S., W.A. Williams, W.G. Duncan, A. Dorvat, and F. Nunez. 1968. Quantitative descriptions of foliage display and light absorption in field communities of corn plants. Crop Sci. 8:352-356.

11. Norman, J.M. 1980. Interfacing leaf and canopy lignt interception models. In J.D. Hesketh and J.W. Jones (eds.) Predicting photosynthesis for ecosystem models. Vol. 2, CRC Press, Boca Raton, FL.

12. Warren, Wilson J. 1960. Inclined point quadrates. New Phytol. 59:1-8.

B. Interception of Photosynthetically Active Radiation in Soybean Canopies

C.C. Brooks, C.S.T. Daughtry, and M.E. Bauer

Introduction

Photosynthetically active radiation (PAR) is defined as radiation in the 0.4 to 0.7 μm wavelength region and is the source of energy for the photosynthetic machinery that converts carbon dioxide and water into plant components. Plant leaves act as convertors of electromagnetic radiation into chemical energy through the process of photosynthesis. The final yield from a plant partly reflects the efficiency of this conversion. The overall efficiency of the conversion is affected by the amount of PAR intercepted by the leaves and the distribution of PAR within the canopy. Agronomists have postulated that crop yields may be limited by less than favorable interception of insolation. Planting pattern plays an important role in the interception of PAR. Soybeans (Glycine max (L.) Merrill) are highly influenced by neighboring plants either within the same row or in adjacent rows. In recent years there has been an increased interest in production of soybeans in narrow rows because of lower labor, energy, and equipment requirements as well as greater seed yields per unit of land. The capability to plant soybeans in narrow row spacings has been greatly enhanced by the introduction of effective chemical weed control and hence the wide spacing needed by mechanical cultivation for weed control may be eliminated. If weeds and excessive lodging can be minimized, then seed yield can be increased.

Weber et al., (1966) noted that plants in wider row widths generally accumulated their leaf area index (LAI) at a slower rate than plants in narrower row widths. At equivalent populations, LAI required to intercept 95% of the solar radiation and days from emergence to 95% interception were greater in wide rows than narrow rows (Hicks et al., 1969; Shibles and Weber, 1966). Thus the growth and/or yield of a crop is directly related to the amount of solar radiation intercepted (SRI) by the crop. This theoretical relationship is expressed by the equation:

$$DM = \int_{e}^{m} E\ P\ SR\ dt$$

where the increase in dry matter (DM) production over time period (t), beginning at emergence and ending at physiological maturity, can be related to the proportion (P) of the incident light (SR) intercepted by the crop and the efficiency (E) of the conversion of solar energy to dry matter (Stevens, 1982).

The above equation can be used to predict dry matter production, if P is known. Direct measurements of P can be obtained by placing a line quantum sensor (LQS) in the canopy or P can be derived from leaf area measurements.

The proportion of solar radiation intercepted (SRI) can be estimated by two different methods. Sakamoto and Shaw (1967) described a method of estimating SRI by using LAI measurements. Using Bouguer's Law, they quantified the expression:

$$I = Io \exp(-k\ LAI)$$

where I = the estimate of solar radiation intercepted
Io = insolation (incoming solar radiation)
k = commonly termed extinction coefficient
LAI = leaf area index

for soybeans. They observed values for k ranging from 0.25 (development stage 7, full pod) to 0.49 (development stage 3, six leaves). Whereas, Ogbuehi and Brandle (1982) reported values of 0.74 (July 25) to 1.16 (August 27). Luxmoore et al. (1971) found a maximum extinction coefficient occurred at the uppermost leaf layers and was greater than 1.4. They also observed that varying the position of the sensor within the canopy produced a minimal k value of 0.35. Norman (1980) reported extinction coefficients ranging from 2.0 to 0.8 for low and high solar elevation angles, respectively. Therefore, additional research is needed to characterize the changes in extinction coefficients if this approach is to be used quantitatively.

However, it would be impossible to make these measurements for use in large scale growth and yield models. Daughtry et al. (1983) described a method using spectral data to predict SRI which may be applicable in large area models. If the proportion of energy available for crop growth can be estimated reliably by using multispectral satellite data, then the capability to estimate crop production for large regions would be greatly improved.

In practice, the amount of SRI is only one of several factors interacting to influence soybean production. Other environmental factors modifying growth and yield are water and temperature, as well as management factors such as planting date, cultivar and fertility.

The objectives of this research are to study the relationships between intercepted photosynthetically active radiation (IPAR), and agronomic and spectral characteristics of soybean canopies throughout the growing season as affected by different cultural practices. Specific objectives are to

1. Study the relationships of accumulated IPAR and LAI, percent canopy cover to total phytomass and total grain yield,

2. Predict IPAR, LAI, percent canopy cover, total phytomass and grain yield using multispectral reflectance data, and

3. Incorporate spectrally estimated variables into crop yield models.

Materials and Methods

Experimental Design

The 1982 soybean cultural practices experiment was conducted on a Chalmers silty clay loam (typic Argiaquoll) at the Purdue Agronomy Farm. The experimental design was a randomized, complete block design which included two blocks, three planting dates (11 May, 25 May, and 14 June), three row widths (38, 76, and 114 cm). Plot size was 6.1 x 15.8 m and all rows were in a north-south orientation. Plots with row widths of 38 and 76 cm were thinned to obtain the desired population (250,000 plants/ha). Plots with a row width of 114 cm were mechanically planted to the desired population (approximately 250,000 plants/ha).

Spectral Measurements

Radiance measurements, used to determine reflectance factor (RF), were acquired with a Landsat-band radiometer (Exotech 100) and a thematic mapper band radiometer (Barnes 12-1000) throughout the growing season (Table 3-2). Procedures outlined by Robinson and Biehl (1979) were used to approximate the bidirectional reflectance factor (BRF) under field conditions. The Exotech 100 is a four-band radiometer with a 15 degree field of view (FOV) and wavelength bands of 0.5-0.6, 0.6-0.7, 0.7-0.8, and 0.8-1.1 μm. The Barnes 12-1000 is an eight band radiometer with a 15 degree FOV and wavelength bands of 0.45-0.52, 0.52-0.60, 0.63-0.69, 0.76-0.90, 1.15-1.30, 1.55-1.75, 2.08-2.35, and 10.40-12.50 μm regions. Data were taken only under near cloud-free conditions when the solar elevation angle was at least 45 degrees above the horizon.

The radiometers and motor-driven camera were attached to a boom mounted on a pickup truck for quick and efficient data collection in the field. The instruments were elevated 7.6 m above the soil surface giving an effective FOV of 3.1 m^2 on the soil surface for both radiometers. Instruments were leveled for a nadir view angle and measurements were taken over two locations in plots with 38 and 76 cm wide rows and four locations in plots

Table 3-2. Summary of IPAR collection for soybeans.

	Planting Date		
Time of Acquisition	11 May	25 May	14 June
	----------number of data sets---------		
Solar noon (+1 hr.)	18	11	11
Before noon	22	15	12
With R.F.*	15	10	8

* IPAR was collected immediately after collection of reflectance factor data.

with 114 cm wide rows. Observations were taken on-row and off-row to obtain a better estimate of the overall canopy response for the plot and to reduce any bias (Daughtry et al., 1982). Measurements from both radiometers were recorded concurrently by a electronic data logger. A vertical photograph was taken of each plot for later crop assessment and soil cover determination.

A line quantum measured shortly after radiometric data was taken. A line quantum sensor (LI-COR, model LI-191s) and a data logger (Omnidata Polycorder 516) were used to measure the average photosynthetic photon flux density throughout the canopy. Two types of measurements were made with the line quantum sensor (LQS). First, the sensor was held level at approximately 1.5 m above the soil surface and incoming PAR was measured (reference measurement). Next the amount PAR transmitted through the canopy was measured by placing the sensor under the canopy on the soil surface in the same east-west orientation in which the reference measurement was taken. Four measurements were taken in series as the LQS was moved through the canopy across four adjacent rows.

Agronomic Measurements

Agronomic data, which were collected weekly, included: plant height, leaf area index, stage of development, total fresh and dry phytomass, dry stem (including petioles), pods, and green leaf blade weight. Percent soil cover was determined by placing a grid over a vertical photograph of each plot and counting the number of dots superimposed over the green vegetation. Area of all green leaves on one or two plants was measured with electronic area meter (LI-COR LI-3100). All plant parts were dried at 75C and weighed. Total leaf area of 10 plants was calculated using the leaf area and dry leaf weight ratio of the subsample of green leaves times the total dry green leaf weight. Leaf area index (LAI) was calculated by dividing total leaf area by the soil area represented. Visual assessment of the soil moisture and crop condition were made during the spectral data collection. Final grain yield was determined by harvesting two, three, or five rows 6.1 m in length for row widths of 114, 76, and 38 cm, respectively. Crop condition assessment included evaluation of lodging, hail, insect, and herbicide damage.

Expected Results

Reflectance factor data will be analyzed, in several individual bands as well as through the use of transformations, to develop the relationships between IPAR and other agronomic variables. Regression and correlation analyses will be used to delineate these relationships. Analysis of variance and mean separation tests will be used to account for the variation due to experimental parameters.

References

1. Hicks, D.R., J.W. Pendleton, R.L. Bernard, and T.J. Johnston. 1969. Response of soybean plant types to planting patterns. Agron. J. 61:290-293.

2. Daughtry, C.S.T., K.P. Gallo, and M.E. Bauer. 1983. Spectral estimates of solar radiation intercepted by corn canopies. Agron. J. 75:(In Press).

3. Daughtry, C.S.T., V.C. Vanderbilt and V.J. Pollara. 1982. Variability of reflectance measurements with sensor altitude and canopy type. Agron. J. 74:758-766.

4. Kauth, R.J. and G.S. Thomas. 1976. The tasselled cap - a graphic description of the spectral-temporal development of agricultural crops as seen by Landsat. Symposium on Machine Processing of Remotely Sensed Data. Purdue University, W. Lafayette, IN 47906.

5. Luxmoore, R.J., R.J. Millington, and H. Marcellos. 1971. Soybean canopy structure and some radiant energy relations. Agron. J. 63:111-114.

6. Norman, J.M. 1980. Interfacing leaf and canopy light interception models. Vol. 2. CRC Press, Boca Raton, FL. pp. 49-67. In Predicting Photosynthesis for Ecosystem Models. J.D. Hesketh and J.W. Jones (eds.).

7. Ogbuehl, S.N. and J.R. Brandle. 1982. Influence of windbreak-shelter on soybean growth, canopy structure, and light relations. Crop Sci. 22:269-273.

8. Robinson, B.F. and L.L. Biehl. 1979. Calibration procedures for measurements of reflectance factor for remote sensing field research. Proc. Photo-Optical Instrumentation Engr. 196-04:16-26.

9. Sakamoto, C.M. and R.H. Shaw. 1967. Light distribution in field soybean canopies. Agron. J. 59:7-9.

10. Shibles, R.M. and C.R. Weber. 1966. Interception of solar radiation and dry matter production by various soybean planting patterns. Crop Sci. 6:55-59.

11. Steven, M.D. 1982. Optical remote sensing for predictions of crop yields. Proc. Soc. Photo-Optical Instrumentation. Engr. 262:137-142.

12. Weber, C.R., R.W. Shibles, and D.E. Byth. 1966. Effect of plant population and row spacing on soybean development and production. Agron. J. 58:99-102.

C. Costs of Measuring Leaf Area Index of Corn

C.S.T. Daughtry, S.E. Hollinger, G. Drape, and E.M. Luke

Introduction

Research on the efficiency of solar radiation interception and utilization by crop canopies requires frequent measurements of leaf area. Because accurate measurements of leaf area for crop canopies are laborous and time-consuming, numerous direct and indirect methods of measuring leaf area for various crops have been developed (5, 7, 9, 10, 12, 14). The many methods reported in the literature have been summarized by reviewers (8, 9, 11) into at least 14 principal methods which vary greatly in their precision, accuracy and difficulty of accomplishing. A researcher's choice of a method to measure leaf area depends largely on (i) morphological features of leaves to be measured, (ii) accuracy required, (iii) amount of material to be measured, and (iv) amount of time and equipment available.

If proper precautions are observed, many of the methods reported in literature are sufficiently accurate for measuring leaf area of individual leaves and plants. In order to estimate leaf area index (LAI) of crop canopies, the variability in leaf area, among plants within a plot also must be considered as an additional source of experimental error. This inherent variability within crop canopies produces different estimates of LAI for the same treatment when more than one sample is acquired per treatment.

In this paper we examined the magnitude of within plot errors for components of corn plants selected from uniform plots and evaluated several methods for estimating LAI with known precision and probability of success. The approximate errors, the number of plants required, and the relative costs in time per sample for each method are also presented.

Materials and Methods

Two field experiments were conducted on a Chalmers silty clay loam (Typic Arqiaquoll) at the Purdue University Agronomy Farm, West Lafayette, Indiana. In 1980 a single-cross corn (Zea mays L. 'Beck 65X') was planted on 22 May in 76 cm wide rows and thinned to 50,000 plants/ha. From a randomly selected starting point in two different rows, 10 consecutive plants were sampled by cutting the plants at the soil line. Each of the 20 plants was weighed immediately and separated into leaf blades (including exposed portions of leaves in the whorl), stalks (including leaf sheaths) and ears. The area of all leaves on each plant was measured using an optically scanning area meter (LI-COR model LI-3000 with conveyor belt). All plant parts were dried at 75 C and weighed. This sampling procedure was followed on four dates when seven, 10, and 16 leaves were fully emerged (collar visible at base of leaf) and at silking, corresponding to development stages 1.75, 2.50, 4.0, and 5.0, respectively (6).

A second experiment was conducted in 1982 on corn (Adler 30X) planted on 12 May in 76 cm wide rows and thinned to 50,000 and 100,000 plants/ha. During the milk stage of grain development 20 randomly selected plants were sampled from each population. As each leaf was removed from the stalk, its length, width, and area were measured. Leaf area was measured using an area meter (LI-COR Model LI-3100) and each leaf was dried at 75C and weighed.

The precision of the area meter was evaluated by repeatedly measuring the area of a calibration plate, a soybean leaflet, and a corn leaf. The coefficients of variation (CV) were 0.08, 0.17, and 0.34% for the plate, soybean leaflet, and corn leaf, respectively. Leaves tend to fold and wrinkle slightly as they move between the rollers of the area meter, causing slight differences in the total area measured. These random errors of measurement associated with the leaf area meter are small compared to other sources of variation discussed later.

The ratio of leaf area per unit leaf dry weight (specific leaf area, SLA) was calculated. Means, standard deviations, and coefficients of variation were calculated for each plant component. Total errors for each sampling scheme were calculated using the appropriate means and standard deviations. These total errors included error due to within plot variation and error associated with the measurement technique.

The minimum number of replications of the basic sampling unit required for a 90% probability ($\beta = 0.10$) of obtaining a significant result at the alpha = 0.05 and 0.01 levels were estimated (1,3). Because the number of degrees of freedom in t_1 and t_2 depends on r, initially r was assumed to be infinity and then adjusted in subsequent calculations until the smallest number of replications that would satisfy the condition was determined (3). The average costs per plant in man-minutes for four methods of measuring leaf area of corn plants were estimated by interviewing agronomists who have extensive experience in growth analysis research. Total cost for each method was calculated by multiplying the minimum number of plants required to detect significant differences times the average cost per plant.

Results and Discussion

Variation Among Plants

Means, standard deviations, and CV of several plant characteristics for the corn plants sampled are presented in Tables 3-3 and 3-4. CV normalizes standard deviations by the mean and is useful for comparing relative variations among stages of development and plant characteristics. The large variations in stalk weights among the plants sampled undoubtedly contributed to the large CVs for total fresh and dry weights (Table 3-3). Care was taken to minimize extraneous errors in stalk dry weights due to non-uniform drying by cutting the stalks into segments 20 to 30 cm long, and by splitting each segment before drying. The largest CVs in total fresh and dry weights occurred prior to silking (Table 3-3) and are similar in magnitude to other reported values for corn (4, 13). The CV of leaf area and leaf weight per plant decreased after silking when all leaves were fully expanded (Table 3-3). In most cases the CVs for leaf area were smaller than CVs for leaf weight (Tables 3-3 and 3-4).

Table 3-3. Descriptive statistics for 20 corn plants sampled at four stages of development in 1980.

Plant Characteristic	Stage of Development†	Mean	S	CV
				%
Total Fresh Weight (g/plant)	1.75	118 a§	18.5	21.8
	2.50	379 b	21.2	80.3
	4.00	880 c	13.2	116.2
	5.00	995 d	11.2	111.4
Total Dry Weight (g/plant)	1.75	11.3 a	19.0	2.1
	2.50	37.2 b	23.9	8.9
	4.00	95.4 c	13.2	12.6
	5.00	154.4 d	13.5	20.8
Stalk Dry Weight (g/plant)	1.75	5.2 a	25.3	1.3
	2.50	20.3 b	29.7	6.0
	4.00	62.0 c	14.5	9.0
	5.00	99.6 c	14.1	14.0
Leaf Dry Weight (g/plant)	1.75	6.1 a	16.3	1.5
	2.50	16.9 b	18.8	3.2
	4.00	33.4 c	12.2	4.1
	5.00	39.7 c	9.9	3.9
Leaf Area (m^2/plant) x 100	1.75	13.8 d	14.4	2.0
	2.50	36.1 b	16.0	5.8
	4.00	64.8 c	10.0	6.5
	5.00	66.0 c	6.8	4.5
Specific Leaf Area¶ (m^2/g) x 100	1.75	2.27 a	4.8	0.11
	2.50	2.16 a	5.7	0.12
	4.00	1.95ab	8.0	0.16
	5.00	1.67 b	6.3	0.11

†Stages of development are 7-, 10-, 16-leaves, and silking, respectively.

§Means of each plant characteristic followed by the same letter are not significantly different at $\alpha = 0.05$ level of Duncan's multiple range test.

¶Specific leaf area = leaf area/leaf dry weight.

Table 3-4. Descriptive statistics for 20 corn plants sampled from two plant densities at milk-stage of development in 1982.

Plant Characteristic	Plant Density	Mean	S	CV
	1000 plants/ha			%
Leaf Dry Weight (g/plant)	50	45.6 a[T]	7.4	16.2
	100	39.6 b	5.2	13.1
Leaf Area (m^2/plant) x 100	50	67.9 a	7.4	10.8
	100	69.2 c	5.5	7.9
Specific Leaf Area[§] (m^2/g) x 100	50	1.51 a	0.13	8.8
	100	1.76 b	0.17	9.4
Leaf Length x Width (m^2/plant)	50	94.0 a	10.8	11.5
	100	93.4 a	6.8	7.3

[†]Specific leaf area = leaf area/leaf dry weight.

[§]Means of each plant characteristic followed by the same letter are not significantly different at $\alpha = 0.05$.

Mean CVs for specific leaf area (SLA), were much smaller than the mean CVs of leaf area, and leaf, stalk, and total dry weights (Tables 3-3 and 3-4). The small CVs observed for SLA are consistent with the expected variances for ratio estimators when the components of the ratio are positively correlated (2,3). These ratios have lower variation than direct measures of area and mass. Based on CV data in Table 3-3, it also appears feasible to estimate leaf area index per plant on a fresh weight basis with approximately the same precision as with the dry weight method. This assumes that moisture losses are minimized and plants are processed rapidly. Estimating LAI on a fresh weight basis has an additional advantage - no fuel is required for drying large volumes of plant material with high moisture contents.

Methods of Measuring LAI

One question facing a researcher is how best to allocate finite resources to measure the area of numerous plants and be reasonably confident of detecting significant differences among crop canopies. We selected four representative methods of measuring LAI to illustrate the advantages and disadvantages of single and multistage sampling schemes. In each of the schemes presented below, plant density (plants/unit area of soil) also must be determined to calculate LAI. We have assumed that the errors in determining plant density are identical for each method and thus may be omitted for these comparisons.

In the first method the area of all leaves (A_L) on n plants is measured directly using a digital electronic area meter (7) and LAI is calculated as

$$LAI1 = A_L/n. \quad (1)$$

The second method employs the relationship between leaf area and leaf weight of a subsample of leaves to convert the weight of a large sample of leaves into leaf area (8,9,15). Leaf area (AL) and leaf weight (WL) are measured on a subsample of leaves and total leaf weight, WTL, only is measured on n plants. This multistage sampling scheme uses a small number of plants to estimate specific leaf area which has a low CV and a larger number of plants to estimate total leaf dry weight which has a high CV (Tables 3-3 and 3-4). LAI is calculated as

$$LAI2 = (AL/WL)(WTL/n) \quad (2)$$

In the third method area of each leaf on n plants is estimated as the product of leaf length (L), maximum leaf width (W), and a constant (b_1). LAI is calculated from the sum of these estimated leaf areas as follows

$$LAI3 = \sum_{j=1}^{n} \sum_{i=1}^{m} (b_1 LiWi)j/n \quad (3)$$

where m is the number of leaves on the jth plant and n is the number of plants sampled. The general form of the relationship of leaf length and width to leaf area is $A = b_0 + b_1 LW$ where b_0 and b_1 are coefficients determined by regression that requires checking if leaf shape changes. Frequently b_0 is not significantly different from zero and the equation can be simplified (7). For example, leaf area of corn may be calculated as $A = 0.75\ LW$ (5,10,15).

The fourth method is an adaptation of the rapid methods of estimating leaf area (5,10). A "leaf area factor" (LAF) is determined by measuring length and width of all leaves for m plants of each treatment in one replication and dividing the total leaf area per plant by the area of the largest leaf per plant. Francis et al. (5) recommended using 10 plants to minimize errors in determining LAF for each genotype. In all other replications only the area of the largest leaf (AL_{max}) would be obtained for n plants and leaf area per plant would be estimated by LAF determined in the first replication. The LAF should be determined for sampling date. LAI is calculated as

$$LAI4 = \sum_{i=1}^{n} b_1(LAF)(AL_{max})i/n \quad (4)$$

Costs of Measuring LAI

The mean CV associated with directly measuring the area of all leaves on each plant using a digital area meter was approximately 11% (Tables 3-3 and 3-4) and was assumed to represent the inherent variability in leaf area per plant with only a minimal contribution due to the measurement technique. Each of the other methods indirectly estimated leaf area and thus contributed additional uncertainty to the measurement of leaf area. The mean CV's associated with measurement methods II, III and IV were 16, 13 and 18%, respectively. These estimated mean CVs will vary from experiment to experiment but should maintain the same relative ranking.

The minimum number of replications of the basic sampling unit (e.g., a plant) required for $\alpha = 0.05$ and 0.01 are shown as functions of the CV and true difference of among treatments (Table 3-5). These data illustrate the value of a reduction in standard error per unit or CV. One cannot have a high probability of detecting a significant difference with any reasonable number of replications unless the CV/d ratio is 1.0 or less. Differences at least twice as large as the CV can be detected in most cases without excessive replication. For example, in order to detect a 10% difference in leaf area using $\alpha = 0.05$ test of significance, at least 73 plants must be measured if the CV is 18% (i.e., method IV). If the CV can be reduced to 11%, only 27 samples are required. Alternatively if the researcher is willing to gamble by accepting a 50% probability ($\beta = 0.50$) of obtaining a significant result then 28 and 8 samples are required for CVs of 18 and 11%, respectively (1). Generally such a high probability of making a Type II error is bad from a researcher's view because one wants to make the right decisions as frequently as possible and avoid losses of time and money on experiments with little chance of success.

In order to evaluate these four methods of measuring LAI the average costs in time (e.g. man-minutes) were estimated for each step (Table 3-6). Costs other than labor were not included in this analysis and it was assumed that the same skill level of labor was used throughout. Destructive sampling was assumed for methods I and II and nondestructive sampling for methods III and IV. Nondestructive measurements may be repeated on the same plants; however, repeated handling and measuring of the same plants may reduce their growth relative to undisturbed plants (13).

Total costs shown in Table 3-7 were calculated by multiplying the mean time required to acquire the necessary measurements on one plant (Table 3-6) by the minimum number of plants required (Table 3-5). For example, in order to detect 20% differences using method I the leaf area of at least eight plants must be measured which would require 64 minutes. The total costs for detecting 20% differences in leaf area are approximately the same for methods I, II, and III (Table 3-7) even though the numbers of plants required doubles (Table 3-5). Method IV, which has the highest CV and requires the largest number plants (Table 3-5), demands the least amount of time (Table 3-6) to estimate leaf area. One major assumption included in method IV is that fixed cost of determining LAF for 10 plants per treatment in one replication can be distributed over four replications. Thus the total costs for method IV in Table 3-7 is 15 man-minutes plus the time required to measure only the largest leaf on n plants (Table 3-5). If an

Table 3-5. Minimum number of observations per sample required to detect time differences among treatments using α = 0.05 and 0.01 tests of significance and 90% probability of success (β = 0.1).

		Test of Significance					
		α = 0.05			α = 0.01		
		True Difference, %					
Method	CV	10	20	50	10	20	50
	%	----------number of samples----------					
I	11	27	8	3	39	11	4
II	16	54	15	4	80	22	5
III	13	39	11	3	55	15	4
IV	18	73	17	4	99	27	6

Table 3-6. Relative costs for measuring leaf area of corn plants with 12 to 14 leaves per plant.

Method	Activity	Time
		man-minutes/plant
I	Measure area of all leaves	
	a. Harvest and transport	1
	b. Remove leaves	3
	c. Measure area	4
II	Measure area and weight of subsample of leaves	
	a. Harvest and transport	1
	b. Remove leaves	3
	c. Measure area	4
	d. Dry and weigh	1
	Measure weight of large sample of leaves	
	a. Harvest and transport	1
	b. Remove leaves	2
	c. Dry and weigh	1
III	Measure length and width of all leaves	6
IV	Measure length and width of all leaves in one replication	6
	Measure length and width of largest leaf in other replications	1

Table 3-7. Total costs (in time) for measuring leaf area of corn plants.

		Test of Significance					
		α = 0.05			α = 0.01		
		True Difference, %					
Method	CV	10	20	50	10	20	50
	%	----------number of minutes----------					
I†	11	216	64	24	312	88	32
II§	16	221	65	21	325	93	25
III¶	13	234	66	18	330	90	24
IV#	18	88	32	19	114	42	21

†Cost1 = n(8 min/plant)
§Cost2 = (9 min/plant) + (n-1)(4 min/plant)
¶Cost3 = n(6 min/plant)
#Cost4 = (10/r)(6 min/plant) + (n)(1 min/plant), where r is number of replications and n is number of plants on which only largest leaf is measured.

experiment has less than three replications, the cost advantages of method IV will be diminished greatly. The additional costs of determining the coefficient (i.e., b_1 in Eq. 3 and 4) which relates measurements of length and width to area are not included in these analyses. If the frequently cited coefficient of 0.75 for corn is used rather than actually determined for each treatment, the estimated leaf area may be biased (7). This bias may be acceptable if leaf shape remains constant from treatment to treatment and only relative estimates of LAI are required.

Summary

Leaf area index is an important biophysical descriptor of crop canopies. Many methods of measuring LAI have been developed which vary greatly in their accuracy, precision, bias and ease of measurement. We examined relative errors, number of plants, and labor costs in time associated with four methods of measuring leaf area of corn plants. The natural variability of leaf area per plant in a uniform field of corn exceeds 10%. Additional variability is introduced by methods which estimate

leaf area based on area to weight ratios or measurements of leaf length and width. Direct measurement of leaf area (method I) had the lowest CV, required the fewest plants, but demanded approximately the same amount of time as the leaf area/weight ratio method (method II) and the leaf length and width method (method III) to detect comparable differences. The fourth method which is based on a relationship between the area of the largest leaf and total leaf area per plant had the highest CV and required the most plants, but demanded the least time to detect 10 to 20% differences in LAI. When the true differences in LAI exceed 50%, all methods require approximately the same amount of time. The method of choice depends on the resources available, the differences to be detected, and what additional information such as leaf weight or stalk weight is also desired. Efficient and creative multistage sampling schemes can minimize experimental error and cost.

References

1. Anderson, V.L. and R.A. McLean. 1974. Design of Experiments: A Realistic Approach. Marcel Dekker, New York.

2. Cochran, W.G. 1963. Sampling Techniques. 2nd ed., pp. 154-164. Wiley, New York.

3. Cochran, W.G. and G.M. Cox. 1957. Experimental Designs. pp. 15-29. John Wiley, New York.

4. Edmeades, G.O. and T.B. Daynard. 1979. The development of plant-to-plant variability in maize at different planting densities. Can. J. Plant Sci. 59:561-576.

5. Francis, C.A., J.N. Rutger, and A.F.E. Palmer. 1969. A rapid method for plant leaf area estimation in maize (Zea mays L.). Crop Sci. 9:537-539.

6. Hanway, J.J. 1963. Growth stages of corn (Zea mays L.). Agron. J. 55:487-492.

7. Hatfield, J.L., C.D. Stanley, and R.E. Carlson. 1976. Evaluation of an electronic foliometer to measure leaf area in corn and soybeans. Agron. J. 68:434-436.

8. Kvet, J. and J.K. Marshall. 1971. Assessment of leaf area and other assimulating plant surfaces. pp. 517-574. In Z. Sestak, J. Catsky, and P.G. Jarvis (eds.) Plant Photosynthetic Production: Manual of Methods. Dr W. Junk. The Hague, Netherlands.

9. Marshall, J.K. 1968. Methods for leaf area measurement of large and small leaf samples. Photosynthetica 2:41-47.

10. Pearce, R.B., J.J. Mock, and T.B. Bailey. 1975. Rapid method for estimating leaf area per plant in maize. Crop Sci. 15:691-694.

11. Ross, J. 1981. The Radiation Regime and Architecture of Plant Stands. Dr W. Junk Publishers, The Hague, Netherlands.

12. Stickler, F.C., S. Wearden, and A.W. Pauli. 1961. Leaf area determination in grain sorghum. Agron. J. 53:187-188.

13. Stuff, R.G., H.F. Hodges, R.F. Dale, W.E. Nyquist, W.L. Nelson, and K.L. Scheeringa. 1979. Measurement of short-period corn growth. Research Bull. 961. Agr. Exp. Stn., Purdue Univ., West Lafayette, Ind.

14. Wiersma, J.V. and T.B. Bailey. 1975. Estimation of leaflet, trifoliate, and total leaf areas of soybeans. Agron. J. 67:26-30.

15. Williams, W.A., R.S. Loomis, and C.R. Lepley. 1965. Vegetative growth of corn as affected by population density. Crop Sci. 5:211-215.

4. LANDSAT SPECTRAL INPUTS TO CROP MODELS

The objective of this research was to develop methods of incorporating Landsat MSS data into crop yield models to improve the accuracy of yield estimates. Two variables were examined, spectrally estimated development stage, and a spectral estimate of stress at a field level.

Due to budget reductions, it was impossible to evaluate the effects of the development stage and stress estimate on meteorological yield models. However, it was possible to evaluate the accuracy of the development stage estimates, and to a lesser extent the stress estimates.

Two sections are included in this report, the application of a greenness index to assess crop stresses at the field level, and the evaluation of the spectral estimation of development stage of corn and soybean.

A. Use of Greenness Index to Assess Crop Stress

S.E. Hollinger

Introduction

Information obtained using Landsat satellite data has the potential to assist in identifying stressed crops. During the southern corn leaf blight outbreak in 1971, MacDonald et al. (1972) applied pattern recognition methods to multispectral scanner data to identify diseased corn fields. Although the spectral sensor was flown on an aircraft rather than a satellite, the experiment demonstrated the usefulness of using spectral data to identify three levels of leaf blight severity. Thompson and Wehmanen (1979) developed a procedure using Landsat MSS data to assess the moisture stress experienced by wheat. The stress index applied to the entire segment rather than to fields within the segment. The same authors (1980) later extended this procedure to corn and soybean segments.

The objective of this investigation is to expand the application of the Thompson-Wehmanen Green Index Number (GIN) to a field basis, and obtain an estimate of stress on each field within a segment.

Experimental Procedure

Landsat data for 32 Corn Belt segments in 1978 and 30 segments in 1979 were used to estimate the Green Index Number (GIN) for a sample of corn and soybean fields in the segments. Several spectral acquisitions were available throughout each growing season. In 1978, 693 observations were

made on 284 corn fields and 616 observations were made on 274 soybean fields. The corresponding figures for 1979 were 731 observations on 348 corn and 983 observations on 449 soybean fields.

A sample of the fields in the segments were observed periodically by USDA personnel as a part of the AgRISTARS program. In addition to observing development stages, notes were made concerning the condition of the crop. These condition reports along with the crop moisture index were used to check the accuracy of the stress estimates.

Thompson and Wehmanen (1980) calculated the stress index for corn and soybeans by determining the percent of pixels within a field or segment that exceed the bare soil greenness plus a greenness threshold (arbitrarily set equal to 20). Determination of a stress-no stress condition is a function of the stage of crop development. From planting to corn stage 3.5 (Hanway, 1971) and soybean stage R2 (Fehr and Caviness, 1977) the percent of pixels that must have a greenness greater than the above criteria increases linearly from 0 to 30%. From corn stage 3 and soybean stage R^2 to maturity, 30% or more of the pixels must have greenness that exceeds the stress criteria for an area to be non-stressed.

In applying GIN to the field level, two major modifications were made to the procedure. These modifications were elimination of screening for mixed and nonagricultural pixels, and a different method of calculating the bare soil green line. Elimination of the screening procedure was possible because we worked only with pure pixels, and the pixels were known to be a part of the field of interest and therefore were assumed to be pixels of corn or soybeans only.

Thompson and Wehmanen (1979, 1980) used the ten percent of the "agricultural" pixels with the smallest green numbers to designate the bare soil green line in the segment. For this application, the bare soil green line was determined by calculating the mean greenness of the field using an acquisition prior to June 1 (Method 1). If the first acquisition for the field was after June 1, then the bare soil green line was calculated as Thompson and Wehmanen calculated it (Method 2). In this case, the mean of the ten percent of the pixels in the field with the lowest greenness was used as the bare soil green line. June 1 is an arbitrary date and was selected because "spectral emergence" had not occurred prior to this date in most segments.

An estimate of the crop development stage is necessary since the stress index is a function of development stage. Two estimates of development stage were available for this purpose. One was the observed development stage from the AgRISTARS segment data. The other was an estimate of development stage calculated from spectral data using the Badhwar and Henderson (1981) temporal profile model.

Results and Discussion

To fully understand the accuracy of the method as applied to the field level, three aspects of the procedure must be examined. These aspects are the effects of calculation of the soil green line, the effects of using a development stage obtained from a spectral estimate, rather than the observed development stage, and finally the accuracy of stress asssessment using the field observations and Crop Moisture Index (CMI) as standards.

Soil Green Line Calculation

AgRISTARS segment 133 in Whitely County, Indiana, was used as a test segment to evaluate the effects of calculating the soil green line by Methods 1 and 2 described above. Segment 133 was selected because it is included in both the 1978 and 1979 data bases.

Plots of bare soil greenness calculated using Methods 1 and 2 are shown in Figure 4-1. The data points are connected using a spline fit and as such have no significance. The significant fact is that using Method 2, the bare soil greenness varies throughout the season beginning at a low value early in the season and rising to a greenness ranging from four to eight when the crop begins to cover the soil. This variation may be associated with the size of the fields. With Method 2 only one to five pixels are used in estimating bare soil greenness and may not give an adequate estimate of bare soil greenness.

It is interesting to note that early in the season, the mean greenness of the field (Method 1) results in a bare soil greenness greater than the bare soil greenness obtained from using the 10 percent of pixels with the lowest green number in each field (Method 2). The larger early season bare soil greenness using Method 1 is due to using all the pixels in the field rather than the small number used in Method 2.

The data plots also indicate a variation of bare soil greenness from year to year. This variation could be due to the fact that different fields were used within the same segment between the years, or because of different soil moisture conditions. It is not appropriate to make major conclusions relative to this variation but it does warrant further consideration with a larger data set.

The two methods of calculating bare soil greenness do not result in a significantly different stress index. Tables 4-1 and 4-2 show the contingency tables used to evaluate the difference between the two methods. The χ^2 statistic was tested using a two tail test with an α of 95% and 5% and 1 degree of freedom.

The conclusion from this data is that both methods of calculating bare soil greenness are the same when calculating a stress-nostress index. If the stress index were a multilevel stress index (i.e. no stress, moderate stress, moderately severe stress, severe stress) the method of calculating the bare soil greenness might become more important.

ORIGINAL PAGE IS
OF POOR QUALITY

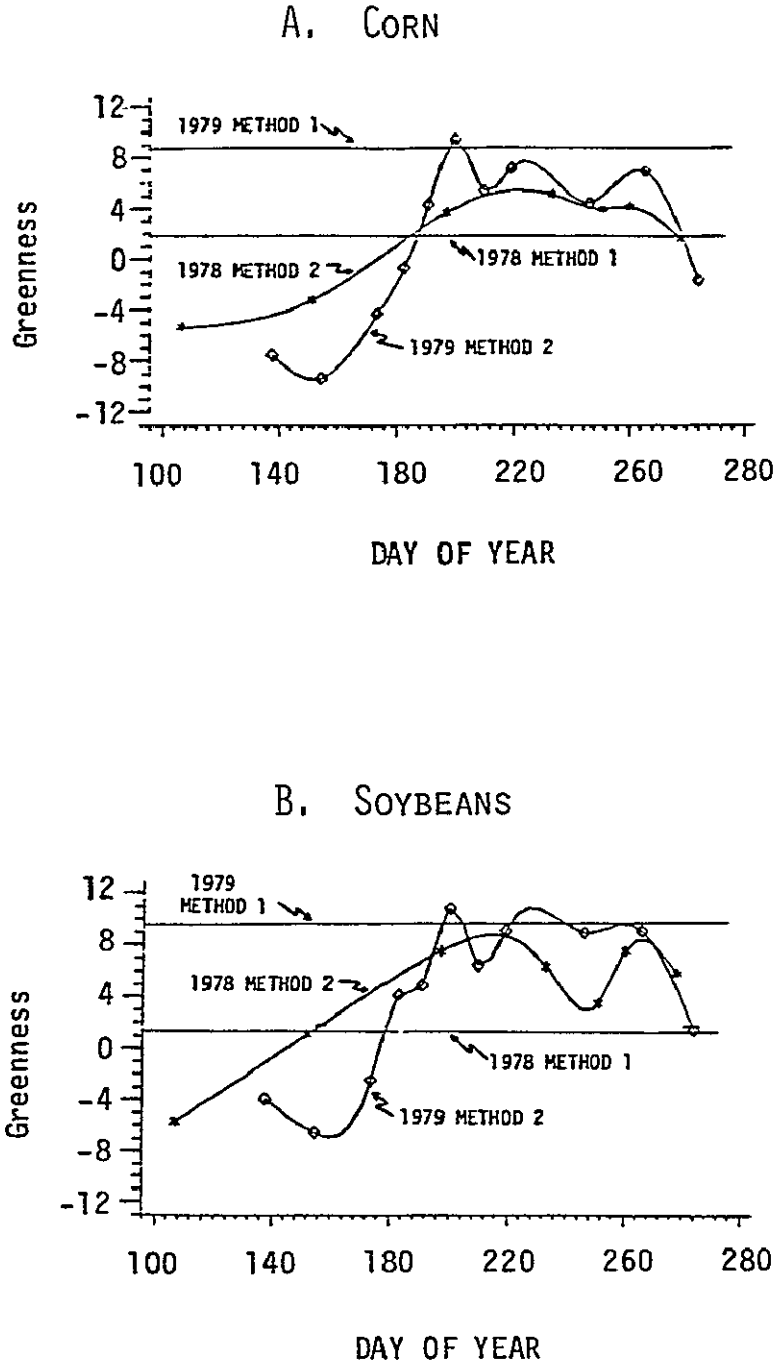

Figure 4-1. Bare soil greenness calculated using Method 1 and Method 2 for segment 133 Whitely County, Indiana.

Table 4-1. Contingency tables showing effect of two methods of calculating bare soil greenness on stress calculation for corn.

	1978			1979		
	No Stress	Stress	Total	No Stress	Stress	Total
Method 1	23 (21.5)	17 (18.5)	40	13 (17.0)	25 (21.0)	38
Method 2	20 (21.5)	20 (18.5)	40	21 (17.0)	17 (21.0)	38
Total	43	37	80	34	42	76
	$\chi^2 = 0.45$			$\chi^2 = 3.40$		

Table 4-2. Contingency tables showing effect of two methods of calculating bare soil greenness on stress calculation for soybeans.

	1978			1979		
	No Stress	Stress	Total	No Stress	Stress	Total
Method 1	13 (11)	9 (11)	22	12 (15.0)	36 (33)	48
Method 2	9 (11)	13 (11)	22	18 (15.0)	30 (33)	48
Total	22	22	44	30	66	96
	$\chi^2 = 1.45$			$\chi^2 = 1.75$		

Development Stage Calculation

The result of using spectrally derived development stages is compared to using the observed development stage in Table 4-3 for corn and in Table 4-4 for soybeans. Using a two-tailed χ^2 test with 1 degree of freedom and an α of 95% and 5% reveals that only corn in 1979 gives the same stress result for both methods of estimating development stage. The corn results in 1978 and soybeans in both years result in a different stress index when spectral data is used to estimate the development stage.

The results lead to the conclusion that the use of this spectral estimate of development stage in GIN is not accurate enough to estimate stress conditions. Therefore, a more accurate model to depict development stage from spectral data is needed. In the interim an observed development stage should be used with the GIN model.

Comparison to Crop Moisture Index (CMI)

Two comparisons to the crop moisture index were made using the 1978 crop data. One considered a stress to be present when the CMI was less than 0.0, the other when the CMI was less than -1.0. The first case is a very slight stress condition, while the second would result in a deteriorating crop condition. In the second case, some droughty fields would begin to show signs of stress.

A comparison of the predicted results to the observed CMI is presented in Table 4-5. In making the comparison between stress predicted at the field level to a stress indicated by the CMI, it was assumed that if the CMI for the crop reporting district indicated a stress on the day of the spectral acquisition, than all the fields in the segment were observed as stressed. *The data in Table 4-5 include all acquisitions for the Indiana, Illinois, and Iowa segments. The stress index showed a much higher degree of accuracy (90% vs. 60%) when a stress was assumed to occur when the CMI was less than -1.0. When this assumption was made, only the Northwest crop reporting district in Indiana had an observed stress condition, and this occured in late August. On this date, stress was determined for two corn fields and one soybean field.

The high percent of correct predictions is encouraging. However, it is difficult to make any conclusions based on this set of data because no prolonged moisture stresses occured in 1978. In addition, the CMI is based on a very large area, and the soil and moisture variations are removed from the index. Thus droughty fields may show a stress spectrally where the CMI would not indicate the stress. The reverse is also true, a field may not show a stress where the CMI indicates a stress. This is the case in the Northwest CRD of Indiana. Both segments are located in prime agricultural areas, with deep, clayey, poorly-drained soils while the majority of the district is composed of old sandy lake shores. The large area of sandy soils in this district masks the smaller areas with good soil moisture characteristics. Therefore, it is not unreasonable for a small number of fields to show a stress spectrally while the majority of the fields do not. It is encouraging that the only day that the fields in this district show a stress is when the CMI indicates a stress (CMI -1.0).

Table 4-3. Results of using spectrally derived development stage versus observed development stage to predict a stress-no stress condition using GIN for corn.

Development Stage	1978			1979		
	No Stress	Stress	Total	No Stress	Stress	Total
Spectrally	665 (640)	28 (53)	693	513 (516)	218 (215)	731
Observed	615 (640)	78 (53)	693	519 (516)	212 (215)	731
Total	1280	106	1386	1032	430	1462
	$\chi^2 = 13.746$			$\chi^2 = 0.118$		

Table 4-4. Results of using spectrally derived development stage versus observed development stage to predict a stress-no stress condition using GIN for soybeans.

Development Stage	1978			1979		
	No Stress	Stress	Total	No Stress	Stress	Total
Spectrally	513 (531)	103 (85)	616	820 (754)	163 (230)	983
Observed	549 (531)	67 (85)	616	687 (754)	296 (230)	983
Total	1062	170	1232	1507	459	1966
	$\chi^2 = 8.232$			$\chi^2 = 9.00$		

Table 4-5. Results of comparing spectral stress index with CMI.

	Crop	
	Corn	Soybeans
Stress: CMI = 0		
No. Predictions	471	419
No. Correct	290	262
Percent Correct	61.6	60.1
Stress: CMI = -1.0		
No. Predictions	471	419
No. Correct	426	383
Percent Correct	90.4	91.4

Comparing the results of the stress calculations is an incomplete test of the procedure. By definition, a stress would occur anytime the greenness of less than 30 percent of the pixels had a greenness less than 20 plus the bare soil greenness. By this definition the stress could occur because of excessively wet conditions, disease, nutrient stresses and poor stands in addition to a low moisture stress. Excessively wet conditions for short periods in Indiana, Illinois, and Iowa could result in drowning of crops in many fields with poorly drained conditions. If a major portion of any field were experiencing this problem, the spectral data would indicate a stress, while the CMI would show adequate soil moisture conditions and no stress. Likewise, the CMI gives no indication of disease or nutrient stresses. Unfortunately, the periodic observations in 1978 do not give adequate information to check for these other stresses.

Comparison of Spectral Stress With Periodic Observation

In making the comparisons of spectral stress with the AgRISTARS periodic observations, a segment was found that had adequate notes describing field conditions. A judgement was then made as to whether the field should be classified as stressed or non-stressed for each day a spectral stress estimate was available. A field was classified as stressed if the observer described the field as poor or having a thin stand.

The results for AgRISTARS segment 133 in Whitely County, Indiana, are shown in Table 4-6 as a contingency table. The χ^2 test indicates that there is a difference between the observed stress and the predicted stress. The χ^2 statistic was tested with an $\alpha = 5\%$ with 1 degree of freedom.

Table 4-6. Comparison between spectrally predicted and observed stress.

	Corn		
	Stress	No Stress	Total
Predicted	25 (15.5)	13 (22.5)	38
Actual	6 (15.5)	32 (22.5)	38
Total	31	45	76

$\chi^2 = 19.667$

	Soybean		
	Stress	No Stress	Total
Predicted	46 (25.0)	12 (33.0)	58
Actual	4 (25.0)	54 (33.0)	58
Total	50	66	116

$\chi^2 = 62.007$

Firm conclusions cannot be drawn from these results because of the small sample size and because the fields did not exhibit moisture stress during 1979. Also, it is difficult to observe field problems due to the causes mentioned above from ground level. These observations at ground level are possible only by an extensive walking of the fields and this was not practical in taking the periodic observations. Therefore some stresses may actually be present but not noted. Additional tests need to be made using other years when moisture and other environmental stresses were experienced.

Summary

The Thompson-Wehmanen GIN procedure has been applied to Landsat spectral data at the field level. Although no firm conclusions can be drawn at this time due to the limited ground truth data bases, the procedure does not seem to be overly sensitive to the method of calculating bare soil greenness. It is sensitive to errors in estimating development stages and therefore, observed development stages should be used to calculate the stress index if the data is available.

Before any major conclusions can be made concerning the validity of applying the procedure to a field level, tests should be run using Landsat spectral data collected during a year when soil moisture was limiting. Such a year would be 1980. These tests are currently being run.

References

1. Badhwar, G.D. and K.E. Henderson. 1981. Estimating Development Stages of Corn from Spectral Data: An Initial Model. Agron. J. 73:748-766.

2. Fehr, W.R. and C.E. Caviness. 1977. Stages of Soybean Development. Iowa State University Coop. Ext. Ser. Special Report 80. CODEN:IWSRBC (80) 1-12 (1977).

3. Hanway, J.J. 1971. How a Corn Plant Develops. Iowa State Univ. Coop. Ext. Ser. Special Report 48. pp. 17.

4. Kauth, R.J. and G.S. Thomas. 1976. The Tasselled CAP - A Graphic Description of the Spectral-Temporal Development of Agricultural Crops as Seen by Landsat. Proc. Symp. on Machine Processing of Remotely Sensed Data, Purdue University, West Lafayette, IN. IEEE Cat. 76, CH11032-1-MPRSD.

5. MacDonald, R.B., M.E. Bauer, R.D. Allen, J.W. Clifton, J.D. Erickson, and D.A. Landgrebe. 1972. Results of the 1971 Corn Blight Watch Experiment. Proc. Eighth Int'l. Symp. on Remote Sensing of Environment, pp. 157-190, Ann Arbor, Michigan, Oct. 2-6, 1972.

6. Palmer, W.C. 1968. Keeping Track of Crop Moisture Conditions Nationwide, The New Crop Moisture Index, Weatherwise, 21:156-161.

7. Thompson, D.R. and O.A. Wehmanen. 1979. Using Landsat Digital Data to Detect Moisture Stress. Photogrammetric Engineering and Remote Sensing, 45(2):201-207.

8. Thompson, D.R. and O.A. Wehmanen. 1980. Using Landsat Digital Data to Detect Moisture Stress in Corn-Soybean Growing Regions. Photogrammetric Engineering and Remote Sensing, 46(8):1087-1093.

B. Evaluation of Landsat MSS Data for Estimating Corn and Soybean Development Stages

S.E. Hollinger

Introduction

Before crop yields can be accurately estimated using meteorological models, an accurate estimate of development stage must be available. This is important because short term weather stresses can have a profound impact on yields if they occur at a critical stage of crop development (i.e. for corn at silking). Thus it is necessary to know the time of year these critical development stages occur so the weather impacts on yields can be accurately evaluated.

A second reason for estimating development stage of crops is the identification of crops in a scene. In classifying crops, analysts need to know the development stage of the various crops in the scene.

Meteorological models and remote sensing techniques can be used to estimate crop development stage. The application of meteorological models to this task is routinely used to estimate yields. These models, however, require ground based knowledge of the date of planting and weather data. In the United States, estimates of the planting date can be obtained at the crop reporting district (CRD) level. Estimates of the variation of the planting date within a CRD, and during the season the variation of development stages within the CRD can be estimated with these data. However, more accurate estimates of yields could be obtained if this information were available on a county or subcounty size area. The information on this small an area is not available since in many cases a county may not have a planting date estimate. A second drawback is that the weather stations are not dense enough to accurately determine the mean or variation of weather within the CRD/county. Therefore, there are two sources of error in the meteorological estimates. In foreign countries these data are often not available at all.

Estimation of development stages using remote sensing could help alleviate the problems associated with the meteorological estimates. Since remotely sensed spectral data provides a picture of the land surface, using remote sensing will give an estimate of the mean development stage for areas that are county size or smaller and an estimate of the variation within the areas.

Badhwar and Henderson (1981) have developed a method of estimating development stages using spectral data and a "greenness" profile. The greenness profile is obtained by fitting a nonlinear curve through daily greenness values of a field throughout the season. The greenness referred to here is the green component of the Kauth-Thomas tasseled cap

transformation (Kauth and Thomas, 1976). The greenness profile shows a characteristic green up stage, a plateau of greenness and then a senesence stage where greenness returns to the greenness of the bare soil. The area remaining under the curve on any day of the season is linearly related to the stage of development. This method has been tested on plot size areas as well as on selected AgRISTARS segments.

The objective of this paper is to use the method developed by Badhwar and Henderson and apply it to a greater number of segments in a semi-operational mode. By semi-operational we mean applying the method to segments where little or no screening of the data has occurred for clouds or other noise in the scene.

Methods

The Badhwar-Henderson (1981) model was used to determine the stage of development for each corn and soybean field from selected segments in 1978 and 1979. Selection of the segments was based on the availability of ground truth and spectral data. All fields larger than two pixels were included in the study.

A total of 284 corn and 274 soybean fields from 32 segments in 1978 were used in this study. In the analysis, the states were divided into three regions: Corn Belt (Iowa, Illinois, Indiana, Missouri), South (Kentucky, Mississippi), and North (Michigan, Minnesota, South Dakota). In 1979, 348 corn and 449 soybean fields from 30 segments were used. The segments were located in four Corn Belt states (Iowa, Illinois, Indiana, Nebraska), five Southern states (Alabama, Arkansas, Louisiana, Mississippi) and five Eastern states (Delaware, Georgia, Maryland, North Carolina, South Carolina).

Ground observation data were collected periodically throughout the growing season by USDA personnel as a part of the AgRISTARS project. Development stages were observed on or within one day from the date of each satellite pass. The development stage classification scheme for both years is presented in Table 4-7 for corn and Table 4-8 for soybeans.

Evaluation of the accuracy of the predicted development stages was accomplished by regressing the predicted development stage against the actual development stage and examining the coefficient of determination (r^2), and the slope and intercept of the regression. Tests of whether the slope equals 1.0 and the intercept equals 0.0 were made using a two-tailed test with $\alpha = 0.05$. The error or difference between the predicted and observed development stages was examined to see if it had a mean equal to zero. Mean errors equal to zero indicate no bias in the predicted development stages. Additionally the standard error (SE) of the errors was evaluated to determine the precision of the estimates. Smaller SE's indicate more precision in the development stage estimates.

The above analyses were conducted on the total segments within each year, by regions of the country and by state to determine the universality of the procedure.

Table 4-7. Development stage schemes used to classify corn development in 1978 and 1979.

Stage of Development		
1978	1979	Description of Development
0.0	1.0	Planting
0.0	1.5	Planting complete not emerged
0.0	2.0	Emerged
0.5	-	2 leaves fully emerged
1.0	-	4 leaves fully emerged
1.5	3.0	6 leaves fully emerged
2.0	-	8 leaves fully emerged
2.5	-	10 leaves fully emerged
3.0	3.5	12 leaves fully emerged
3.5	-	14 leaves fully emerged
4.0	-	16 leaves fully emerged
5.0	4.0	Tassels emerged, silks visible, pollen beginning to shed
-	4.2	Silking and pollen shed 80% complete
6.0	5.0	Kernels at blister stage
7.0	-	Dough stage
8.0	5.5	Beginning dent stage
9.0	5.8	Full dent stage
10.0	6.0	Physiologic maturity
11.0	7.0	Harvest

Results

A total of 756 corn and 691 soybean development stage predictions were evaluated from the 1978 data. Using the 1979 data, 822 corn and 1125 soybean development stage predictions were evaluated. These data represent less than one-half the spectral data available for use. The data not used were screened out because ground observations were not available to evaluate the predicted development stages, or because the curve fitting technique could not converge on a solution. Failure to converge on a solution was due to greenness values in some areas failing to follow the normal "green up" and "green down" of the fields within the segments.

The results of the analysis of the data for both corn and soybeans are presented in Table 4-9. In both 1978 and 1979 a significant positive bias was found in the corn development stage estimations. The data are the combinations of all fields from all the areas. Corn and soybean development stages were calculated using a linear relationship to the area remaining under the greenness profile curve.

Table 4-8. Development stage schemes used to classify soybean development in 1978 and 1979.

Stage of Development			
1978		1979	Description of Development
numerical/Fehr-Caviness			
0	V0	1.0	Pre-emergence, crop planted
		1.5	Planting complete but not emerged
0.25	VE	2.0	50% of plants have cotyledons above soil surface
0.50	VC		Unifoliolate leaves unrolled so that leaf edges not touching
0.75	V1		Fully developed leaves at unifoliolate node
1.00	V2		Fully developed trifoliolate leaf at node above the unifoliolate nodes
	V3		Three nodes on the main stem with fully developed leaves
2.00	V4	3.0	Four nodes on main stem with fully developed leaves
4.00	R1	3.4	Beginning bloom
5.00	R2		Full bloom
6.00	R3	3.6	Beginning pod
7.00	R4	4.0	Full pod, pods about 2 cm long on top nodes of main stem
		4.2	Full pod on 80% of plant
8.00	R5	4.5	Beginning seed
9.00	R6	5.0	Full seed
10.00	R7		Beginning maturity
		5.8	20% of plants with pods at mature color
11.00	R8	6.0	Full maturity
12.00	R9	7.0	Harvest and post harvest

$$S = \gamma_0 + \gamma_1 A \qquad (1)$$

where S is the calculated development stage, A is the area remaining under the greenness curve on the day of interest, and γ_0 and γ_1 are constants. The constants used to calculate the development stages are given in Table 4-10. The soybean development stages show a significant positive bias in their estimate in 1979 and a negative bias in 1978.

Table 4-9. Evaluation of estimated development stages for all regions combined in 1978 and 1979 for both corn and soybean.

Year	N	Bias	RMSE	Regression Analysis		
				r^2	β_0	β_1
		Corn				
1978	756	0.28*	1.11	0.815	1.04*	0.80**
1979	822	0.13*	0.72	0.670	0.69*	0.81**
		Soybean				
1978	691	-1.19*	1.49	0.759	0.78*	1.08**
1979	1125	0.77*	0.68	0.672	-0.78*	1.00

* Significantly different from zero at $\alpha = 0.05$, two-tailed test.
** Significantly different from 1.0 at $\alpha = 0.05$, two-tailed test.

Table 4-10. Coefficients used to relate the area remaining under the greenness profile curve to development stage.

Year	Corn		Soybeans	
	γ_0	γ_1	γ_0	γ_1
1978	11.0	-10.0	9.0	-8.0
1979	6.5	-3.9	6.0	-2.9

When the same data are examined on a regional basis (Table 4-11), a bias in the corn development stage estimates is found in each of the regions except the southern region in 1978. The bias is positive in the corn belt both years and in the northern region in 1978. The eastern region shows a negative bias in 1979. Estimates of the soybean crop are negatively biased in 1978 in all regions and positively biased in 1979 in all regions.

Table 4-11. Analysis of estimated development stage on a regional level for corn and soybean in 1978 and 1979.

Region	Year	N	Bias	RMSE	γ^2	β_0	β_1
			Corn				
Corn belt	1978	627	0.18*	1.08	0.832	1.16*	0.79**
North	1978	89	0.99*	1.11	0.695	0.64	0.75**
South	1978	40	0.24	0.82	0.857	-1.04	1.10
Corn belt	1979	637	0.24*	0.51	0.804	0.58*	0.80**
East	1979	185	-0.26*	1.06	0.357	1.60*	0.70**
			Soybeans				
Corn belt	1978	580	-1.30*	1.48	0.771	0.85*	1.08**
North	1978	40	-0.46	1.60	0.556	0.39	1.02
South	1978	71	-0.67*	1.27	0.774	0.62	1.01
Corn belt	1979	618	0.61*	0.51	0.818	-1.11*	1.12**
East	1979	201	1.41*	0.75	0.213	0.96*	0.47**
South	1979	306	0.66*	0.57	0.772	-0.99*	1.07**

* Significantly different from zero with $\alpha = 0.05$, two-tailed test.
** Significantly different from 1.0 with $\alpha = 0.05$, two-tailed test.

The bias in the estimates can be removed using the regression coefficients in Table 4-9 and equations 2 and 3.

$$\gamma_0^1 = \beta_0 + \beta_1\gamma_0 \quad (2)$$

$$\gamma_1^1 = \beta_1\gamma_1 \quad (3)$$

New development stage estimates can be calculated by substituting γ_0^1 and γ_1^1 into equation 1. The new coefficients for all areas combined are given in Table 4-12, and the result of the analysis of the revised development stage estimates in Table 4-13. There is no bias in the revised estimates. Regression analysis shows a one to one relationship between the predicted and observed development stages in both years for both crops. Even though all bias is removed from the combined data, it is obvious from the regional data that there will still be a bias in these data. Thus it is necessary to calculate coefficients for equation 1 for each region and state. Changing the coefficients for equation 1 did not affect the root mean square error. Thus the results are not any more precise; however, they are more accurate.

Table 4-12. Revised coefficients for calculating development stage.

Year	Corn		Soybean	
	γ_0^1	γ_1^1	γ_0^1	γ_1^1
1978	9.8	-8.0	10.5	-8.6
1979	6.0	-3.2	5.2	-2.9

Table 4-13. Analysis of development stage estimates calculated from revised coefficients.

Year	N	Bias	RMSE	Regression Analysis		
				γ^2	β_0	β_1
			Corn			
1978	756	-0.03	1.11	0.814	0.04	1.00
1979	822	0.03	0.72	0.670	0.02	0.99
			Soybean			
1978	691	0.04	1.49	0.758	-0.04	1.00
1979	1125	-0.03	0.68	0.672	0.02	1.00

Coefficients that result in an unbiased estimate at the state and regional level are presented in Table 4-14 for 1978 data and Table 4-15 for 1979 data. A third variable, $\rho_s(t_0)$, is also listed in Tables 4-14 and 4-15. This variable represents the stage of development that must be attained before the crop becomes spectrally separable from the soil. It is encouraging that in both years, the development stage when the crop becomes differentiated from the soil background is descriptively the same even though the development stage scales used are significantly different. In most cases, this occurs when 4-8 leaves are fully emerged in corn and when 2-4 nodes are present in soybeans. Exceptions to this are the 1978 Illinois and Michigan soybeans fields, the 1979 Mississippi soybean fields, and the 1979 Georgia and South Carolina corn fields. Note also that the Nebraska

Table 4-14. Coefficients that provide an unbiased estimate of development stage on regional and state level in 1978.

Region/ State	Corn			Soybean		
	γ_0^1	γ_1^1	$\rho_s(t_0)$	γ_0^1	γ_1^1	$\rho_s(t_0)$
Corn belt	9.9	-7.9	2.0	10.6	-8.6	2.0
Iowa	10.1	-8.2	1.9	11.4	9.7	1.7
Illinois	10.1	-7.6	2.5	11.1	6.1	5.0
Indiana	10.0	-8.1	1.9	10.6	-9.0	1.6
Missouri	8.9	7.4	1.5	9.8	9.7	0.1
North	8.9	7.5	1.4	9.6	-8.2	1.4
Michigan	9.2	8.8	0.4	12.1	-7.2	4.9
Minnesota	7.5	5.6	1.9	9.5	-8.3	1.2
South Dakota	9.6	8.0	1.6	8.6	-7.4	1.2
South	11.1	-11.0	0.1	9.7	-8.1	1.6
Kentucky	11.1	-11.0	0.1	14.1	-12.4	1.7
Mississippi	-	-	-	7.8	-5.4	2.4

and North Carolina soybean coefficients in 1979 are erroneous. In the Nebraska case, the development stage is a constant 2.8. In North Carolina, the crop is estimated to be at full pod stage when the crop is separable from the soil then the development stage moves toward emergence rather than maturity. These errors are a result of greenness profiles in the states for these crops. In these cases, the greenness profile shows a green up only with no plateau or green down portion in the profile. In cases such as this, the Badhwar-Henderson method does not apply and procedures should be developed to screen these data out and flag the segments and fields.

Discussion

The results of estimating development stage with the Badhwar-Henderson technique in this study are not as good as the results obtained by Badhwar and Henderson (1981). To a certain extent this is to be expected because this study was designed to use the method with a minimum of human screening of the data. All available segments with an adequate number of Landsat MSS acquisitions without clouds were used. Also all acquisitions from the segments that were registered within two pixels were used. We also included some smaller fields that were not in the original Badhwar-Henderson study.

Table 4-15. Coefficients that provide an unbiased estimate of development stage on regional and state level in 1979.

Region/ State	Corn			Soybean		
	γ_0^1	γ_1^1	$\rho_s(t_0)$	γ_0^1	γ_1^1	$\rho_s(t_0)$
Corn belt	5.8	-3.1	2.7	5.6	-3.2	2.4
Iowa	5.9	-3.3	2.6	5.5	-3.3	2.2
Illinois	5.8	-2.8	3.0	5.9	-3.0	2.9
Indiana	5.6	-2.9	2.7	5.6	-3.1	2.5
Nebraska	6.6	-4.5	2.1	2.8*	0.0*	2.8
East	6.2	-2.2	4.0	3.8	-1.4	2.4
Delaware	6.2	-3.2	3.0	4.1	-1.6	2.5
Georgia	6.9	-2.9	4.0	3.8	-1.7	2.1
Maryland	5.6	-2.6	3.0	4.4	-2.1	2.3
North Carolina	5.6	-2.0	3.6	3.1*	1.1*	4.2
South Carolina	7.9	-3.2	4.7	-	-	-
South	-	-	-	5.4	-3.1	2.3
Alabama	-	-	-	5.3	-2.5	2.8
Arkansas	-	-	-	5.0	-2.6	2.4
Louisiana	-	-	-	5.2	-3.2	2.0
Mississippi	-	-	-	5.4	-1.3	4.1
Texas	-	-	-	5.5	-2.8	2.7

* Atypical greenness profile.

The results of this study show the validity of the technique. The descriptive stage of development when the crop became spectrally separable from the soil are the same regardless of the numerical scale used to describe the development stage. The assumption by Badhwar and Henderson that the crop becomes spectrally visible when four leaves are fully emerged in corn is not always valid but varies by region and state. The variation of the stage where the crop becomes spectrally visible would be a function of the soil background greenness, and the amount of green vegetation that surrounds the fields, such as forest around small fields. The green vegetation surrounding the field would be a factor due to the atmospheric scattering of the radiation reflected from the scene.

Although some of the coefficients are greater than the numerical value assigned to the harvested field, the coefficients could be adjusted by substracting a constant so that the maximum stage would be close to maturity. The same constant would need to be substracted off each

coefficient for a given area so that the stage, when spectral emergence would occur, would be the same. The important value is the stage where the crop becomes spectrally visible ($\rho_0(t_0)$).

In the two years of data, the stage when the crops became spectrally visible in Iowa, Illinois, and Indiana was about the same. Therefore, it appears that this value may be relatively constant from year to year within a given area. If this is so it would mean that once the stage when the crop becomes spectrally visible is determined for an area, the method could be used with a considerable degree of accuracy.

In conclusion, the Badhwar-Henderson method of estimating development stages of corn and soybeans appears to be applicable to a given region providing the stage when the crop becomes spectrally visible is known and assuming the crop has been accurately identified. A major problem that limits its use for real time crop inventory analysis is that it requires a full season's data before the developed stages can be determined. This deficiency of the method limits its usefulness in real time evaluation of crop yields. Therefore, a method needs to be developed to use this technique for early season detection of crop development stages.

References

1. Badhwar, G.D. and K.E. Henderson. 1981. Estimating development stages of corn from spectral data: an initial model. Agron. J. 73:748-766.

2. Kauth, R.J. and G.S. Thomas. 1976. The tasseled cap - a graphic description of the spectral-temporal development of agricultural crops as seen by Landsat. Proc. Symp. on Machine Processing of Remotely Sensed Data, Purdue University, West Lafayette, IN. IEEE Cat. 76, CH11032-1-MPRSD.

5. FIELD RESEARCH--EXPERIMENT DESIGN, DATA ACQUISITION AND PREPROCESSING

L.L. Biehl

Introduction

This section describes the results of work conducted under Task 4, Field Research - Experiment Design, Data Acquisition, and Preprocessing. The overall objectives of this task are to (1) plan, acquire and preprocess the field research data required to support the crop identification, development stage estimation, and condition assessment objectives of corn/soybean scene radiation research, (2) manage and distribute the field data required to support all scene radiation groups, i.e., corn/soybeans and small grains, and (3) train and coordinate researchers in the use of instruments and data acquisition procedures. The data are being used for analysis and modeling to obtain a quantitative understanding of the radiation characteristics of crops and their soil backgrounds and to assess the capability of current, planned and future satellite sensors to capture available, useful spectral information.

Based on the previous, proven experience since 1974, there were two kinds of test sites for 1982 - controlled experimental plot sites and commercial field sites. The data from experiments in commercial field test sites provide a measure of the natural variation in the temporal-spectral characteristics of the cover type. The data from experiments in controlled plots enable more complete understanding and interpretation of the spectra. The test sites are summarized in Table 5-1. The emphasis of this report is on the corn and soybean experiments conducted by LARS.

Experiment Objectives

The experiments for 1982 at the Purdue University Agronomy Farm include some that have been continued from previous years to sample different seasonal weather patterns and new experiments to obtain measurements related to canopy geometry and view angle - sun angle.

The following overall objectives were selected for the experiments:

- To determine relationship of crop canopy variables (development stage, LAI, biomass, soil background, etc.) to reflectance and radiant temperature of corn and soybeans.

- To determine and model the relationship of leaf area index and solar radiation interception to spectral reflectance of corn and soybean canopies.

- To determine effects of varying agronomic practices (planting date, row spacing, plant population, cultivar, soil type) on spectral response of corn, soybeans, sorghum, and sunflowers.

Table 5-1. Summary of 1982 field research test sites and their respective crops.

Location	Major Crop(s)
Commercial Fields	
Cass County, N. Dakota	Spring wheat, barley, sunflower, soybean
Agriculture Experiment Station	
W. Lafayette, Indiana	Corn, soybean, sorghum, sunflower, soil residue
Lawrence, Kansas	Corn, soybean, wheat
Manhattan, Kansas	Small grains
St. Paul, Minnesota	Corn, soybean
Sandhills, Nebraska	Corn, soybean
Corvallis, Oregon	Small grains
Brookings, S. Dakota	Small grains
College Station, Texas	Rice, sorghum
CIMMYT, Mexico	Wheat

- To support the development of corn and soybean yield models which use spectral response as a function of crop development stage as an input.

- To determine the dynamic nature of spectral reflectance of canopies at many sun and view angles as a function of crop development stage.

- To determine effects of crop residue and tillage practices on early season crop reflectance.

Experiment Descriptions and Data Acquisition

Several experiments were developed at the Purdue Agronomy Farm to accomplish the objectives stated above. The experiments included treatments of cultural practices and sun-view angle/canopy geometry (Table 5-2). Spectral and agronomic measurements (Table 5-3) were collected on every day that solar illumination conditions were favorable, i.e. no clouds over or in the vicinity of the sun.

The spectral measurements of the experiments were made by the Exotech 100 (Landsat MSS bands) and Barnes 12-1000 multiband (Landsat TM bands) radiometer field systems. The system also includes a 35 mm camera, sighted to view the same area as the spectral sensors (Figure 5-1).

Table 5-2. Summary of the 1982 field research experiments at the Purdue Agronomy Farm.

Experiments and Treatments
Corn Cultural Practices
3 Planting dates (May 14; June 8, 24)
4 Populations (25, 50, 75, 100 thousand plants/ha)
2 Soil types (Chalmers-darker, Fincastle-lighter)
2 Replications
Soybean Cultural Practices
4 Planting dates (May 11, 15; June 14, 24)
3 Row widths (38, 76, 114 cm)
2 Soil types (Chalmers-darker, Fincastle-lighter)
2 Replications
Sorghum Cultural Practices
3 Planting dates (May 19; June 9, 24)
2 Hybrids (NK300-semi-dwarf, BR64-dwarf)
2 Replications
Sunflower Cultural Practices
3 Planting dates (May 19; June 8, 24)
2 Populations (37.5, 75 thousand plants/ha)
2 Replications
Solar Radiation Interception
Corn: 2 Planting dates (May 14, June 24)
2 Plant populations (50, 100 thousand plants/ha)
2 Replications
Soybeans: 4 Planting dates (May 14, 25; June 14, 24)
3 Row spacings (38, 70, 114 cm)
2 Replications
Corn Sun-View Angle
View zenith angles (0, 7, 15, 22, 30, 45, 60, 70 degrees)
View azimuth angles (0, 45, 90, 135, 180, 225, 270, 315 degrees)
Solar zenith (20-70 degrees)
Solar azimuth (90-270 degrees)
Soil Residue
3 Crops (corn, soybean, wheat)
3 Tillage systems (moldboard plow, chisel plow, no-till)
4 Crop rotations (continuous corn, continuous soybean, corn-soybean, corn-soybean-wheat)
2 Replications

ORIGINAL PAGE IS
OF POOR QUALITY

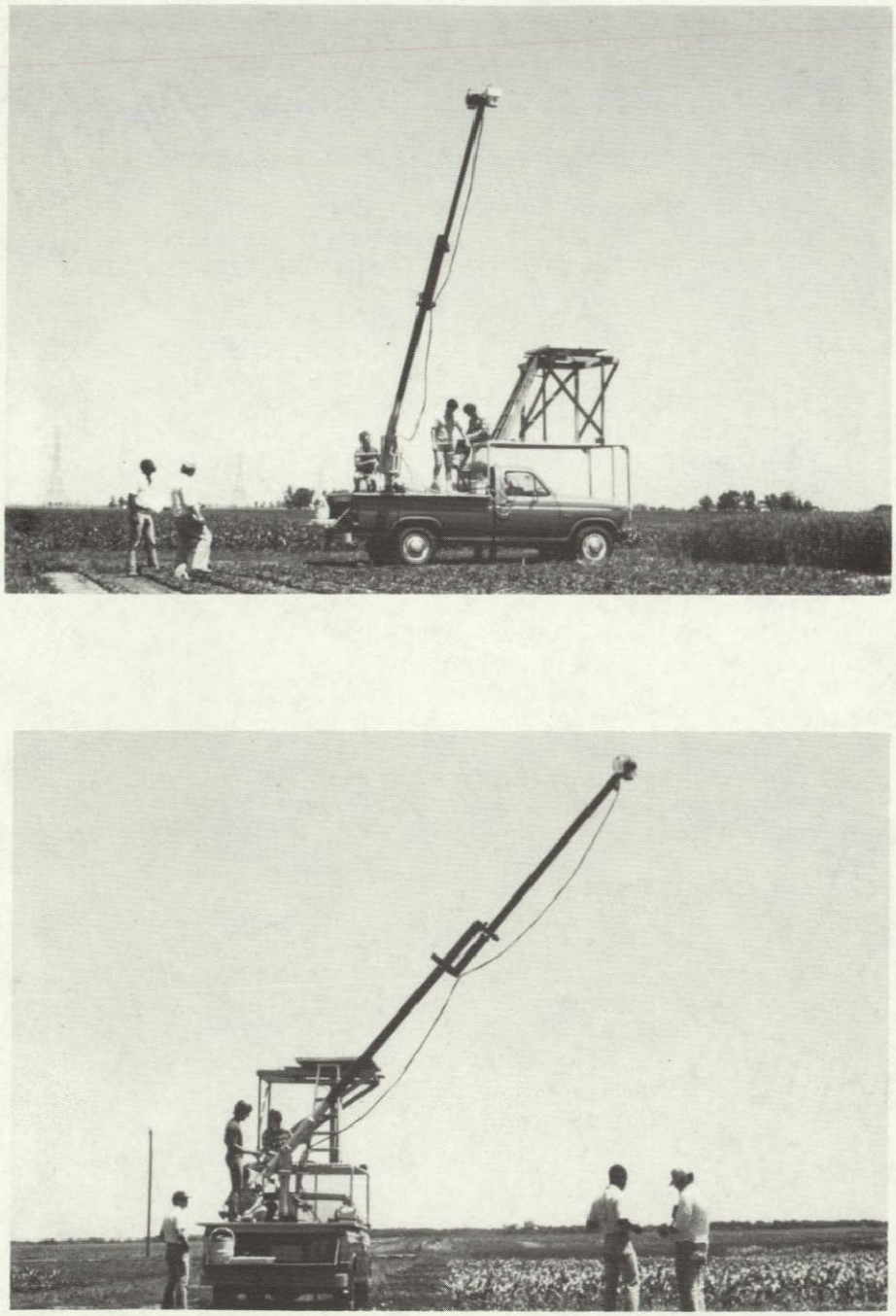

Figure 5-1. Multispectral data acquisition system. The system includes two radiometers (MSS and TM) bands, camera, calibration panel, data logger, and aerial boom. The sensors are normally operated at height of 8 meters and measurements are made of approximately 50 plots per hour.

To obtain data which can be readily compared, the instrument systems are operated following defined, established procedures. The instruments are operated from aerial towers at seven to ten meters above the target to minimize any row effect and shadowing of skylight. Care is taken to ensure that the field of view of the instrument includes only the desired subject. The routine data taking mode of the instrument is straight down for determination of bidirectional reflectance factor. Measurements of the painted barium sulfate reflectance reference panel are made at 15-20 minute intervals. Two to six measurements of each plot are typically made by moving the sensor so that a new scene within the plot fills the field of view.

Spectral measurements, along with agronomic and meteorological data, were acquired on each day that weather conditions permitted (Table 5-4). During 1982 over 19000 spectra of corn, soybeans, sorghum, sunflowers, and soil were acquired on 30 days. Crop maturity stages from seedling to senescence are represented in these data.

A specially designed tower and boom were fabricated for the sun-view experiment. The tower and boom were used for all sun-view angle data collected after August 1 (before August 1, a truck-mounted aerial boom was used). The apparatus includes a 10 meter tower, a 3 meter boom to mount the Barnes 12-1000 radiometer, and a platform for a reflectance reference panel. The radiometer can be positioned for a selected view azimuth and rotated to different viewing zenith angles, including the sky. A complete hemisphere of data (8 zenith and 8 azimuth angles) can be obtained within 6 minutes. This experiment is fully described in section 6.

Laboratory Measurements

The painted barium sulfate reflectance reference panels used by the several truck-mounted systems were prepared and calibrated by Purdue to support the acquisition of comparable data from site to site. During this past year, 22 panels were prepared and calibrated. The reference panels were calibrated with a bidirectional reflectance factor reflectometer (4). Reflectance measurements of the panels were obtained for illumination zenith angles from 10 to 55 degrees. The reference panels and their calibrations were distributed to several field research teams including University of Nebraska; Kansas State University; Oregon State University; South Dakota State University; University of Kansas; University of Minnesota; Rutgers University; North Dakota State University; NASA/JSC; NASA/ERL; and USDA-ARS stations at Phoenix, Arizona; Bushland, Texas; and Lubbock, Texas.

Data Preprocessing

The spectral, agronomic, and meteorological data are calibrated and preprocessed into comparable formats for easy access and analysis by researchers. The spectrometer/radiometer data are preprocessed into LARSPEC format (2) and the aircraft scanner data are preprocessed into LARSYS format.

Table 5-4. Summary of 1982 data acquisition by field radiometer systems at the Purdue Agronomy Farm.

Measurement Date	Experiment: Cultural Practices: Corn	Cultural Practices: Soybeans	Cultural Practices: Sorghum	Cultural Practices: Sunflowers	SRI: Corn	SRI: Soybeans	Soil Residue	Sun-View Angle
week of	number of data sets acquired during week†							
April 11	-	-	-	-	-	-	1	-
May 9	-	-	-	-	-	-	1	-
30	-	-	-	-	-	-	1	-
June 6	H	H	-	-	3	2	1	-
13	M	1	-	2	4	4	-	15
20	1	1	S	1	4	5	-	24
27	-	-	-	-	-	-	-	-
July 4	S	S	-	-	1	1	-	5
11	1	2	1	1	3	2	-	11
18	2	1	2	2	2	1	-	17
25	H	H	1	-	2	2	-	11
Aug 1	-	-	-	-	-	-	-	-
8	1	1	2	2	4	5	-	41
15	1	M	1	1	2	2	-	18
22	-	H	-	-	1	1	-	7
29	1	2	2	2	4	5	-	24
Sept 5	-	-	-	-	-	-	-	-
12	-	-	-	-	-	-	-	-
19	-	-	-	-	-	-	-	-
26	1	1	1	-	2	1	-	-
Oct 24	H	H	-	-	1	1	-	9

†H = half of treatments, M = more than half of treatments, S = less than half of treatments.

During this year preprocessing of the 1980 FSS (helicopter spectrometer) data was completed. Also, preprocessing of all the 1981 spectral data except for the FSS data were completed early in the year. Preprocessing of the 1982 Exotech 100 and Barnes 12-1000 data collected at the Purdue Agronomy farm and the 1981 FSS data is nearly complete. The preprocessing accomplishments for 1982 and the present status are summarized in Table 5-5.

Table 5-5. Summary status of field research data preprocessing accomplishments during 1982 (1980-82 crop years).

Instrument/Data Type	Completed	In Processing
Aircraft Multispectral Scanner (dates/flightlines)	3/7	-
Helicopter Mounted Field Spectroradiometer (dates/observations)		
Field Averages	19/1,476	17/
Individual scans	19/30,432	17/
Helicopter Mounted Multiband Radiometer (dates/observations)		7/
Truck Mounted Field Multiband Radiometer (dates/observations)		
Purdue/LARS Exotech 100	19/3,691	27/
Purdue/LARS Barnes 12-1000 systems	10/4,781	49/
Laboratory Spectroradiometer (dates/observations)		
Purdue/LARS Exotech 20C	5/418	-

Data Library and Distribution

The development of the field research data library at Purdue/LARS was initiated in the fall of 1974 by NASA Johnson Space Center as a part of the Large Area Crop Inventory Experiment (3). The purpose of the data base is to provide fully annotated and calibrated multitemporal sets of spectral, agronomic, and meteorological data for agricultural remote sensing research. Spectral, agronomic, and meteorological measurements were made primarily over wheat for three years. In 1978 and 1979 the data base was expanded to include data collected for corn and soybean experiments in Indiana, Iowa, and Nebraska, as well as from a major U.S. soils experiment. In 1980 the library was expanded again to include data collected for spring wheat, barley, sunflowers, and soybeans in North Dakota, and cotton, rice, and soybeans in Texas.

Milestones achieved during the past year have been: inclusion of most 1981 crop year data and distribution of data to researchers at 27 locations.

The data have been collected over several test sites and crops as illustrated in Table 5-6. The test sites are of two types, controlled experimental plots and commercial fields. The instruments used to collect the spectral data are listed in Table 5-7. The spectroradiometer data are processed into comparable units, bidirectional reflectance factor, in order to make meaningful comparisons of the data acquired by the different sensors at different times and locations (4). The multispectral scanner data are approximately linearly related to scene radiance and the information is available for the researcher to calibrate the scanner data to in-band bidirectional reflectance factor if desired.

The Field Research Data Library Catalog summarizes the data available. The catalog includes a separate volume for each crop year during which data were collected. In the past twelve months, seven aircraft scanner runs and more than 40,000 additional spectrometer/multiband radiometer observations have been made available to researchers. The data includes spectral observations of corn, soybeans, and wheat. A summary of the spectral data in the library is given in Table 5-8. Listed in Table 5-9 are 27 institutions which have received or accessed field research data during the past year. A report summarizing the scene radiation data base was published in July (4).

Hardware Development

Hardware acquired or developed during the past year to improve our capability to obtain accurate and timely spectral measurements includes:

-3/4-ton pickup to replace aging 1/2-ton pickup as platform for boom,

-tower and boom for sun-view angle experiments (described above),

-portable data loggers,

-special boom designed and built for researchers CIMMYT, Mexico,

-portable spectroradiometer for measuring leaf reflectance and transmittance in the field

Software Development

Major achievement during the past year are twofold. First, a copy of the LARSPEC software system was implemented on the NASA/JSC EODL computer system and copies of the 29 LARSPEC data tapes were sent to NASA/JSC. This provides the capability for increased access to the data by researchers at NASA/JSC and their remote sites and duplication of the data base in case data is lost at one of the sites due to a catastrophe.

The second major achievement is well under way. A portion of LARSPEC field research data base is being converted to a disk-oriented data base as a test pilot using the commercial data base management system, ADABAS. The purpose of the pilot test is to determine if the disk-oriented data base software will provide increased efficiency in analysis and management of the field research data.

Table 5-6. Summary of field research test site locations and major crops.

Test Sites		Experiment Type†	Major Crop	Crop Years
State	County			
Indiana	Tippecanoe	P	Corn & Soybeans Winter Wheat	1978-81 1979-80
Iowa	Webster	C	Corn & Soybeans	1979-81
Kansas	Finney	C,P	Winter Wheat	1975-77
Nebraska	McPherson	P	Corn & Soybeans	1979-81
North Dakota	Cass	C	Spring Wheat Barley Sunflowers Soybeans	1980-81
North Dakota	Williams	C,P	Spring Wheat	1975-77
Oregon	Linn	P	Small Grains	1982
South Dakota	Brookings	P	Small Grains	1981-82
South Dakota	Hand	C	Spring Wheat Winter Wheat	1976-79
Texas	Wharton	C	Cotton Rice Soybeans	1980
U.S. & Brazil		L	250 Soil Types	1978

†C - commercial fields, P - controlled plot, L - laboratory

Table 5-7. Summary of major sensor systems used for field research, 1975-82.

Platform and Sensor	Years
Spacecraft Multispectral Scanners	
Landsat-1 MSS	1975-77
Landsat-2 MSS	1975-79
Landsat-3 MSS	1978-80
Landsat-4 MSS and TM	1982
Aircraft Multispectral Scanners	
24-Channel Scanner (MSS)	1975-76
11-Channel Modular Multispectral Scanner (MMS)	1975-79
8-Channel Thematic Mapper Simulator (NS001)	1979-81
Helicopter-Mounted Spectroradiometer	
NASA/JSC Field Spectrometer System (FSS)	1975-81
Helicopter-Mounted Multiband Radiometer System	
NASA/JSC Barnes 12-1000 MMR	1982
Truck-Mounted Spectroradiometer Field Systems	
NASA/ERL Exotech 20D	1975
NASA/JSC Field Signature Acquisition System (FSAS)	1975-77
Purdue/LARS Exotech 20C	1975-80
Truck-Mounted Multiband Radiometer Field Systems	
Purdue/LARS Exotech 100 Radiometer	1977-82
Purdue/LARS Barnes 12-1000 MMR	1981-82
University of Nebraska Barnes 12-1000 MMR	1981-82
University of Nebraska Exotech 100	1981-82
Oregon State University Barnes 12-1000 MMR	1982
South Dakota State University Barnes 12-1000 MMR	1982

Table 5-8. Summary of spectral data in the field research data library by instrument and data type for 1975-82 crop years.

Instrument/Data Type	Dates	Number of Observations or Flightlines
Landsat MSS		
Whole Frame CCT	124	124
Aircraft Multispectral Scanner	79	448
Helicopter-Mounted Field Spectroradiometer		
Field averages	108	9,267
Individual scans	108	162,826
Truck-Mounted Field Spectroradiometer		
NASA/JSC FSAS	44	813
Purdue/LARS Exotech 20C	131	7,613
NASA/ERL Exotech 20D	45	644
Truck-Mounted Field Multiband Radiometer		
Purdue/LARS Exotech 100	105	25,182
Purdue/LARS Barnes 12-1000	10	4,781
Laboratory Spectroradiometer		
Purdue/LARS Exotech 20C	42	1,622

Field Measurement Workshops and Training

The AgRISTARS Supporting Research Project is supporting the development of field research programs at several universities in the Midwest and Great Plains states. The purpose of the program is to obtain calibrated, meaningful measurements at several sites with different soils and climatic conditions to further the communities' understanding of the reflective and radiative properties of crops and soils. LARS has supported these activities during 1979-81 in the development of the Barnes 12-1000 eight-band radiometer, truck-mounted booms, calibration platforms, and calibration panels (1).

Table 5-9. Recipients of field research data during 1982.

Organization	Means of Distribution
USDA/ARS, Water Conservation Lab Phoenix, Arizona	Mail
Colorado State University Fort Collins, Colorado	Mail
University of Hawaii Honolulu, Hawaii	Mail
Purdue University West Lafayette, Indiana	Computer Terminal
Kansas State University Manhattan, Kansas	Mail
University of Kansas Lawrence, Kansas	Mail
NASA Goddard Space Flight Center Greenbelt, Maryland	Mail
Environmental Research Institute of Michigan Ann Arbor, Michigan	Mail
University of Minnesota St. Paul, Minnesota	Mail
University of Nebraska Lincoln, Nebraska	Mail
State University of New York Binghamton, New York	Mail
Goddard Institute for Space Studies New York, New York	Mail
State University of New York Syracuse, New York	Computer Terminal
SCIPAR, Inc. Williamsville, New York	Mail
North Dakota State University Fargo, North Dakota	Mail

Table 5-9, cont.

Organization	Means of Distribution
Phillips Petroleum Company Bartesville, Oklahoma	Mail
Oregon State University Corvallis, Oregon	Mail
South Dakota State University Brookings, South Dakota	Mail
USDA/ARS Bushland, Texas	Mail
Texas A&M University College Station, Texas	Mail
Pan American University Edinburg, Texas	Mail
NASA Johnson Space Center Houston, Texas	Computer Terminal
Texas Agricultural Experiment Station Lubbock, Texas	Mail
USDA/ARS, Remote Sensing Research Unit Weslaco, Texas	Mail
Canada Centre for Remote Sensing Ottawa, Canada	Mail
CIMMYT (Centro International de Mejoramiento de Maiz y Trigo) Mexico City, Mexico	Mail
National Aerospace Laboratory Amsterdam, The Netherlands	Mail

During this past year, personnel at LARS have held a field measurement workshop, visited several sites to review data acquisition procedures, and provided much support via the mail and phone for other university and USDA field research programs. On May 11 and 12, 1982, a workshop was held at Purdue/LARS for personnel from the University of Minnesota and the NASA Earth Resources Laboratory. A mini-workshop was also held with personnel from NASA Goddard Space Flight Center. Visits were made to the field research programs at:

University of Minnesota
South Dakota State University
CIMMYT, Mexico
Oregon State University
North Dakota State University (helicopter test site)
NASA Johnson Space Center

Acknowledgements

The experiment design was led by Marvin Bauer, Larry Biehl, Craig Daughtry and Richard Weismiller. The plot preparation and agronomic measurements of corn, soybeans, sorghum, sunflowers, and soil experiments were directed by Craig Daughtry and Richard Weismiller. Larry Biehl was responsible for the spectral measurements and data preprocessing. Jon Ranson, Chris Brooks, Lois Grant, Kevin Gallo, Ted Rappaport, Tom Poland, Bill Sever, Jim Long, Vic Fletcher, Ken Draves, Jim Meyers, Dwight Lindman, and Randy Simms assisted in plot preparation and data collection. Ching-Neu Lue, Cathy Kozlowski, Gay Benson, Mary Rice, and Drew Duncan assisted in data preprocessing. Jerry Majkowski, Todd Plantenga, and Jim VanMilligan assisted with the data base management, distribution and software development. Barrett Robinson, Ted Rappaport, Bill Sever, and Tom Poland assisted with hardware development. Barrett Robinson coordinated the workshops and training for field measurement programs at other universities and institutions.

References

1. Bauer, M.E. and Staff. 1982. Remote sensing of agricultural crops and soils. AgRISTARS Tech. Report SR-P2-04266 and Purdue Tech. Report 113081. pp. 65-72.

2. Biehl, L.L. 1982. LARSPEC spectroradiometer-multiband radiometer data formats. AgRISTARS Tech. Report SR-P2-04277 and Purdue/LARS Tech. Report 050182.

3. Biehl, L.L., C.S.T. Daughtry, and M.E. Bauer. 1981. Crop and soils field research data base experiment summaries. AgRISTARS Tech. Report SR-P2-04280 and Purdue/LARS Tech. Report 042382.

4. Biehl, L.L., M.E. Bauer, B.F. Robinson, C.S.T. Daughtry, L.F. Silva and D.E. Pitts. 1982. Proc. Eighth Int'l Symp. Machine Processing of Remotely Sensed Data, Laboratory for Applications of Remote Sensing, Purdue University. July 7-9, 1982.

5. DeWitt, D.P. and B.F. Robinson. 1976. Description and evaluation of a bidirectional reflectance factor reflectometer. Laboratory for Applications of Remote Sensing, Purdue University, West Lafayette, Indiana. LARS Information Note 091576.

6. Robinson, B.F. and L.L. Biehl. 1979. Calibration procedures for measurement of reflectance factor in remote sensing field research. SPIE Vol. 196. Measurements of Optical Radiation, SPIE, Box 10, Bellingham, WA. pp. 16-26.

6. SUN-VIEW ANGLE STUDIES OF CORN AND SOYBEAN CANOPIES IN SUPPORT OF VEGETATION CANOPY REFLECTANCE MODELING

K. J. Ranson, L. L. Biehl and M. E. Bauer

Introduction

The interaction of sunlight with a crop canopy is a complex system consisting of reflection, transmission and absorption. The reflected portion of the solar radiation incident on a canopy provides the basic source of information for remote sensing systems sensitive to visible and reflective infrared wavelengths. The amount of light reflected from a field into a given direction is a function of numerous variables. Agronomic variables such as leaf area index (LAI), biomass, canopy cover and cultural practices and biophysical variables that include foliage angle distribution, leaf reflectance and transmittance and soil reflectance all determine, in part, the amount and distribution of sunlight reflected from a canopy. Physical scene variables such as sun position, wind, and atmospheric characteristics affect the reflectance by altering the shadowing, leaf orientation and the distribution of light incident on the canopy, respectively. The effect of temporal variables, particularly crop development stage, are a function of the above agronomic and biophysical variables.

The estimation of agronomic variables with remote sensing data is important for providing accurate information about the type, amount and status of crops. This information can then be used as input for crop assessment and yield estimation models (Bauer, 1975). Results of empirical studies have demonstrated useful relationships between canopy reflectance and agronomic variables. Daughtry et al. (1980) found relatively high correlations between spectral reflectance and such agronomic variables as biomass, LAI, percent canopy cover, and development stage of wheat. Leamer et al. (1980) indicated that reflectance might be used to monitor development stage of wheat. Holben et al. (1980) found significant correlations between spectral radiance and soybean LAI and biomass. A strong relationship between spectral radiance and grain yield of wheat was reported by Tucker et al. (1980). These studies utilized either truck-mounted or hand-held nadir-viewing sensors.

In the past, however, researchers have noted that identification of agronomic variables from remote sensing data is affected by a dependence of canopy reflectance on the solar illumination and sensor viewing geometry. Studies of angular reflectance of individual corn and soybean leaves conducted by Breece and Holmes (1971) showed increasing reflectance as the angle between the leaf normals and the sensor was increased. Farrar and Mapunda (1977) showed similar trends for African crop plants including maize, soybean and sugar beet.

This non-Lambertian behavior has also been shown to exist in studies where the full crop canopy is considered. Egbert and Ulaby (1972) showed a dependence of reflectance from cotton due to solar zenith angle and effects due to changes in sun and view angles for grass canopies. Vanderbilt et al. (1980) identified an angular reflectance dependence due to sun and view angle as well as wavelength for different growth stages of wheat. Ranson et al. (1980) illustrated the angular dependence of soybean canopy reflectance for rowed and closed canopies. Staenz et al. (1980) found significant variations of reflectance from soil, small grains and broad leaved crops with changing view angles. Methy et al. (1981) studied soybeans and concluded that the measured anisotropy was due to view azimuth angle, solar zenith angle and development stage. Kimes (1983) reported that for homogeneous vegetation canopies reflectance was minimum when viewed near nadir and increased as view angle increased. A greater understanding of these off-nadir measurements may provide additional information for estimating agronomic variables as discussed by Jackson et al. (1979).

Several physically based vegetation canopy reflectance models have been developed that predict the angular scattering properties of a canopy described by a set of biophysical and agronomic parameters. The models by Smith and Oliver (1972) and Suits (1972) are well known examples that consider the canopy as parallel layers with infinite horizontal extent. The model by Suits has recently been extended (Suits, 1981) to include canopies with well defined rows. Increased activity in this area has led to the development of other models such as the geometric optics type model of Jackson et al.(1979), the three-dimensional cubicle cell model of Kimes and Kirchner(1982) and the layered plane model of Cooper, et al.(1982). Recently, increased emphasis has been given to validating canopy models so they may be confidently applied to the problem of estimating agronomic variables from remote sensing data (Goel, 1982). Therefore, it is important that comprehensive field measurements be acquired for crop canopies in terms of their directional reflectance properties and agronomic and biophysical parameters.

The need for increased understanding of the angular reflectance properties of canopies becomes more important as the launch of satellites with off-nadir pointing capabilities becomes more likely. One such satellite, the Systeme d' Probatoire Observation de la Terre (SPOT) developed by a consortium of European countries, is scheduled for launch during the next few years. A more sophisticated satellite with increased spectral resolution, the Multiple Resource Sampler (MRS), has been proposed by NASA (Schnetzler and Thompson, 1979).

Objectives

The objectives of this study were designed to increase our understanding of the nature of angular reflectance distributions of two economically important crops: corn (Zea mays(L.)) and soybean (Glycine max(L.)) and to acquire comprehensive data sets that are suitable for validating most vegetation canopy reflectance models.

Specifically the objectives of this reporting period were:

1. Acquire bidirectional reflectance factor data for for corn and soybean canopies over a wide range of sun and view angles.

2. Compile comprehensive data sets of angular reflectance and canopy agronomic and biophysial parameters that are suitable for testing vegetation canopy reflectance models.

Materials and Methods

Soybeans, a crop of major economic importance which maintains a well defined row structure for about half of the growing season before becoming closed as the rows expand and overlap, were selected for the 1980 summer field study. The former case can be decribed by geometric optics types of canopy models while the latter case may be described adequately by layered infinite plane types of canopy models. A corn field was used for the 1982 research. Corn was selected since it is an economically important crop and has some interesting characteristics amenable to an angular reflectance study. One of these characteristics is the highly specular reflectance component that is evident even by casual observation in the field. Another interesting feature that is directly related to development stage is the appearance of tassels. Nadir observation does not appear to detect this phenomenon very well and it is possible that an off-nadir view will enhance the detection of tasseling.

The fields selected were as uniform as possible in terms of slope, soil type, drainage and planting pattern. Both fields had north-south oriented rows with a row width of 76 cm and planting pattern typical of commercial fields and were kept weed free.

Spectral Measurements

Spectral radiometric data for the soybean sun-view angle experiment were acquired with an Exotech Model 100 radiometer (Table 6-1). Field stops were used to restrict the half power angular field of view (FOV) to ten degrees. The instrument was mounted on a pan head capable of movement in the horizontal (azimuth) and vertical (zenith) planes. A Hi-Ranger truck was used to provide an aerial platform for the instrument at a nominal altitude of ten meters above the soil surface (Figure 6-1). The truck was backed into the center of the field and the boom raised to the desired height and rotated to extend out an azimuth angle of 135 degrees from north. From this position the radiometer view zenith angle was set at zero degrees(nadir) and a measurement was made. The view zenith angle was then set at seven degrees and measurements were made at view azimuth angles of 45, 90, 135, and 180 degrees. This procedure was repeated for view zenith angles of 15, 22, 30, 45 and 60 degrees completing a half hemisphere of measurements. The truck boom was then rotated counter clockwise into an azimuthal position of 315 degrees. At this position measurements for the series of view zenith angles were obtained for view azimuths of 225, 270, 315 and 360 degrees completing the measurement hemisphere. The truck boom

Table 6-1. Description of sensor codes, wavelength bands and corresponding satellite sensor channels.

Sensor Code	Wavelength	Corresponds To
mss1	.5 - .6μm	Landsat MSS 1
mss2	.6 - .7μm	Landsat MSS 2
mss3	.7 - .8μm	Landsat MSS 3
mss4	.8 - 1.1μm	Landsat MSS 4
mmr1	.45 - .52μm	Thematic Mapper 1
mmr2	.52 - .60μm	Thematic Mapper 2
mmr3	.63 - .69μm	Thematic Mapper 3
mmr4	.76 - .90μm	Thematic Mapper 4
mmr5	1.15 - 1.30μm	None
mmr6	1.55 - 1.75μm	Thematic Mapper 5
mmr7	2.08 - 2.35μm	Thematic Mapper 6
mmr8†	10.4 - 12.5μm	Thematic Mapper 7

†Not used for 1982 sun-view angle experiments.

was then rotated again counter clockwise to position the instrument over a plot of bare soil where a nadir observation was made. Additional nadir observations of the soybean field were acquired at truck boom azimuths of 90, 160, 270 and 340 degrees. Prior to and after each measurement hemisphere measurements were acquired from a sunlit and shaded barium sulfate painted panel to provide for calculation of bidirectional reflectance factors (Robinson and Biehl, 1979) and estimates of the percent skylight, respectively. Thirty-five mm color slides were taken at each canopy and soil view position to document the field of view.

The spectral data collection procedures for the 1982 corn experiment were modified from those described above. A tower system was under construction at the start of the field season and it was necessary to eliminate the access roadway for the Hi-Ranger in the center of the field.. To solve this problem roadways were placed on the east and west sides of the field. A half hemisphere of data was collected from each side with the radiometer looking into the center of the field. A Barnes Model 12-1000 radiometer with seven spectral bands was used for this experiment. A different instrument mount was also used that improved setting the view zenith angles. To start a data hemisphere the truck was driven down the west roadway and the truck boom extended out at an azimuth of 135 degrees with a sensor elevation of ten meters. From this position measurements of a series of view zenith angles were taken at view azimuth angles of 0, 180, 225, 270, and 315 degrees. The view zenith angles used were the same as those used in 1980 except for the addition of 70 degrees. Nadir measurements of a bare soil plot located adjacent to the truck were also made. The truck was then moved to the east side of the field and a series

ORIGINAL PAGE IS
OF POOR QUALITY

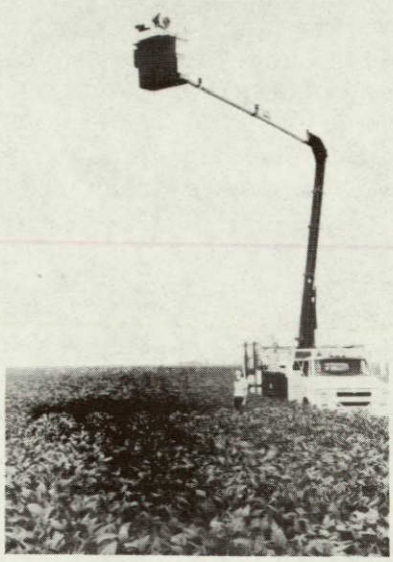

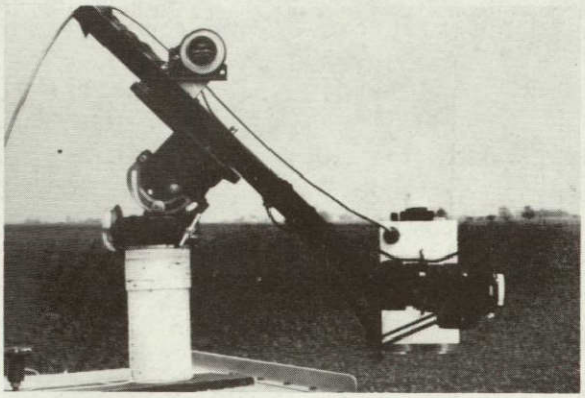

An Exotech Model 100 radiometer (above) mounted on the aerial platform of a Hi-Ranger truck(top left) was used for the 1980 soybean sun-view angle experiments.

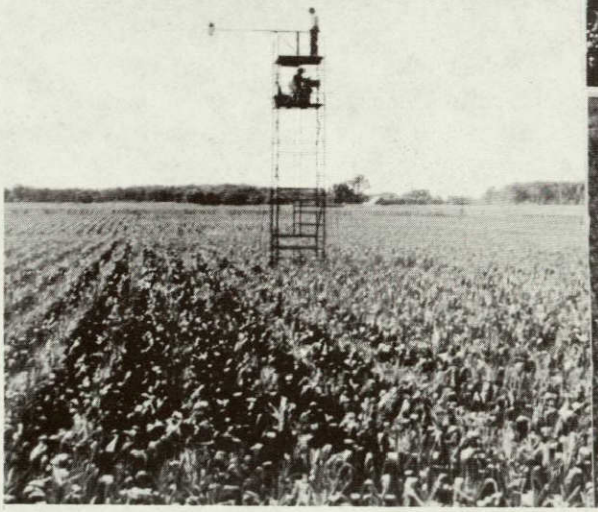

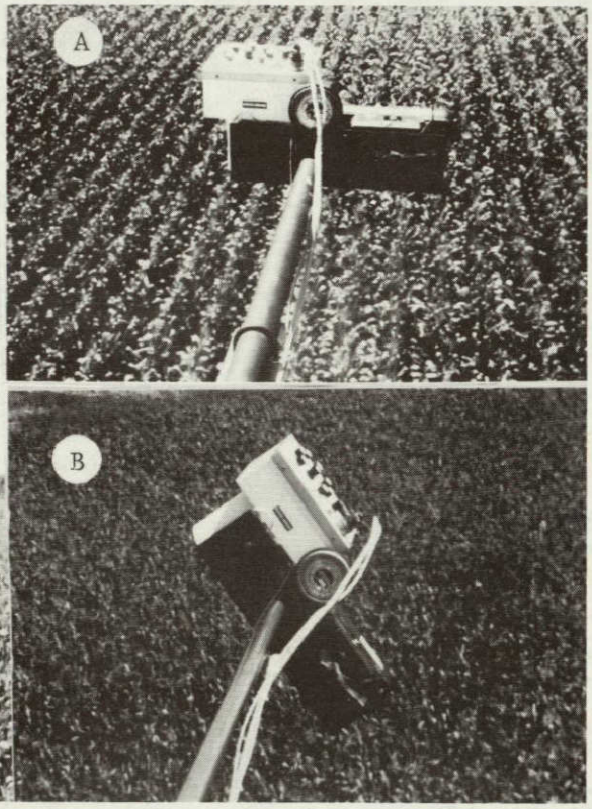

This ten meter tower (lower left) was used during the 1982 corn sun-view angle experiments. A Barnes Model 12-1000 radiometer shown here looking nadir (A) and at 45° (B) was mounted on a 3 meter boom.

Figure 6-1. Instrumentation set-up for sun-view angle experiments.

of view zenith angle measurements were made for view azimuths of 45, 90, 135, 180 and 360 degrees completing the measurement hemisphere. Additional nadir observations of the corn field were acquired at truck boom azimuths of 270 and 315 degrees on the west side and at 45 and 90 degrees on the east side of the field. To document the FOV 35 mm color slides were obtained for each view position. Initially, a 15 degree FOV was used for this experiment, on one measurement day, however, ten degree field stops were used to provide a comparison with the data acquired from the tower as discussed below.

The tower system was erected in the center of the corn field during the first week of August. The tower was constructed of six 1.5 meter sections of construction scaffolding with platforms mounted on the fifth and top sections. A three meter boom was mounted on a pivot base in the center of the top platform (Figure 6-1,lower left). The lower platform accommodated an engineer and data logging equipment. The boom was inserted in a sleeve and could be rotated about the vertical axis by means of wheel attached to one end. The Barnes instrument equipped with ten degree field stops was attached to the other end of the boom (Figure 6-1, lower right). Rotating the boom about its pivot point provided selection of azimuth positions of 0, 45, 90, 135, 180, 225, 270 and 315 degrees. View azimuth angles were measured perpendicular to the boom azimuth direction. For example with the boom pointing east (90 degrees) view azimuths of 0 and 180 degrees were obtained. The procedure consisted of setting the view zenith angle at 70 degrees and making successive measurements as the zenith angle was changed to 60, 45, 30 and so on until the instrument view had passed through nadir. Then view angles were increased through 7, 15, 22 and so on until 70 degrees zenith was reached. The principle here is much like a scanner although slower.

A complete circuit around the tower resulted in two replications of all eight azimuth angles and all eight zenith angles. Calibration measurements were made prior to and after each circuit with a barium sulfate painted panel resting on a platform mounted on the south side of the tower. With this system, it was possible to acquire two complete hemispheres of data and calibration measurements in less than 15 minutes. Due to the increased number of observations acquired with this sysytem color slides documenting the field of view were taken at each view position for complete hemispheres only a few times each day. Slides were acquired, however, whenever the instrument operator determined that a tower shadow might fall within the FOV.

In order to document the effects of changing sun angle measurement hemispheres were obtained at 30 to 60 minute intervals throughout the day for both the soybean and corn experiments as long as cloud conditions would permit. Table 6-2 summarizes the spectral data collected during the summers of 1980 and 1982.

Agronomic and Biophysical Measurements

A standard set of agronomic and biophysical measurements describing the canopies were acquired within one day of the spectral measurements. These

ORIGINAL PAGE IS
OF POOR QUALITY

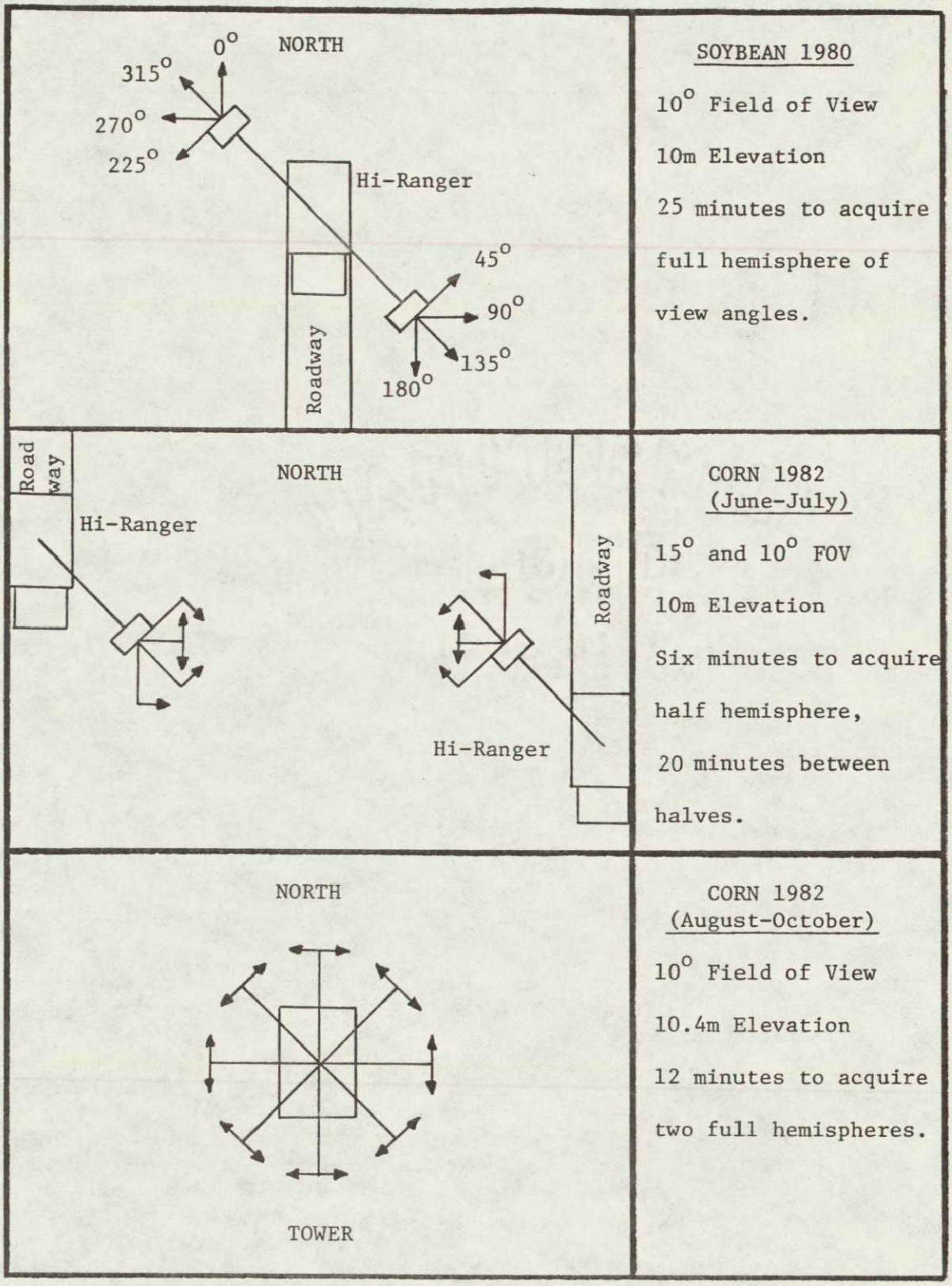

Figure 6-2. Spectral data collection configurations for 1980 and 1982 sun-view angle experiments. Arrows indicate view azimuths.

ORIGINAL PAGE IS
OF POOR QUALITY

Table 6-2. Summary of sun-view angle data sets for soybeans (1980) and corn (1982) canopies.

Date	Start Time (GMT)	End Time (GMT)	Solar Zenith Angle Range (Degrees) Max-Min-Max	Solar Azimuth Angle Range (Degrees)	Number of Data Sets	Cloud Cover (%)
July 18, 1980	17:59	21:35	19-50	183-265	5	10-20
July 25, 1980	15:14	18:49	40-21-24	109-214	6	1-20
Aug 27, 1980	15:15	18:49	40-30-60	132-237	12	0
June 13, 1982	17:24	21:58	18-17-55	162-272	9	1-10
June 14, 1982	15:58	18:01	27-17	118-190	6	10-20
June 21, 1982	14:52	19:16	41-17-25	101-233	9	10-40
June 23, 1982	16:55	18:45	21-17-21	142-218	5	5-30
June 24, 1982	14:07	18:38	49-18-20	92-214	10	5-10
July 6, 1982	15:10	18:21	38-18-19	105-201	3	3-60
July 9,1982	15:26	16:14	36-28	109-123	2	10-17
July 12,1982	14:30	16:43	46-26	110-136	5	0-35
July 14,1982	14:59	15:21	41-37	103-108	2	15-25
July 15,1982	15:07	16:11	40-29	105-123	3	1-10
July 16,1982	16:58	17:07	22-21	144-149	1	15
July 23,1982	14:25	22:42	49-23-64	98-275	17	1-10
July 30,1982	14:01	15:27	54-42	96-109	4	0- 3
July 31,1982	13:46	16:50	57-26	93-143	7	0-32
Aug 11,1982	14:14	18:27	51-25-26	103-197	12	0-20
Aug 12,1982	14:08	19:15	53-25-31	102-222	24	0-20
Aug 19,1982	14:58	19:17	48-31-37	118-219	16	5-20
Aug 28,1982	16:00	17:48	39-31	135-180	7	15-30
Sept 4,1982	14:13	21:30	48-33-70	123-262	24	0- 1
Oct 25,1982	16:30	21:30	53-52-80	170-245	18	10-15

included LAI, total fresh biomass, development stage, percent canopy cover, canopy profile, leaf angle distribution, and leaf spectral reflectance and transmittance measurements.

Soybean leaf angle measurements were made using a modification of the protractor method described by Kyle and Davies (1974) and Nichiporovich (1961). In addition to leaf zenith and azimuth angles, the across row, along row and height locations and area were measured for each leaf sampled (except for the August 27 date when only leaf heights and leaf areas were obtained).

Soybean biomass and leaf area index were estimated from random samples of one meter lengths of row. Each sample was placed in plastic bags and later weighed to determine fresh total biomass. The plants were separated

into green leaflets, yellow leaflets, stems plus petioles and pods, oven dried at 60 degrees Celsius and reweighed. The leaf area from a random subsample of green leaves from each sample was obtained with an optical planimeter and dry weights were obtained. The leaf area to weight ratio was obtained from the subsample data and used to calculate the leaf area index for each one meter of row samples.

An orthogonal photographic technique described by Smith et al. (1977) was used to estimate the leaf angle distribution for corn. This involved obtaining two orthogonal photographs of a corn plant against a reference background gridded into rectangles representing compartments of known height and width. Leaf segments that were located in a particular compartment were cut and labeled and placed in bags for later leaf area measurements. The photographs were digitized by determining the three dimensional cooridinates of the leaf midrib and the leaf angle distributions calculated by a computer program. Five to 15 plants were sampled for leaf angle distribution and leaf area index estimates.

Leaf optical properties (reflectance and transmittance) were acquired with a Beckman DK-2 spectrophotometer in a laboratory. Due to equipment problems, these measurements were acquired for only a few days periodically during both years. In order to maintain the plant in good condition the plants were removed from the field with a substantial root ball in well watered containers and transported to the laboratory in an enclosed vehicle.

Meteorological data consisting of relative humidity, air temperature, barometric pressure, wind direction, wind speed and global solar irradiance were acquired each day at the Purdue Agronomy Farm.

Discussion

Spectral Data Analysis

The spectral data collected during the summers of 1980 and 1982 provide a unique data set useful for documenting the angular reflectance properties of soybean and corn. The following section discusses the types of trends in the these data sets.

When a radiometer views a scene the response and thus BRF is dependent on the scattering properties and proportions of sunlit and shaded scene components. For agricultural scenes such as soybean and corn fields the scene components are vegetation and bare soil. When the sensor looks straight down on a canopy with well defined row structure the effect of sunlit and shaded soil on the scene reflectance is maximized. As the view angle increases proportionately more vegetation is viewed since the sensor now sees the sides of the plant rows. Figures 6-3 and 6-4 illustrate how the scene changes with view angles for rowed canopies of soybean and corn, respectively. The series of photographs were taken with a camera mounted next to the radiometer and include the FOV of the radiometer. The photographs represent a view azimuth angle of 90 degrees with sensor direction perpendicular to the plant rows. The time of acquisition was

ORIGINAL PAGE IS
OF POOR QUALITY

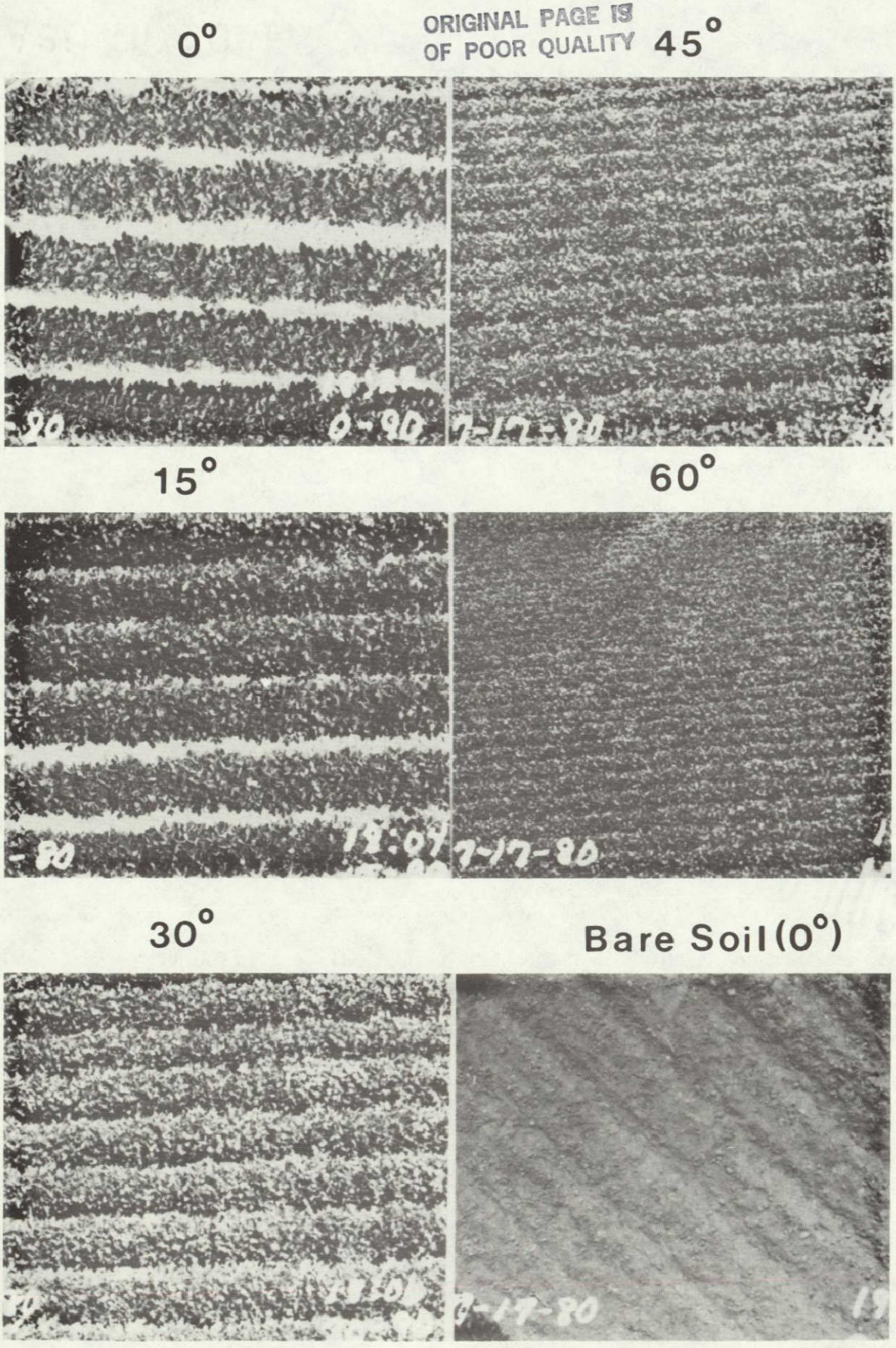

Figure 6-3. Photographs of the soybean field with varying zenith view angle. Date = July 17, 1980, Time = 18:10 GMT, View Azimuth Angle = 90°.

ORIGINAL PAGE IS
OF POOR QUALITY

within 30 minutes of solar noon so shadowing of the soil surface is minimal. As the canopies mature and adjacent rows overlap the sensor sees mainly the tops of the canopies and the amount of bare soil present decreases. A series of photographs for overlapping soybean and corn canopies are presented as Figures 6-5 and 6-6, respectively.

One would expect the BRF from rowed canopies to change with view angle due to the presence of bare soil in the field of view. This can be seen in Figure 6-7a where the BRF's for each wavelength band are plotted against view zenith angle. For the soybean case the BRF in the two visible bands (mss1, mss2) decrease with view angle until about 30 degrees after which it levels off. Note that in the corresponding photographs (Figure 6-3) the bare soil disappears at a view angle between 30 and 45 degrees. The near-IR BRFs (mss3, mss4) decrease only slightly initially and then increase. This is due in part to the relatively high reflectance of the soil in these wavelength bands. For the case of the rowed corn canopy the data presented in Figure 6-7a show a general decrease in reflectance in all bands except mmr4 and mmr5. The canopy was not developed sufficiently to completely mask the soil even at the extreme view angles.

Figure 6-7b presents data for soybean and corn canopies where the adjacent rows have overlapped. The BRFs for all wavelength bands tend to decrease slightly at first, but then increase as view angles are increased past 30 degrees. The initial decrease may be due to the canopy structure where erect leaves in the upper layers of the canopies result in the sensor seeing a significant amount shadowing within the canopy. Analysis of leaf angle data for these canopies tend to support this hypothesis. As the sensor view angle increases the projected area of leaves into the direction increases and the reflectance increases. Another possible factor involved in the increased reflectance observed is the dependence of specularly reflected light on view direction (Vanderbilt,1983).

Figure 6-8 illustrates how reflectance factors may vary over a complete hemisphere. Presented are contours of equal refelectance factors for rowed and closed soybean canopies acquired when the sun was near solar noon and late in the day. View zenith angles are represented as the rings on the polar graphs with nadir view in the center with 15 degree increments increasing outward. View azimuth angles are represented as radial lines with 0 degrees at the top and increase clockwise. For comparison purposes the distribution of reflectance factors for the red (.6-.7μm) band acquired near solar noon can be described as a hill elongated along the north-south row direction. The summit of the hill is located in the vicinity of the hot spot where the sensor views the canopy in line with the sun. Reflectance falls off most rapidly at view azimuths perpendicular to the row direction. The corresponding near-IR (.8-1.1μm) band distribution is more like a ridge, the top of which slopes downward parallel to the solar azimuth direction from the hot spot to a minimum where the sun and sensor view directions coincide. This local minimum occurs where the sensor would see the maximum amount of canopy shadowing. The polar plots for the closed canopy data acquired near solar noon show similar distributions for both wavelength bands with maximum reflectance occuring when the sensor looks in line, but away from the sun and minimums occuring when the sensor looks towards the sun direction. The angular distributions for data collected late in the day

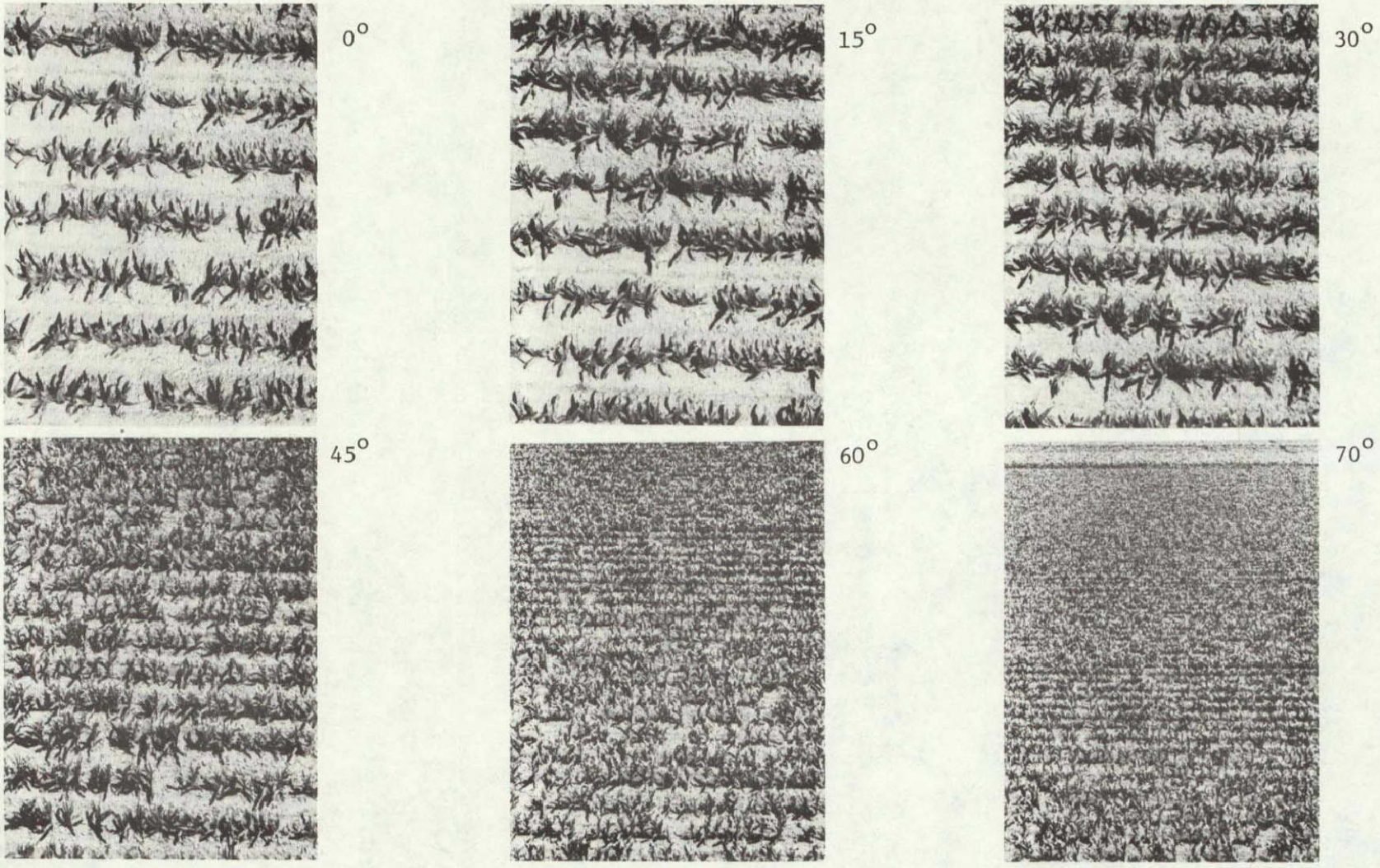

Figure 6-4. Photographs of the corn fields taken at various view zenith angles. Date = June 21, 1982, Time = 17:56 GMT, View Azimuth Angle = 90°.

ORIGINAL PAGE IS
OF POOR QUALITY

ORIGINAL PAGE IS
OF POOR QUALITY

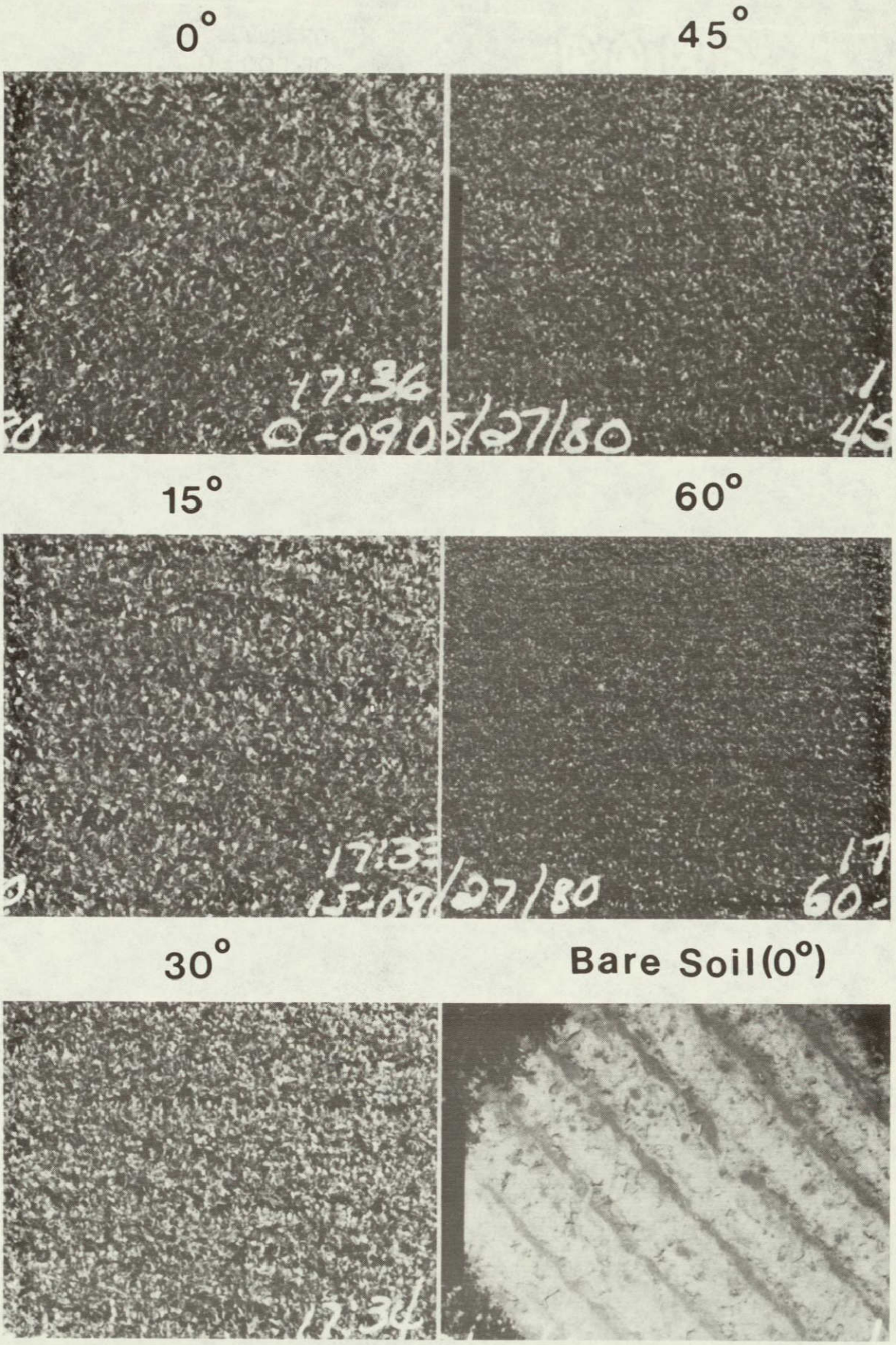

Figure 6-5. Photographs of the soybean field with varying zenith view angle. Date = August 27, 1980, Time = 17:35 GMT, View Azimuth Angle = 90°.

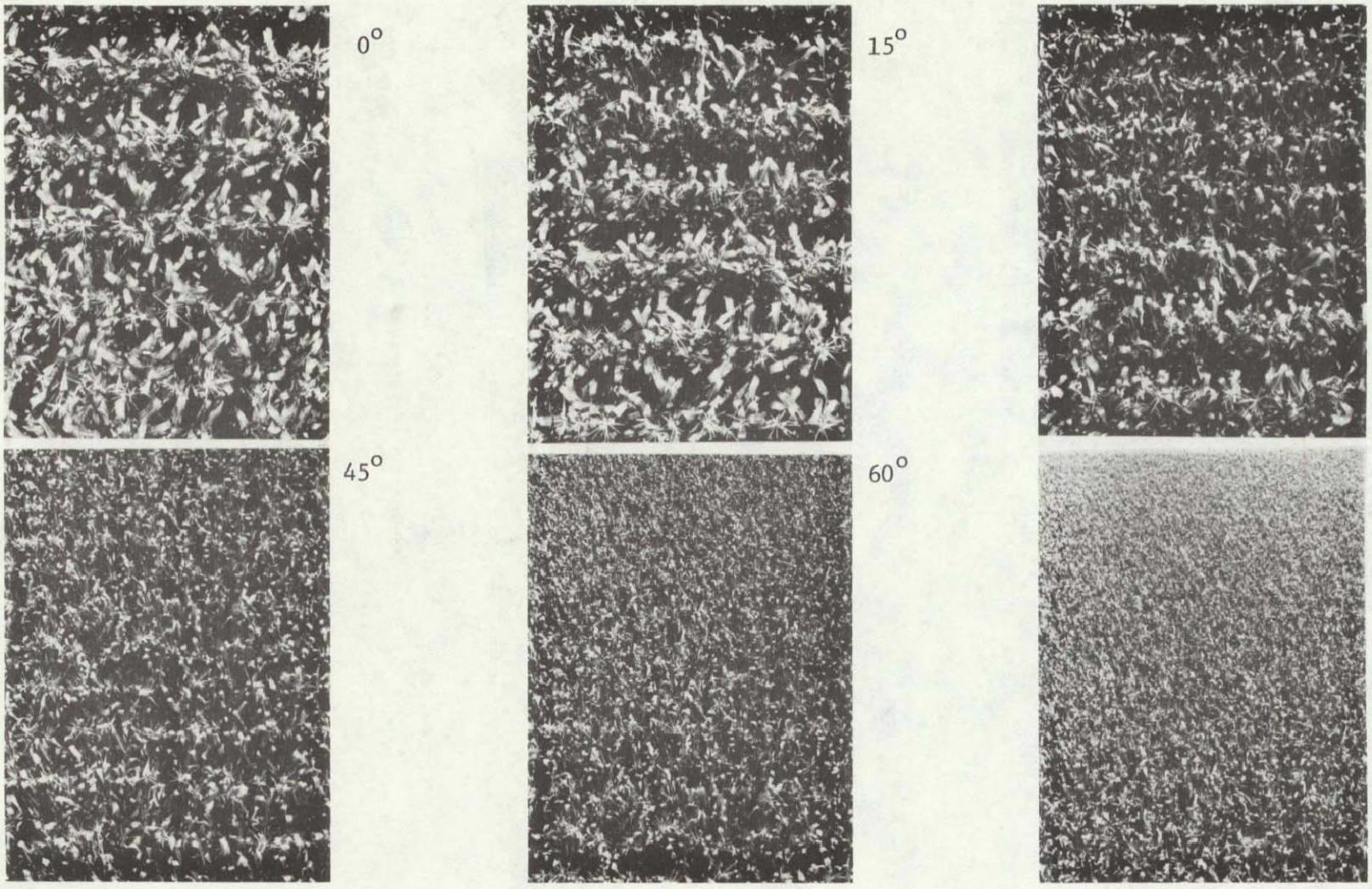

Figure 6-6. Photographs of the corn field taken at variuos view zenith angles. Date = July 31, 1982, Time = 16:48 GMT, View Azimuth Angle = 90°.

ORIGINAL PAGE IS
OF POOR QUALITY

ORIGINAL PAGE IS
OF POOR QUALITY

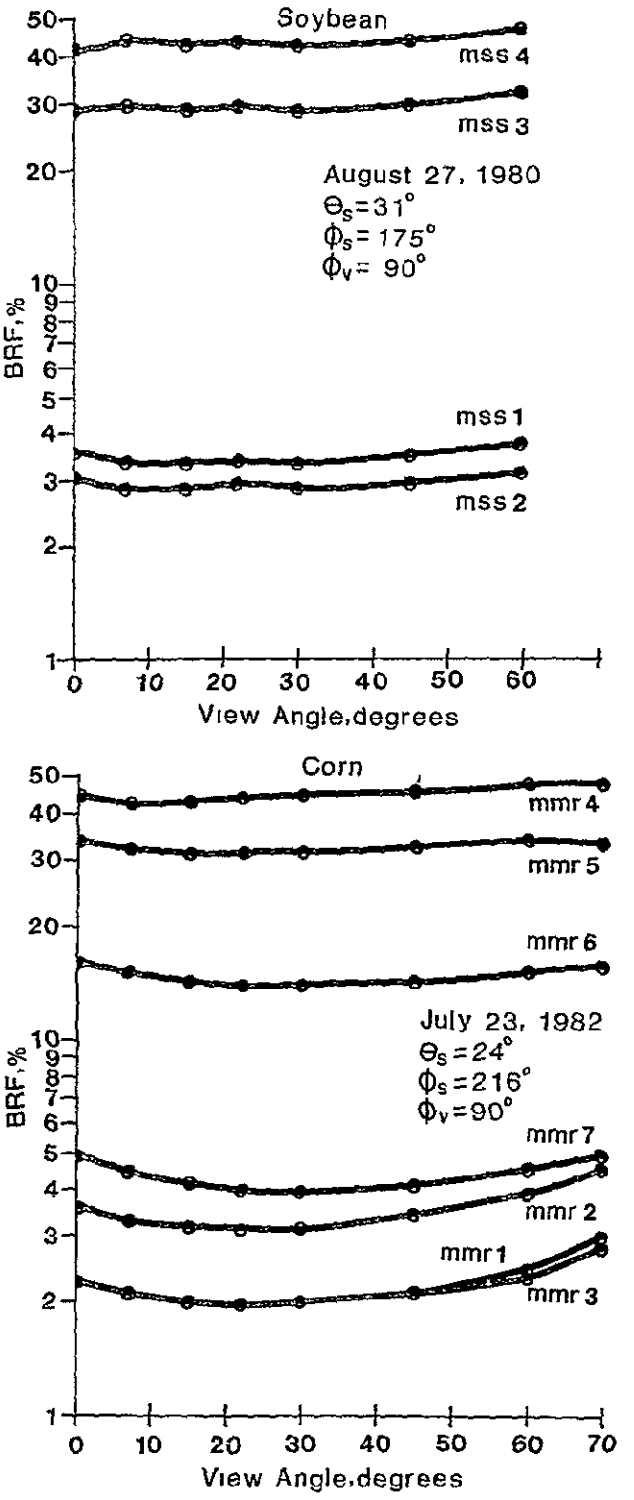

Figure 6-7b. Relationships of spectral bidirectional reflectance factors with view zenith angle for overlapping soybean and corn canopies. θ_s = solar zenith angle, ϕ_s = solar azimuth, ϕ_v = view azimuth angle. Wavelength band codes are explained in Table 2.

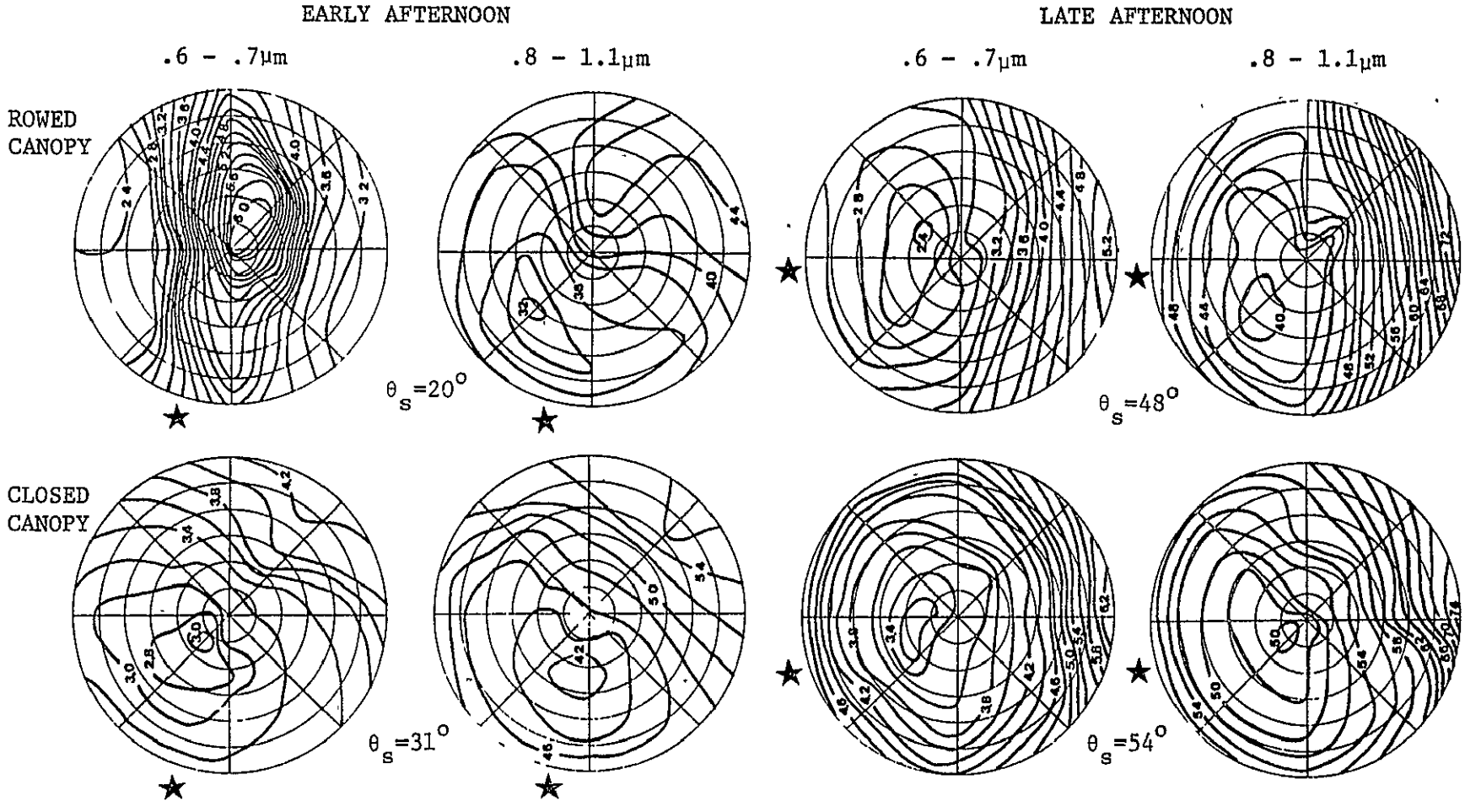

Figure 6-8. Contours of equal reflectance factors for rowed and closed soybean canopies for red (.6-.7μm) and near-infrared wavelength bands. Bullseye circles represent view zenith angles with 0° at the center and outward to 60° in 15° increments. Radial lines indicate view azimuth angles with 0° at top and increasing clockwise. Stars indicate average solar azimuth position during hemisphere acquisition. Date of rowed canopy data = July 17, 1980. Date of closed canopy data = August 27, 1980.

ORIGINAL PAGE IS
OF POOR QUALITY

ORIGINAL PAGE IS
OF POOR QUALITY

are similar for both canopies but the magnitude of reflectance is greater for the closed canopy. In each case the distributions are concave with a steeply sloped sides in the direction away from from the sun. Minimums occur for sensor azimuth directions towards the sun azimuth with view zenith angles approaching nadir.

Examples of spectral reflectance factor distributions for rowed and overlapping corn canopies are presented in Figures 6-9 and 6-10, respectively. The distribution for the rowed canopy in the red band (.63-.69μm) in the early afternoon aprroximates the hill shaped pattern found for soybean. The distribution for the near-IR band (.76-.90μm) is also similar, whereas that for the middle-IR band (2.08-2.35μm) is similar to the red band. The data hemispheres collected in the morning show definite maximums at the hot spot for the red and middle-IR bands with regions of local minimums occuring when the sensor looks toward the sun azimuth. For the overlapping canopy reflectance increases for view directions parallel with the solar azimuth with minimums located for view zenith angles approaching nadir. The large increase in reflectance observed from morning to early afternoon is probably due to an increased specular component occuring at the larger solar zenith angle.

Canopy Modeling Data Modules

The second objective of this reporting period was to compile data modules for selected measurement dates that include the angular reflectance factors and biophysical and agronomic parameters required for validating most vegetation canopy reflectance models. To date, two data sets have been assembled for this purpose. The first set was acquired during August 1980, and was representative of a closed soybean canopy. This data set has been used as input for several canopy models (eg. Cooper et al.,1982) and was found to be acceptable for the needs of most models. A second data module, acquired for a rowed soybean canopy on July 17, 1980 has been compiled and released on a limited basis. The data acquired for the corn canopy in 1982 is currently being reduced and a number of complete data modules for rowed and overlapping canopies will be made available in the near future.

References

1. Bauer, M.E. 1975. The role of remote sensing in determining the distribution and yields of crops. Adv. Agron. 27:271-304.

2. Breece, H.T.(III) and R.A. Holmes. 1971. Bidirectional scattering characteristics of healthy green soybean and corn leaves in vivo. Appl. Opt. 10:119-127.

3. Cooper, K., J. Smith and D. Pitts. 1982. Reflectance of a vegetation canopy using the adding method. Appl. Opt. 21(24):

4. Daughtry, C.S.T., M.E. Bauer, D.W. Crecelius and M.M. Hixson. 1980. Effects of management practices on reflectance of spring wheat canopies. Agron. J. 72(6):1055-1060.

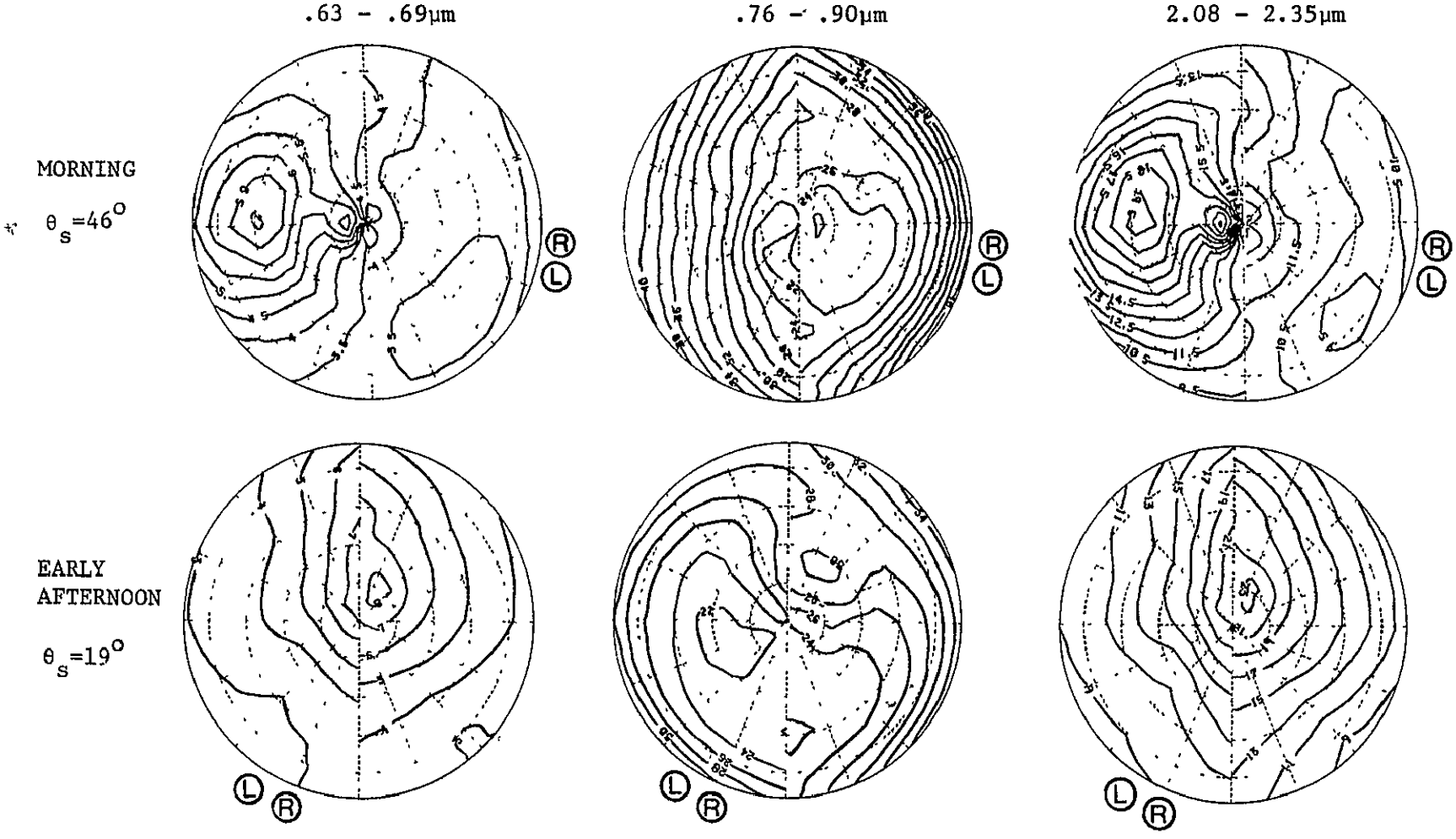

Figure 6-9. Contours of equal reflectance factors for a rowed corn canopy in the morning and early afternoon. Data is presented for three wavelength bands: .63-.69μm, .76-.90μm and 2.08-2.35μm. Bullseye circles represent view zenith angles with 0° at the center and outward to 15, 30, 45, 60 and 70°. Radial lines represent view azimuth angles as in Figure 6-8. Circled letters indicate average solar azimuth position during acquisition of each half hemisphere; R = right side, L = left side. Date of data acquisition was June 24, 1982.

ORIGINAL PAGE IS
OF POOR QUALITY

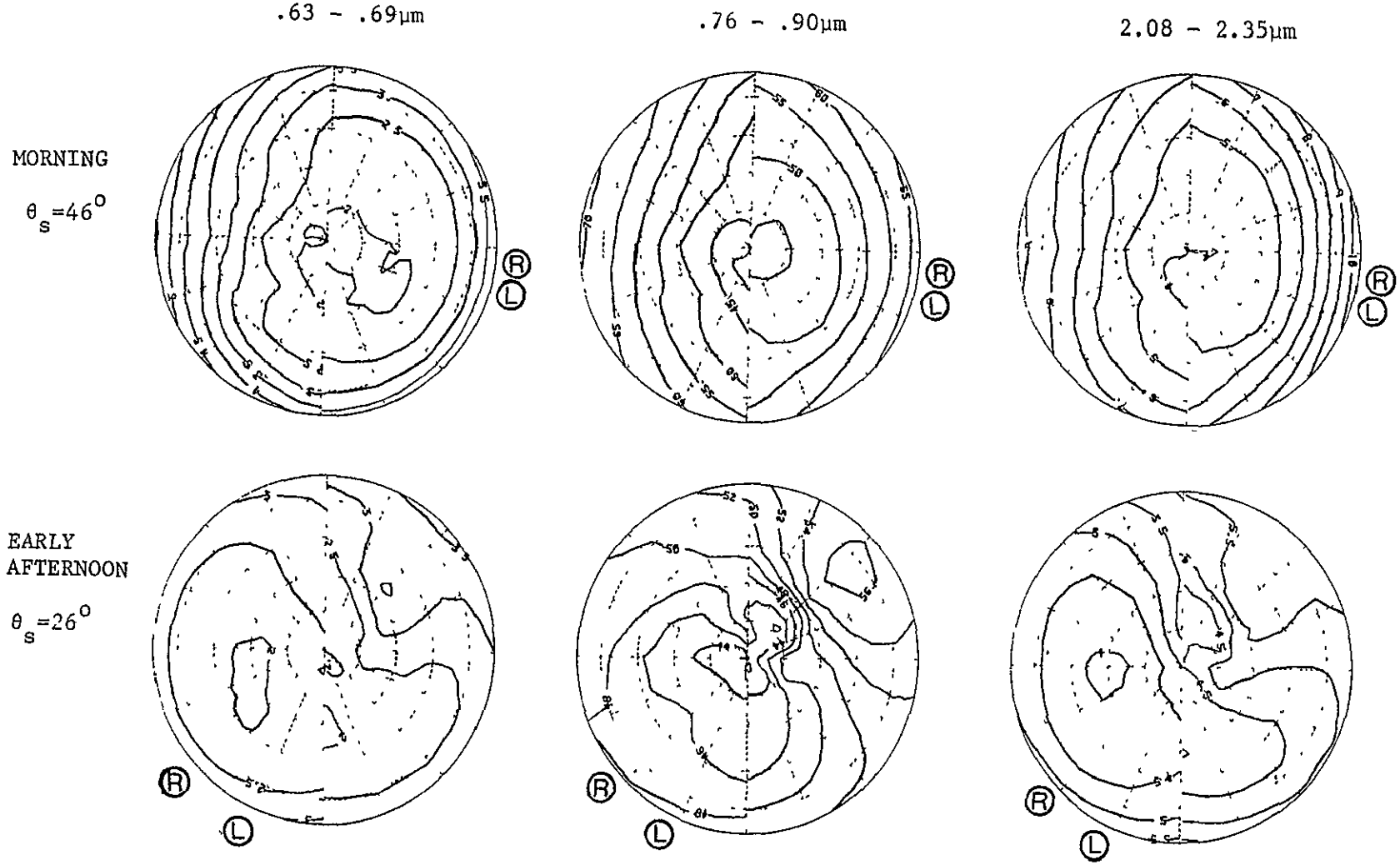

Figure 6-10. Contours of equal reflectance factors for an overlapping corn canopy in the morning and early afternoon. Data is presented for three wavelengths: .63-.69μm, .76-.90μm and 2.08-2.35μm. Angular coordinates are the same as described in Figure 6-9. Date of data acquisition was July 23, 1982.

ORIGINAL PAGE IS
OF POOR QUALITY

5. Egbert, D.E. and F.T. Ulaby. 1972. The effect of angles on reflectivity. Photogramm. Eng. Rem. Sens. 38:556-564.

6. Farrar, J.F. and O.P. Mapunda. 1977. Optical properties of the leaves of some African crop plants. Appl. Opt. 16(1):248-251.

7. Goel, N.S.(ed). 1982. Modeling of vegetation canopy reflectance: status, issues, and recommended future strategy. JSC-18666. NASA/JSC, Houston, TX, 77058. 76 pp.

8. Holben, B.N., C.J. Tucker and C. Fan. 1980. Spectral assessment of soybean leaf area and leaf biomass. Photogramm. Eng. Rem. Sens.46(5):651-656.

9. Jackson, R.D., R.J. Reginato, P.J. Pinter, Jr. and S.B Idso. 1979. Plant canopy information extraction from composite scene reflectance of row crops. Appl. Opt. 18(22):3775-3782.

10. Kimes, D.S. 1983. Dynamics of directional reflectance factor distibutions for vegetation canopies. Submitted to Applied Optics (Jan,1983).

11. Kimes, D.S and J.A Kirchner. 1982. Radiative transfer model for heterogeneous 3-D scenes. Appl. Opt. 21(22):4119-4129.

12. Kyle, W.J. and J.A. Davies. 1974. Quantitative comparison of foliage display in two plots of corn. Can. J. Bot. 52:2465-2471.

13. Leamer, R.W., J.R. Noriega and A.H. Gerberman. 1980. Reflectance of wheat cultivars as related to physiological growth stages. Agron J. 72(6):1029-1032.

14. Methy, M., B. Lacaze and J. Dauzant. 1981. Cinetiques journalieree et saisonniere des factors spectraux de reflectance directionelle d'une culture de soja, et implications pour l'utillsation des donnes du satellite SPOT. In:Signatures spectrales d'objects en teledetection. Avignon. Sept 8-11,1981.

15. Nichiporovich, A.A. 1961. Properties of plant crops as an optical system. Sov. Plant Physiol. 8:428-435.

16. Ranson, K.J., V.C. Vanderbilt, L.L. Biehl, B.F. Robinson and M.E. Bauer. 1980. Soybean canopy reflectance as a function of view and illumination geometry. Proc. 15th Int. Symp. Rem Sens. Environ., Ann Arbor, MI, pp. 853-866.

17. Robinson, B.F. and L.L. Biehl. 1979. Calibration procedures for measurement of reflectance factor in remote sensing field research. Proc. Soc. Photo-Optical Instrumentation Engr. 23rd Annual Tech. Symp. on Measurements of Optical Radiation, Bellingham, WV, pp. 16-26.

18. Schnetzler, C C. and L.L. Thompson. 1979. Multiple resource sampler:an experimental satellite sensor for the mid-1980's. Proc. SPIE Tech. Symp., Huntsville, AL. Vol. 183.

19. Smith, J.A and R.E. Oliver. 1972. Plant canopy models for simulating composite scene spectroradiance in the 0.4 to 2.05 micrometer region. Proc. Eighth Int. Symp. Rem. Sens. Environ., Univ. Mich., Ann Arbor, 2:1333-1353.

20. Smith, J.A., R.E. Oliver and J.K Berry. 1977. A comparison of two photographic techniques for estimating foliage angle distribution. Aust. J. Bot. 25:545-553.

21. Staenz, K., F.J. Ahern and R.J. Brown. 1980. The influence of illumination geometry on the reflectance factors of agricultural targets. Proc. 15th Int. Symp. Rem. Sens. Environ., Ann Arbor, MI.

22. Suits, G.H. 1972. The calculation of the directional reflectance of a vegetative canopy. Remote Sens. Environ. 2:117-125.

23. Suits, G.H. 1981. The extension of a uniform canopy reflectance model to include row effects. ERIM Tech. Rep. No. SR-E1-04065, Ann Arbor, MI. 48 pp.

24. Tucker, C.J., B.N. Holben, J.H. Elgin and J.E. McMurtry III. 1980. Relationship of spectral data and grain yield variation. Photogramm. Eng. Rem. Sens. 46(5):657-666.

25. Vanderbilt, V.C.,B.F. Robinson, L.L. Biehl, M.E. Bauer and A.S. Vanderbilt. 1980. Simulated response of a multispectral scanner over wheat as a function of wavelength and view-illumination directions. ISP Congress, Hamburg, W. Germany. (also AgRISTARS Tech. Rep. No. SR-PI-04202, Purdue/LARS, W. Lafayette, IN, 47906)

26. Vanderbilt, V.C, L. Grant, L.L Biehl and B.F. Robinson. 1983. Specular and diffuse reflectance of two wheat canopies measured at many view angles. Presented at National Radio Science Meeting, Jan 5-7,1983, Boulder,CO.

III. Soil Moisture Research

7. SPECTRAL ESTIMATION OF CORN CANOPY PHYTOMASS AND WATER CONTENT

S.E. Hollinger and V.C. Vanderbilt

A goal of remote sensing is to estimate the amount of phytomass in the canopy as an intermediate step to estimating the condition of the crop and ultimately its yield. Canopy phytomass is composed of water and solid plant material and it is the solid plant material, dry phytomass, or dry matter, that is important in estimating yields. The combined dry phytomass plus the water it holds is also responsible for the appearance of the canopy as seen by the optical sensor.

Total water content in a canopy increases as the canopy grows, then decreases as the canopy senesces. Superimposed upon these general trends are diurnal fluctuations (Wilson et al., 1953; Millar and Denmead, 1976). All plant parts exhibit diurnal fluctuations in water content with leaves and stems varying the most. Maximum water contents were observed at night and minimums in midafternoon when evaporative demands were greatest. Millar and Denmead found that leaf relative water content (RWC) responded to radiation intensity with the highest RWCs occurring under low irradiances and the lowest RWCs under high irradiances.

The energy reflected by a plant canopy is related to the fresh and dry phytomass and water content of the canopy (Daughtry et al., 1980; Carlson et al., 1971; Thomas et al., 1966; Tucker, 1979, 1980; Tucker et al., 1979; Holben et al., 1980). In wheat canopies, Daughtry et al. (1980) found that canopy fresh phytomass, dry phytomass, and water content were correlated with (1) reflectance factor in the visible wavelengths and (2) the greenness (Kanth, et al., 1979). Fresh and dry phytomass and water content were negetatively correlated with reflectance in the visible wavelengths and were positively correlated with the greenness.

Reflectance in wavelengths greater than 1.1 μm have shown the highest correlation with RWC of canopies. Carlson et al. (1971) found the reflectance in the 1.0-2.5 m wavelength band was positively correlated to RWC for corn and soybeans. Thomas et al. (1966) found a nonlinear relationship between RWC and reflectance of cotton at wavelengths greater than 0.54 μm. When RWC was greater than 80%, there was no change in the reflectance of individual leaves dried from a fully turgid state to a wilted state. In a simulation study, Tucker (1980) reported that the wavelength band from 1.5 to 1.63 μm showed the greatest spectral radiance changes with leaf dehydration. However, he concluded that the best band to detect water content from space was 1.55 to 1.75 μm because of the atmospheric water absorption bands that attenuate and scatter radiation in this region of the spectrum.

In a blue grama (Bouteloua gracilis) canopy, Tucker (1979) found combinations of near infrared (IR) (0.75-0.80 μm) and red (0.63-0.69 μm) wavelength bands to be sensitive to the amount of photosynthetically active vegetation present. Other IR bands (0.75-0.90 μm and 0.80-0.90 μm) used in

PAGE 118 INTENTIONALLY BLANK PRECEDING PAGE BLANK NOT FILMED

conjunction with the red band exhibited the same response as the 0.75 to 0.80 μm band. All combinations of IR band and red band reflectance were found to be linearly correlated with the leaf water content except for the IR+red and the (IR+red)/(IR-red) combination. The coefficient of determination (r^2) ranged from 0.68 to 0.85 for the various combinations. The two combinations noted as exceptions above had r^2s of 0.

Holben et al. (1980) measured the radiance of a soybean canopy in the Red (0.65-0.70 μm) and IR (0.775-0.825 μm) wavelength bands and found that both the ratio, IR/Red, and the normalized difference, (IR-Red)/IR+Red); were the functions of area and mass of green leaves. The IR/Red ratio showed a linear relationship and the normalized difference, an exponential relationship.

The objective of this study was to estimate canopy phytomass and total water content using multispectral data.

Methods

The crop data used in this study were collected from experimental plots on the Purdue Agronomy Farm 10 km northwest of Lafayette, Indiana, in 1979, 1980, and 1981. Included in the experiment design were three plant populations (25000, 50000, and 75000 plants per hectare), three planting dates in 1979 (2 May, 16 May, and 30 May), seven planting dates in 1980 (7 May, 16 May, 22 May, 29 May, 11 June, 18 June, and 2 July), and four planting dates in 1981 (8 May, 29 May, 11 June, and 29 June). Only one population (50,000 plants/ha) was planted on 16 May, 29 May, 18 June, and 2 July 1980. Each treatment was replicated twice on two soils, a dark Chalmers soil (fine silty mixed mesic typic Haplaquolls) and a lighter Fincastle soil (fine silty mixed, mesic aeric Ochraqualfs). Color differences between the two soils are greatest when they are dry. The populations were established by overseeding in 76 cm rows and thinning to the desired population after emergence.

Spectral reflectance data were collected throughout the growing season on clear days using an Exotech 100 spectral radiometer with a 15 degree field of view. These data were used to calculate the reflectance factor (Nicodemus, et al., 1977; Robinson and Biehl, 1979) which approximates the bidirectional reflectance factor (BRF). The radiometer was mounted on the boom of a pickup truck and elevated to a height of 5.2 μm in 1979 and 7.6 μm in 1980 and 1981. The Exotech 100 has the following wavelength bands: 0.5-0.6, 0.6-0.7, 0.7-0.8, and 0.8-1.1 μm.

In 1979 and 1980, each day that spectral data was obtained, five plants were sampled the same day or the day immediately following the date of spectral sampling. In 1981 each plot was sampled once a week. The total fresh phytomass, leaf area index, total dry phytomass, percent ground cover, mean stage of development (Hanway, 1963), and total water content were measured for each plot.

Total water content (Wh) is the mass of water in the canopy (g/M^2) and is calculated by:

$$Wh = Wf - Wd \quad (1)$$

where Wf is fresh phytomass (g/m^2) and Wd is dry phytomass (g/m^2) after the plants have been dried at 60 C until their weight is constant.

The agronomic data (total fresh phytomass, total dry phytomass, and total water content) were plotted as functions of development stage. Each treatment mean was plotted so the effects of the treatments could be observed. These plots were then used to decide what treatments should be used in the study. The treatments selected were those that showed the most significant difference in the agronomic variables.

Various combinations and transformations of the spectral bands commonly used in remote sensing work were linearly correlated with the three agronomic variables, Table 7-1. In addition, an angular transformation of greenness and brightness was developed and tested. The angular transformation was the arctangent of the ratio of greenness to brightness and was related by an exponential function to the agronomic variable, i.e., fresh phytomass, dry phytomass, and water content. The angular transformation is

$$A_v = a + b\ \mathrm{Exp}(c(\tan^{-1}(G/B))) \quad (2)$$

where A_v is the predicted agronomic variable of interest, G and B are greenness and brightness transformations (from Table 7-1), respectively, and a, b, and c are coefficients determined by the nonlinear regression program (NLIN) of SAS (Helwig and Council, 1979).

The angular transformation model was developed by studying the relationship of the various agronomic variables to the greenness and brightness. Figure 7-1 is a plot of eleven fresh phytomass classes (0-10). Class 0 represents all measurements with fresh phytomass less than 5% of the maximum fresh phytomass in the data set. Class 1 represents all observations from 5% to 15% of maximum phytomass. Classes 2 through 10 represent similar class divisions. A plot of the angular transformation vs. the log of the fresh phytomass measurements (Figure 7-2) indicates that this transformation is related to fresh phytomass by an exponential function. The nonlinearity in the relationship at low angles represents (1) the noise in the measurements of small phytomass, and (2) the error introduced by sampling the canopy phytomass outside the field of view of the radiometer. When evaluating crop condition to estimate eventual final yields, accurate estimates of phytomass are less critical in young (low phytomass) than older corn canopies (larger phytomass). Therefore, the scatter of the data at low phytomass and angle should not significantly limit the utility of the model. Similar results were obtained with plots of dry phytomass and water content.

Table 7-1. Transformations of Landsat band used to relate spectral data to fresh and dry canopy phytomass and water content.

Name of Transformation	Equation
IR3/Red	R3/R2†
IR4/Red	R4/R2
Normalized Difference	(R4-R2)/(R4+R2)
Transformed Vegetative Index	((R4-R/(R4+R2) + 0.5))0.5
Brightness	0.374R1 +0.461R2 +0.544R3 +0.594R4
Greenness	-0.447R1 -0.619R2 +0.145R3 +0.629R4
Yellowness	-0.809R1 +0.571R2 +0.134R3 -0.050R4
Nonsuch	0.038R1 +0.289R2 -0.816R3 +0.499R4

† R1,...R4 = reflectance factor for wavelength bands 0.5-0.6, 0.6-0.7, 0.7-0.8, and 0.8-1.1 μm, respectively.

ORIGINAL PAGE IS
OF POOR QUALITY

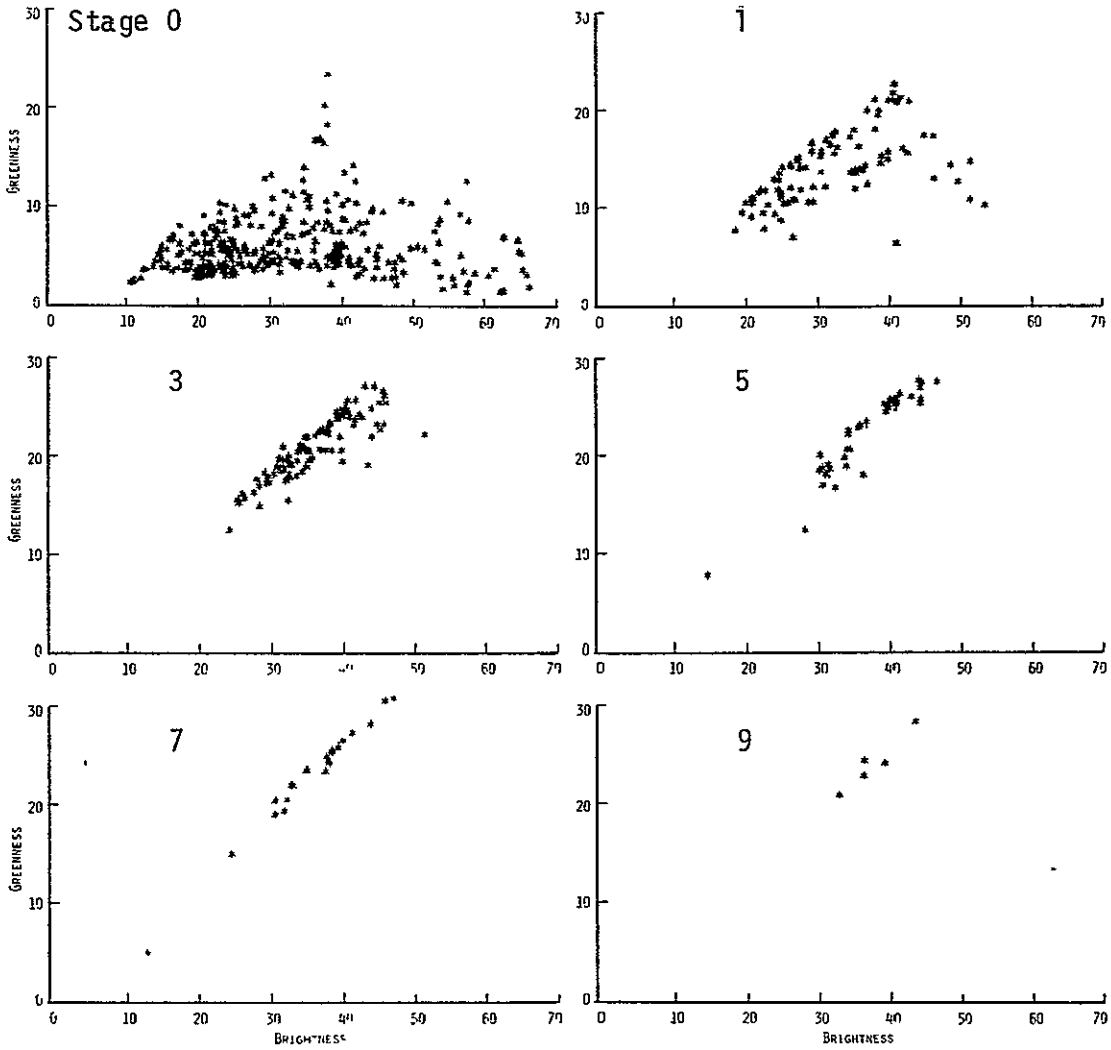

Figure 7-1. Distribution of phytomass classes as a function of greenness and brightness.

ORIGINAL PAGE IS
OF POOR QUALITY

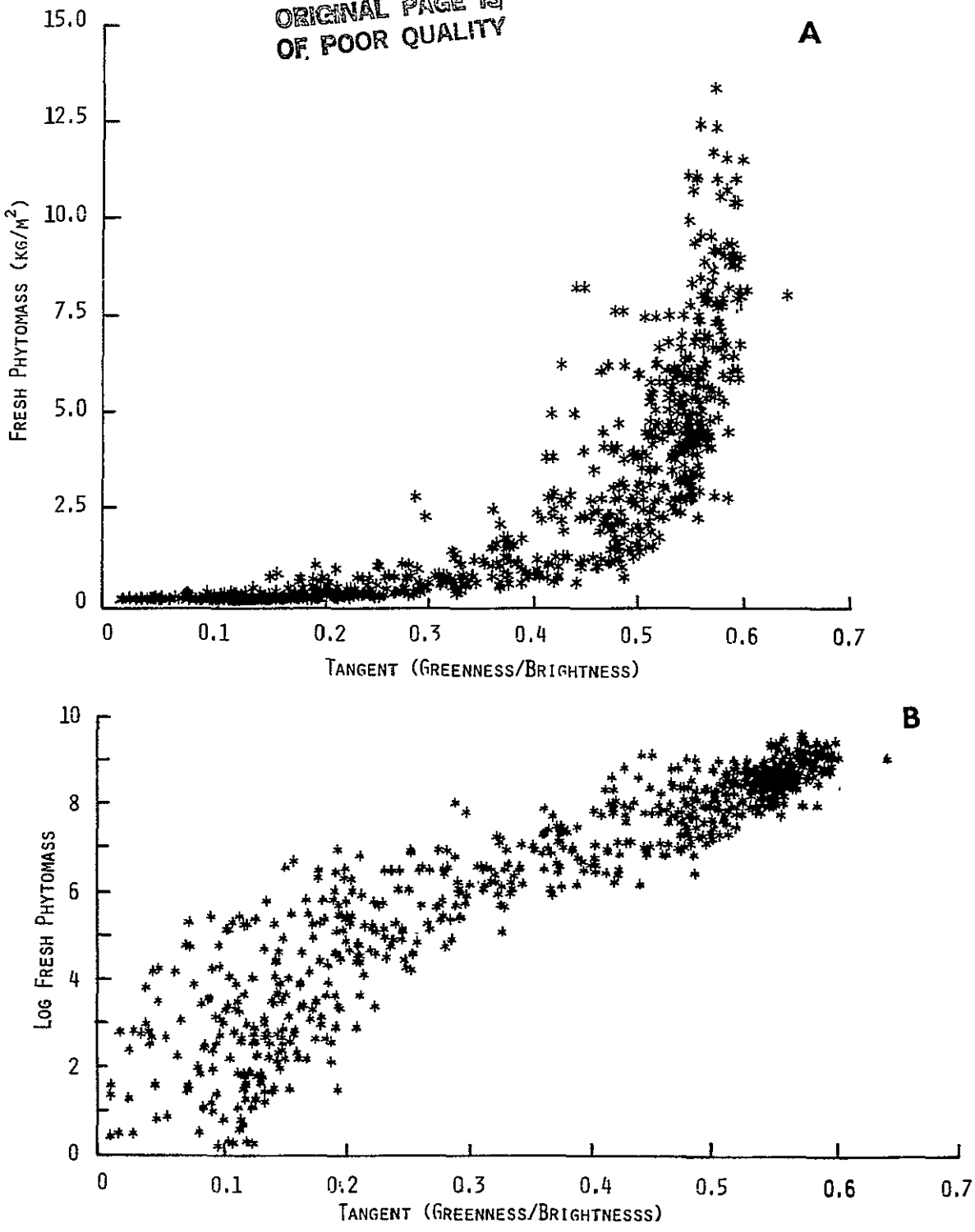

Figure 7-2. Relationship between the greenness-brightness angular transformation and the log of fresh phytomass.

Results

The agronomic data (total fresh phytomass, total dry phytomass, and total water content) were examined to determine the effects of treatments. The treatments that showed the greatest differences in the agronomic variables were evaluated with the spectral data to determine how well the spectral data explained the observed agronomic differences.

Agronomic Data. Canopy phytomass and water content (Figure 7-3) were distinctly different in the two years (1979 and 1980) used to develop these models. The weather in 1979 was wetter than normal with normal temperatures. Rainfall in June, July, and August was -3.5, +84, and +50 mm different from normal, respectively. Mean daily temperatures were 0.2, 1.4, and 1.3 C below normal for June, July, and August, respectively. During the 1980 growing season, the rainfall was above normal for June and July (+63 and +64 mm, respectively) and slightly below normal in August (-2.5 mm). However, the mean daily temperature was 1.7 and 1.8 C above normal in July and August. The high temperatures in 1980 resulted in 47 mm more water being evaporated during June, July, and August than in 1979. Under normal conditions in West Central Indiana, more water will be lost by the corn crop through evapotranspiration than it receives in the form of rain during the growing season. The additional water use in 1980 resulted in a greater stress during the late vegetative stage and therefore reduced vegetative phytomass.

Differences in canopy phytomasses and water content were observed in population treatments in 1979 and 1980 (Figure 7-3). After blister stage (maturity = 6) in 1980, corn plants from 25,000 plant/ha had a greater phytomass than plants from 50,000 and 75,000 plants/ha. This may be attributed to the less favorable weather conditions in 1980 and was probably the result of these more dense populations running out of subsoil moisture earlier than the 25,000 plant/ha population. This increase in phytomass was due to a larger grain yield in the least dense population than in the more dense populations in 1980. Since the phytomass in the 25,000 plant/ha population became greater than the phytomass in the 50,000 and 75,000 plant/ha populations after the canopy was fully established, it was not evident in the spectral data.

Soil types had no statistically observed effect on canopy phytomass or water content. Planting date treatments had an effect when the data were examined as a function of the day of year. This is because the more mature plots had greater amounts of phytomass and water content than less mature plots on the same day. These differences become discernible for plots with planting dates greater than two weeks apart. When the same data were studied as a function of development stage, the effect of planting date was not discernible.

ORIGINAL PAGE IS
OF POOR QUALITY

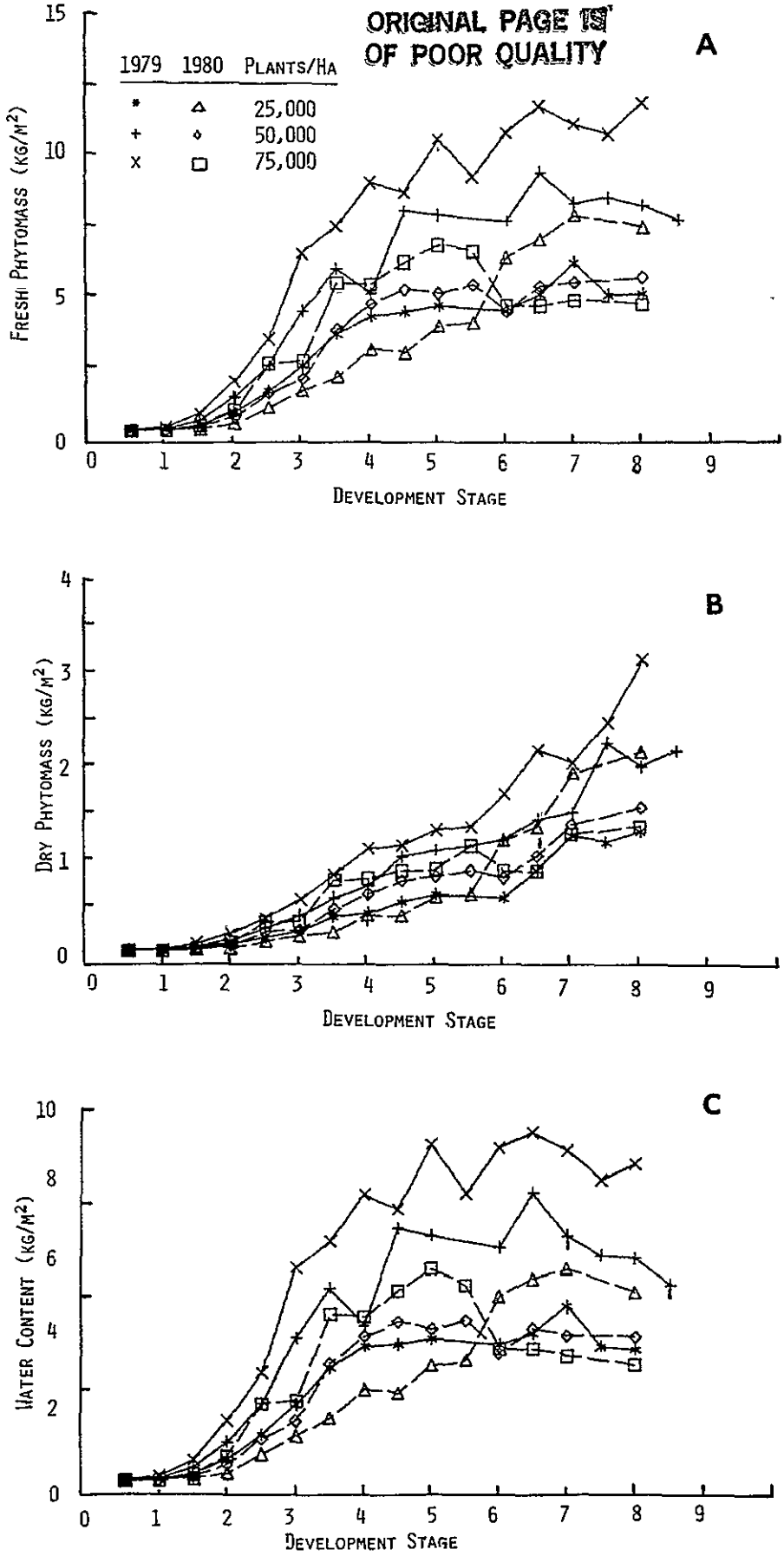

Figure 7-3. Effect of population and year on fresh phytomass, dry phytomass, and water content.

Spectral Data. The linear coefficient of determination (r2) for fresh and dry phytomass and water content as a function of the spectral transformations are presented in Table 7-2. The highest linear correlation to the three canopy variables was obtained with IR4/Red ratio which explained 76% of the fresh phytomass variability, 49% of the dry phytomass variability, and 79% of the water content variability. Similar results were obtained for the IR3/Red band ratio. Plots of the greenness, normalized difference, and transformed vegetative index transformations revealed a strong curvilinear relationship with fresh and dry phytomass and water content. Therefore, the smaller linear coefficient of determination with these later transformations should be expected.

Table 7-3 shows a comparison of the root mean square error (RMSE) of the nonlinear model using the angular transformation and the linear IR-Red ratio model. In all three populations and for all three variables, the angular transformation of the greenness/brightness ratio shows a higher degree of precision. The angular transformation, involving the greenness and brightness of the four bands rather than just two bands, provides more precise information about the condition of the crop.

Coefficients for the general model (Eq. 2) for each of the three population treatments were determined using nonlinear regression techniques (Table 7-4). The table includes the model coefficient with their corresponding 95% confidence intervals. The only coefficient with values significantly different from each other was a in Eq. 2. The difference was due to population. Therefore, to estimate canopy phytomass and water content accurately, plant density must be known or estimated.

To test the performance of the model throughout the crop season, the models for the three separate populations were used to predict values for each population. The residuals of the three models were summed for all the development stages to determine how the models performed as a group. Of particular interest was how well the models performed at different development stages. Plots of the predicted fresh phytomass, dry phytomass and water content in 1979 and 1980 are shown in Figure 7-4.

The predicted phytomass and water content fall within the 95% confidence interval when the canopy is between the 12-14 leaf stage of development and blister stage (e.g. maturity stages 3 to 6) Before the 12-14 leaf stage, the models overpredict phytomass and water content and after blister stage they underpredict. Failure of the models to predict phytomass and water content during reproductive stages of development was a result of leaf senescence which reduces greenness and as a result of dry matter being accumulated mainly in the ear. Since the area of the ear is small compared to the green leaves and contributes very little to the reflectance of the canopy, detection of ear phytomass increases is not possible with passive remote sensing techniques. Results of a test of the models on an independent set of data, 1981, are presented in Figure 7-5. Note that for fresh phytomass, the results are the same as for the 1979, 1980 data. Results for dry phytomass and water content in 1981 are similar to the 1979, 1980 results. The steep decrease in predicted phytomass in 1981 following dent stage is a result of reduced canopy reflectence due to senescence.

Table 7-2. Linear coefficients of determination between spectral band combinations and canopy fresh and dry phytomass and water content.

Spectral Combination	Coefficient of Determination (r^2)		
	Phytomass		
	Fresh	Dry	Water Content
IR3/Red	0.74	0.46	0.77
IR4/Red	0.76	0.49	0.79
Normalized Difference	0.61	0.43	0.63
Transformed Vegetative Index	0.59	0.41	0.60
Brightness	0.10	0.05	0.10
Greenness	0.63	0.42	0.65
Yellowness	0.17	0.11	0.18
Nonsuch	0.08	0.15	0.07

Table 7-3. Comparison of root mean square errors (RMSE) of angular transformation model to RMSE of linear infrared/red ratio model.

	Population (plants/ha)					
	25000		50000		75000	
	Spectral Model					
Variable	G/B†	IR/R§	G/B	IR/R	G/B	IR/R
Fresh phytomass	1162	1304	377	395	820	946
Dry phytomass	1138	1247	315	343	920	981
Water content	1581	1749	418	447	1264	1391

† $A_V = a + b\ \mathrm{Exp}(c(\tan^{-1}(G/B)))$

§ $A_V = a + b\ (R4/R2)$

Table 7-4. Coefficients and 95% confidence interval of coefficients for the general model (Eq. 2).

Agronomic Variable/ Population	General Model Coefficients a	b	c
Fresh Phytomass			
25000	-916.6 ± 904.1	515.9 ± 545.7	4.3 ± 1.7
50000	-138.0 ± 264.2	60.0 ± 42.0	8.1 ± 1.2
75000	58.7 ± 378.5	7.0 ± 8.3	12.2 ± 2.1
Dry Phytomass			
25000	-194.8 ± 350.5	109.9 ± 9.6	3.9 ± 3.2
50000	-35.4 ± 78.3	12.6 ± 9.7	7.6 ± 2.1
75000	-19.8 ± 109.6	3.0 ± 6.0	10.3 ± 3.4
Water Content			
25000	-721.1 ± 612.9	406.6 ± 362.7	4.4 ± 1.4
50000	-103.7 ± 211.2	48.0 ± 32.2	8.3 ± 1.2
75000	80.1 ± 288.2	4.7 ± 5.4	12.6 ± 2.0

ORIGINAL PAGE IS
OF POOR QUALITY

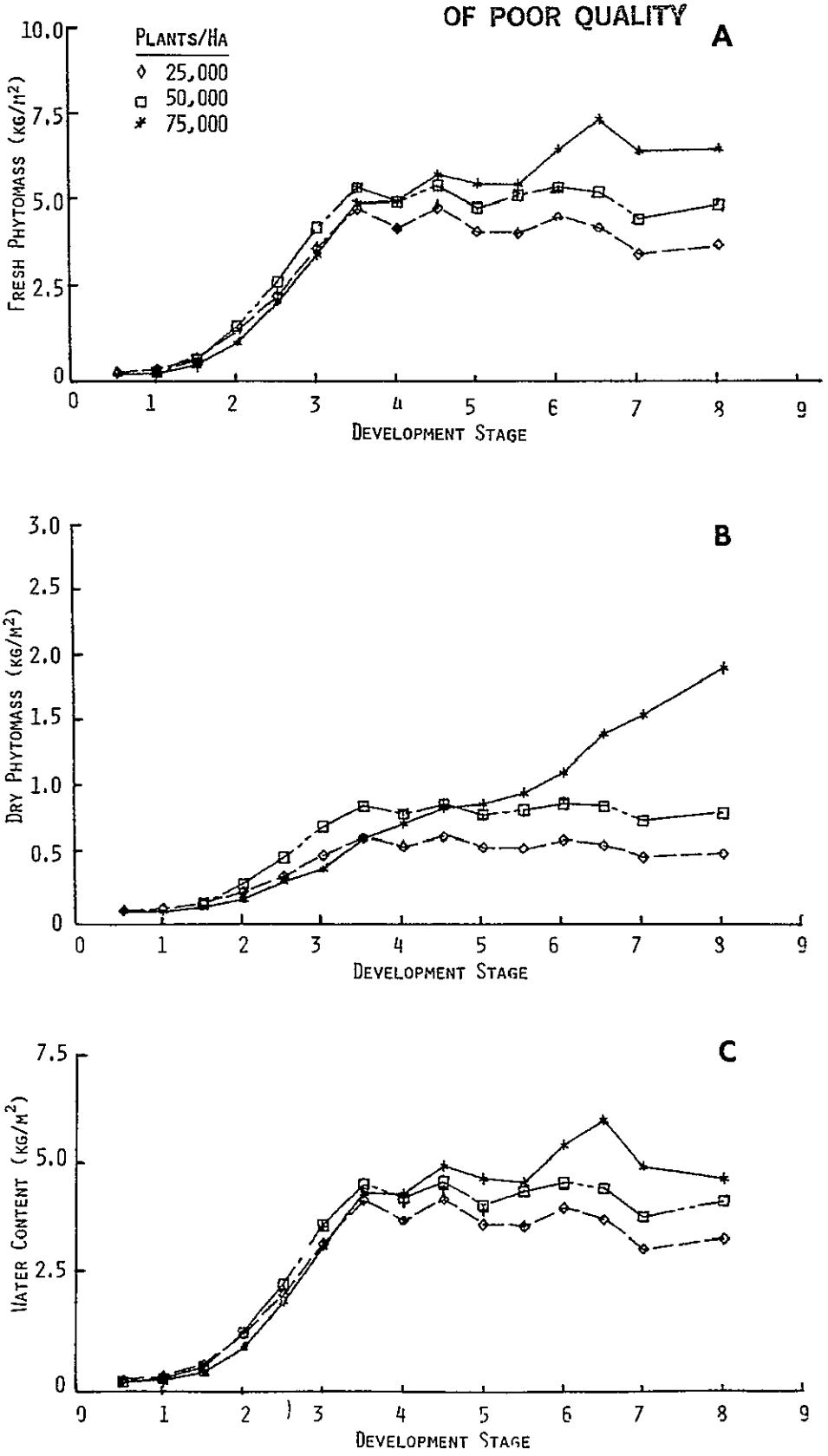

Figure 7-4. Results of predicting 1979 and 1980 fresh phytomass (a), dry phytomass (b), and water content (c) using the equations developed with the 1979 and 1980 data for each of the three plant populations.

ORIGINAL PAGE IS
OF POOR QUALITY

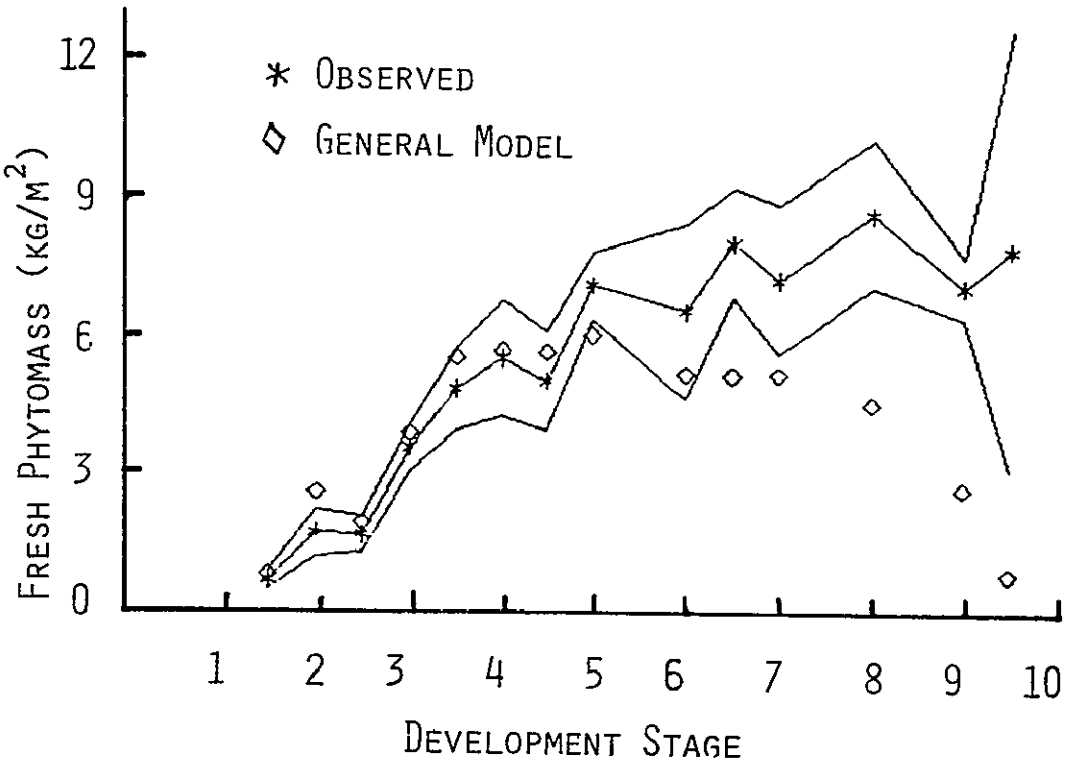

Figure 7-5. Results of applying the models for fresh phytomass to 1981 field plot data.

Microwave backscattering is sensitive to the mass of ears and stems of a corn canopy (Eger et al., 1982). This has led to the speculation that a combination of microwave and multispectral data could be used throughout the season to determine canopy phytomass and to estimate eventual yield. A particular time of interest would be the period after blister stage of corn development.

The estimates of phytomass using this method could be made even more accurate if independent estimates of crop population density and development stage were known. These estimates may be possible from other spectral models. Potentially, the angular transformation models could improve the accuracy of surface soil moisture estimates from microwave remote sensing. Such estimates are subject to large errors because sensors cannot differentiate between water in the soil surface and water in the canopy.

The estimate of phytomass is most accurate when the vegetation phytomass is at a maximum. Since the final yield of corn is related to the amount of vegetative plant material, these estimates could be combined with meteorological crop models or some harvest index model to more accurately estimate final yields over a large area.

It is important to remember that the spectral signature of any canopy is an integration of the reflectance properties of the soil and of the canopy structure and geometry. As such, the model will be most sensitive to changes in canopy characteristics from planting until the canopy is fully developed. Once the canopy is fully developed, additional phytomass increases will not be easily detected with the models since the increase in phytomass does not greatly affect the canopy's spectral signature.

Summary

A transformation of greenness and brightness was related to fresh and dry phytomass and water content. The transformation included the angle of rotation to the greenness level from the soil brightness line and a logrithmic transformation of the phytomass and water content data. Improvements in the relationship between the spectral data and the canopy variables were obtained using this technique. The model performed best during the period from the 12-14 leaf fully emerged stage of development to blister stage. This is fortunate because it provides an estimate of phytomass and water content at a stage of growth when the corn crop is most susceptible to weather extremes.

Thus, a better estimate of the soil surface water content might be obtained by subtracting the canopy water content (provided by the angular transformation) from the total surface water content (obtained from microwave measurements).

References

1. Carlson, R. E., D. N. Yarger, and R. H. Shaw. 1971. Factors affecting the spectral properties of leaves with special emphasis on leaf water status. Agron J. 63:486-489.

2. Daughtry, C. S. T., M. E. Bauer, D. W. Crecelius, and M. M. Hixson. 1980. Effects of management practices on reflectance of spring wheat canopies. Agron J. 72:1055-1060.

3. Eger, G. W., F. T. Ulaby, and E. T. Kanemasu. 1982. A three-part geometric model to predict radar backscatter from wheat, corn, and sorghum. AgRISTARS Support Research Project Report SR-K2-04313, University of Kansas, Center for Research, Inc., Lawrence, KS.

4. Helwig, J. T. and K. A. Council. 1979. SAS user's guide. SAS Institute, Raleigh, NC.

5. Holben, Brent N., Compton J. Tucker, and Cheng-Jeng Fan. 1980. Spectral assessment of soybean leaf area and leaf biomass. Photogrammetric Engineering and Remote Sensing 46:651-656.

6. Kauth, R. J., P. F. Lambeck, W. Richardson, G. S. Thomas, and A. P. Pentland. 1979. Feature extraction applied to agricultural crops as seen by landsat. In Proc. of Technical Sessions, Vol 2, LACIE Symposium, July 1979. JSC16015. NASA/Johnson Space Center, Houston, TX 77058.

7. Millar, B. D. and O. T. Denmead. 1976. Water relations of wheat leaves in the field. Agron. J. 68:303-307.

8. Nicodemus, F. E., J. C. Richmond, and J. J. Hsia. 1977. Geometrical considerations and nomenclature for reflectance. NBS Monogr. 160. Inst. for Basic Standards, Washington, DC 20234.

9. Noggle, G. R., and G. J. Fritz. 1976. Introductory Plant Physiology. Prentice-Hall, Inc., Englewood Cliffs, NJ. 688p.

10. Robinson, B. F., and L. L. Biehl. 1979. Calibration procedures for measurement of reflectance factor for remote sensing field research. Proc. Soc. Photo-optical Instrumentation Engr. 196:16-26. 23rd Annual Tech. Symp. on Measurements of Optical Radiation. Bellingham, WA.

11. Thomas, J. R., V. I. Myers, M. D. Heilman, and C. L. Wiegand. 1966. Factors affecting light reflectance of cotton. Remote Sensing of Environment Symp. Proc. (Institute Science and Technology, Univ. of Mich.) 4:305-311.

12. Tucker, Compton J. 1979. Red and photographic infrared linear combinations for monitoring vegetation. Remote Sensing of Environment 8:127-150.

13. Tucker, Compton J. 1980. Remote sensing of leaf water content in the near infrared. Remote Sensing of Environment 10:23-32.

14. Tucker, Compton J., J. H. Elgin Jr., and J. E. McMurtrey III. 1979. Temporal spectral measurements of corn and soybean crops. Photo. Eng. and Remote Sensing 45:643-653.

15. Wilson, C. C., W. R. Boggess, and P. J. Kramer. 1953. Diurnal fluctuations in moisture content of some herbaceous plants. Amer. J. Bot. 40:97-100.

IV. Registration Research

PRECEDING PAGE BLANK NOT FILMED

8. CORRELATIVE AND NONCORRELATIVE APPROACHES TO IMAGE REGISTRATION

P.E. Anuta

Introduction

Image registration research during the period covered in this report addressed several topics relevant to improving registration performance on time-sequential scenes of the earth's surface. Several approaches to preprocessing and correlation were evaluated as alternatives and one was tested on Landsat data. Results were not promising and attention was turned to noncorrelative methods for scene-matching with the intent of developing a method which performs well for scenes which are very dissimilar. These investigations are reported in the following sections.

Alternative Image Correlation Methods

The most-often used approach to image correlation for registration is to use a gradient preprocessing operation followed by product correlation to determine translational misregistration between two images. Numerous approaches to the preprocessing and correlation process have appeared in the literature, each claiming performance advantage over others. Among those studied are phase correlators (Chan, 1978) which measure the phase shift between two images to estimate misregistration and others which use various preprocessing approaches. Knapp (1976) presents a very good review and comparison of registration processors and carries out a solution for the optimum processor. The optimum turns out to be a phase-shift detection approach with a frequency weighting which is the inverse of the cross-spectral density of the signals or images being registered. The only assumption made for the development is that the signal and noise are Gaussian. The problem with this method is that the spectral density must be known or predicted and performance degrades as the estimate accuracy degrades. A method showing promise for alleviating the prediction problem was presented by (Chan, 1980) which models the misregistration as a digital filter and solves for the unknown shift by estimating the parameters of the filter which would produce an observed shift. This method demonstrated good performance in the literature and was chosen for implementation and testing.

A product of the development of the optimum correlators is an expression for the variance of the misregistration estimate. A form of this expression is given in Knapp as:

$$\mathrm{VAR}[D] = \frac{\int_{-\infty}^{\infty} |\psi(f)|^2 (2\Pi f)^2 \, G_{x_1 x_1}(f) \, G_{x_2 x_2}(f) \left[1 - |\alpha(f)|^2\right] df}{T\left[\int_{-\infty}^{\infty} (2\Pi f)^2 \, | \, G_{x_1 x_2}(f) \, | \, \psi(f) df\right]^2}$$

PAGE 138 INTENTIONALLY BLANK PRECEDING PAGE BLANK NOT FILMED

where: $\psi(f)$ is the preprocessing weighting filter

$G_{x_1x_1}$, x_2x_2 , x_1x_2 is the spectral density for the signals or images indicated in the subscript

$\alpha(f)$ is the coherence of the two signals or images:

$$\alpha(f) = \frac{G_{x_1x_2}(f)}{\sqrt{G_{x_1x_1}(f)\, G_{x_2x_2}(f)}}$$

T is the integration time or distance of the correlation process.

Another result is that for the case where the signal-and-noise spectra have the same functional form, several candidate methods have the same variance, are optimum, and achieve the Cramer-Rao lower bound. Evidence has been presented by Svedlow (1976) that Landsat images of the earth scene (the signal) and the temporal change (the noise) between scene times have the same form of spectral density. In this case, the variance can be evaluated in terms of only a signal-to-noise ratio defined as the ratio of the signal variance to the noise variance.

A further relationship can be derived between the correlation coefficient between the two scenes to be registered and the signal-to-noise ratio. In one dimension, the development is:

Let: X_1 = the signal (image at Time 1 which is a zero mean random signal

$X_2 = X_1 + n$ to be the signal (image) at Time 2

Assume the noise n is independent of the signal and that it has zero mean. Then the correlation coefficient between X_1 and X_2 is:

ORIGINAL PAGE IS
OF POOR QUALITY

$$\rho_{12} = \frac{E\left[X_1 X_2\right]}{\sqrt{E\left[X_1^2\right] E\left[X_2^2\right]}}$$

$$= \frac{E\left[X_1 (X_1+n)\right]}{\sqrt{\sigma_1^2 (\sigma_n^2+\sigma_{x_1}^2)}}$$

$$= \frac{E\left[X_1^2\right] + E\left[X_1 n\right]}{\sigma_{x_1} \sqrt{\sigma_{x_1}^2+\sigma_n^2}}$$

Since X_1 and n are independent $E[X_1 n] = 0$ and:

$$\rho_{12} = \frac{\sigma_{x_1}^2}{\sigma_{x_1} \sqrt{\sigma_{x_1}^2+\sigma_n^2}}$$

The signal-to-noise ratio is defined as:

$$SNR = \frac{\sigma_{x_1}^2}{\sigma_n^2}$$

Thus: $$\rho_{12} = \frac{\sqrt{SNR}}{\sqrt{SNR+1}}$$

or: $$\rho_{12}^2 = \frac{SNR}{SNR+1}$$

or: $$SNR = \frac{\rho 12^2}{1-\rho_{12}^2}$$

A signal-to-noise ratio of one corresponds to a correlation between the two images of .707 and this is generally considered to be a threshold between "well" correlated and poorly correlated scenes.

One of the preprocessing methods discussed in Knapp is called the Roth filter and has the same performance as the optimum filter. It has a frequency weighting filter defined by:

$$\psi(f) = \frac{1}{G_{x_1 x_1}(f)}$$

The registration estimate standard deviation is plotted in Figure 8-1 for the case of no preprocessing and for the Roth filter as a function of correlations coefficient between the two signals (scenes) being registered. Current requirements for images registration accuracy are in the .2 to .3 pixel range. With no preprocessing, this error is exceeded when scene correlation goes below .6; but with preprocessing, the error is exceeded below a correlation of .19. The advantage of preprocessing is clear.

Some insight into the variation in scene-to-scene correlation with time between acquisitions was obtained by computing the correlation between registered Landsat MSS data over one season. Correlation coefficients between all pairs of times are plotted in Figure 8-2 as a function of days of separation or acquisition for a span of time of March through October 1981. A wide variation in values is observed and this is expected since during some parts of the season, the scene changes very little and over others the change is dramatic. Nonetheless a steadily decreasing trend is observed and a visually sketched trend line is included in the figure. A rapid drop in correlation in the first 36 days is evident with a slower taper-off after that. The point of this development of scene correlation and registration estimate error properties is to demonstrate the relationship between scene correlation and error and show that error tolerances will be exceeded for scenes differing by relatively short intervals in time using conventional techniques.

Before investigating methods which may give improved performance, a numerical evaluation of several data sets was carried out to evaluate what performance was actually being obtained. The data base available for the evaluation is listed in Table 8-1 and contains segments from Central United States and Argentina. Block correlation without preprocessing was carried out on pairs of these images. The location of the peak of the correlation function relative to the zero shift position is listed in Table 8-2 for six of these data sets. The values of shift are plotted as a function of correlation coefficient in Figure 8-3. The results generally tend to group around the Roth filter curve; however, what is not shown on the curve are the numerous cases which were drastically in error. In the sample here, 17% of the correlations were considered failures. This is a problem not

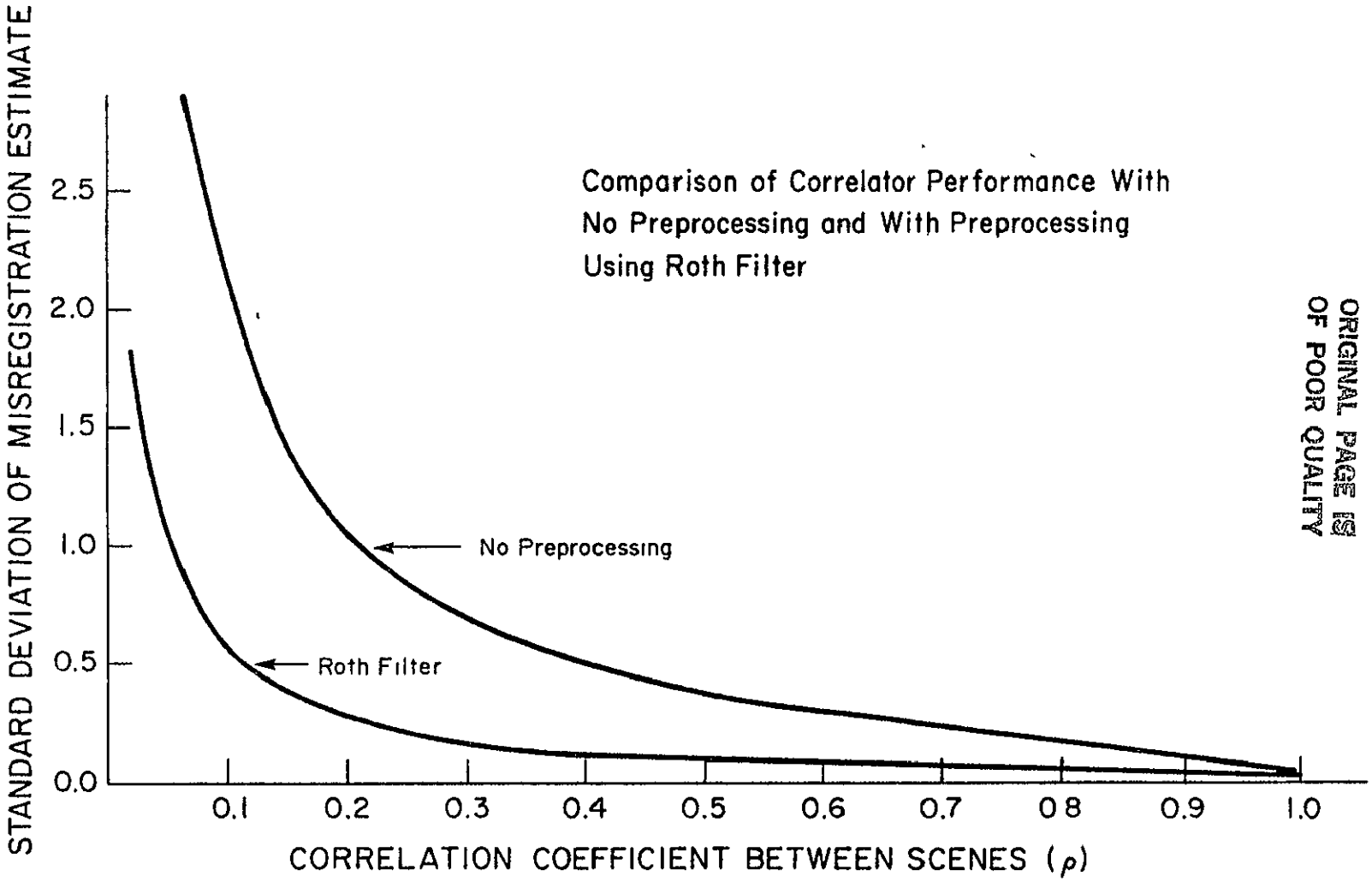

ORIGINAL PAGE IS
OF POOR QUALITY

Figure 8-1. Comparison of correlator performance with no preprocessing and with preprocessing. using Roth filter.

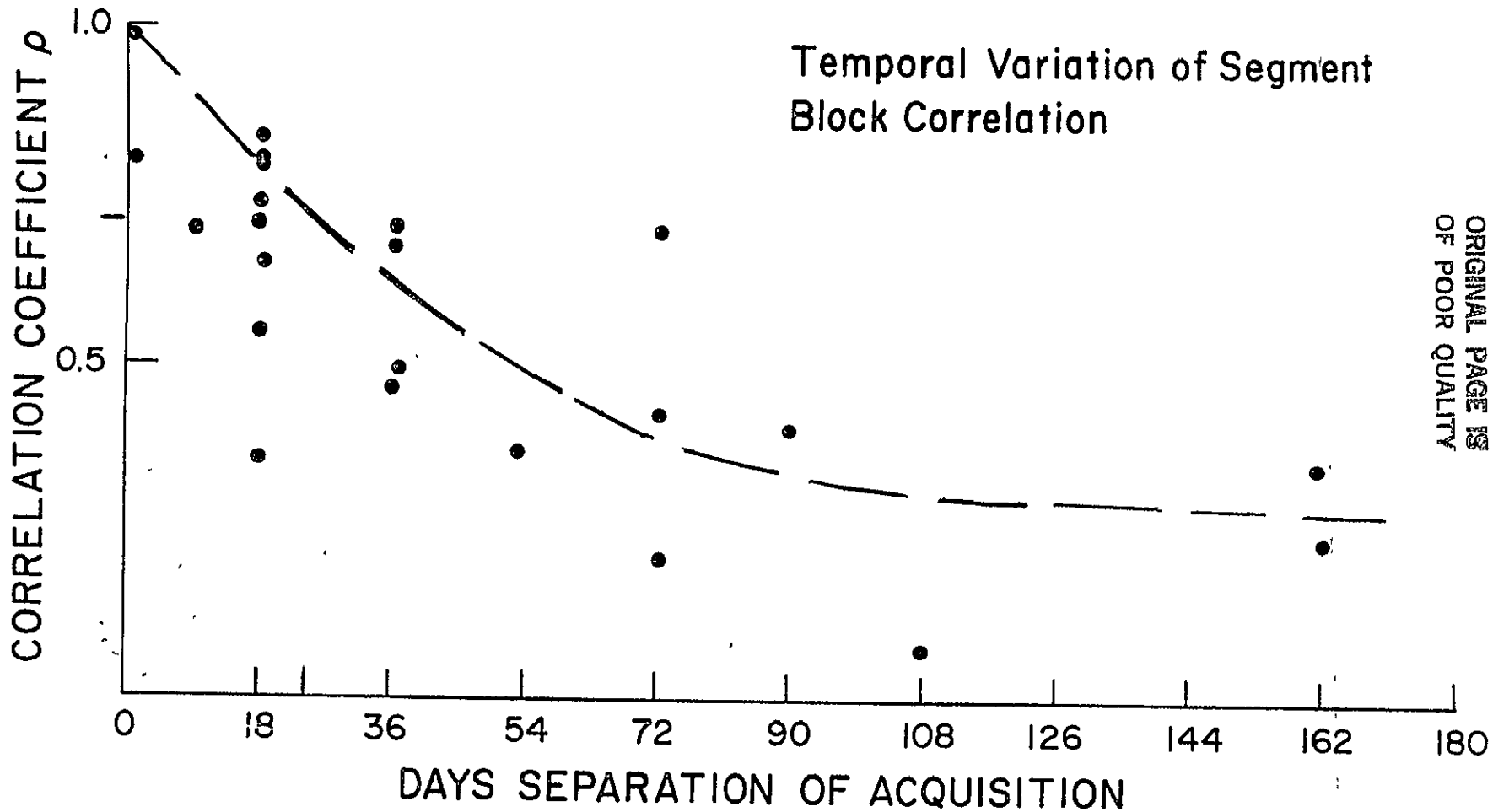

Figure 8-2. Temporal variation of segment block correlation.

ORIGINAL PAGE IS
OF POOR QUALITY

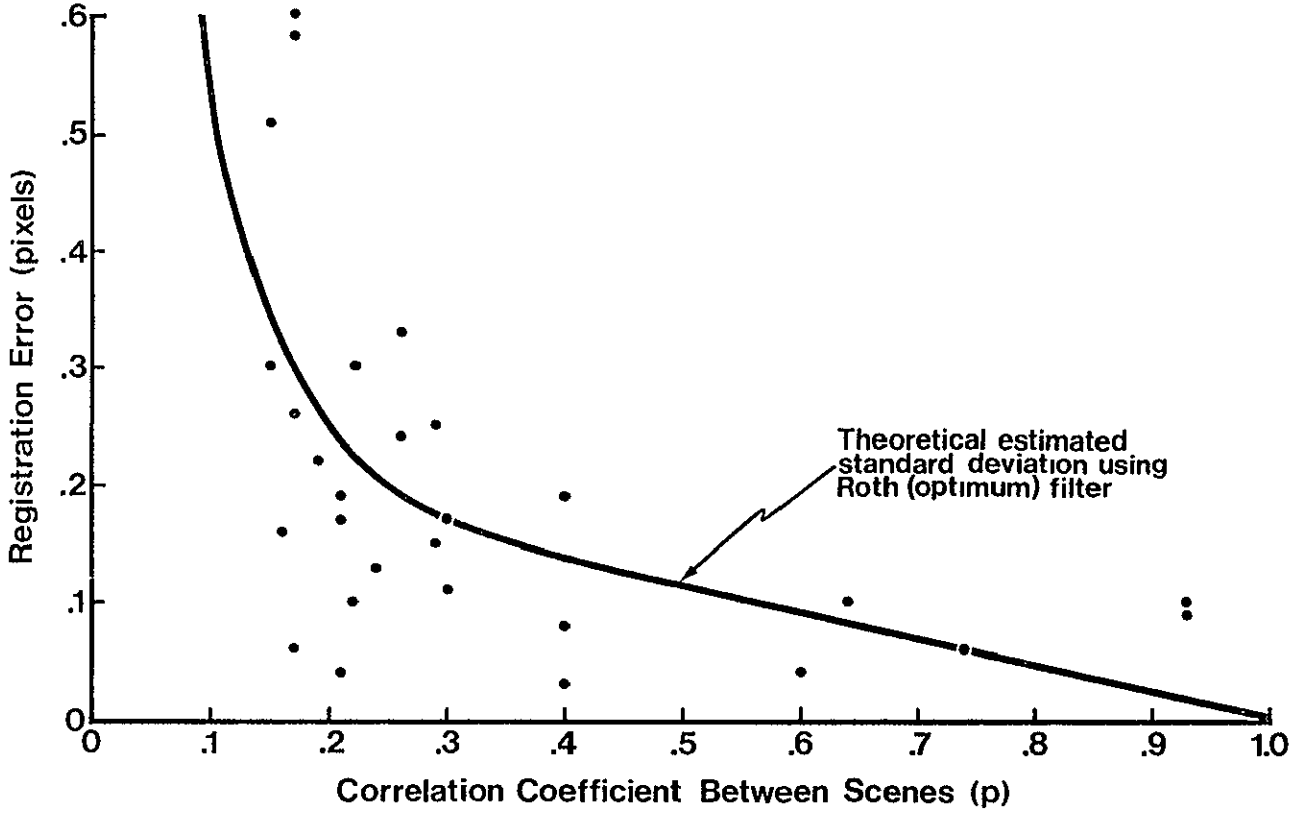

Figure 8-3. Results of correlation tests on registered MSS imagery from AgRISTARS segments.

Table 8-1. Data Base for Registration Algorithm Research

Run I.D.	Segment	Acquisitions	Run I.D.	Segment	Acquisitions
81077000	203	4	81190000	9529	3
81077001	204	4	81064001	9530	3
81202000	---	2	81064002	9531	4
81078000	209	4	81078002	9534	2
81187000	---	3	81065000	9535	2
81078001	1177	2	81092001	9537	4
81183000	9501	2	81236000	9537	2
81183001	9502	2	81183002	9541	2
81092000	9525	4	81092002	9543	4
91204000	9526	2	81236001	9543	2
81107000	9527	2	81092003	9545	3
81107001	9528	3	81079001	893	4
81064000	9529	4	81079002	893	2

ORIGINAL PAGE IS
OF POOR QUALITY

Table 8-2. Evaluation of JSC registration processor output.

RUN: 81064000

	CHANNEL 2 DAY 64					CHANNEL 3 DAY 99					CHANNEL 4 DAY 153				
	ρ_{MAX}	SNR	BLOCK COR. ΔC	BLOCK COR. ΔL	PAR. EST. COR.	ρ_{MAX}	SNR	BLOCK COR. ΔC	BLOCK COR. ΔL	PAR. EST. COR.	ρ_{MAX}	SNR	BLOCK COR. ΔC	BLOCK COR. ΔL	PAR. EST. COR.
CHANNEL 3 DAY 99	0.26	0.07	0.20	-0.13											
CHANNEL 4 DAY 153	0.17	0.03	0.03	-0.05		0.24	0.06	-0.10	0.09						
CHANNEL 1 DAY 172	0.21	0.05	0.11	0.13		0.21	0.05	-0.03	0.03		0.40	0.19	0.13	0.14	

ORIGINAL PAGE IS
OF POOR QUALITY

Table 8-2. (Continued)

RUN: 81092000

	CHANNEL 2 DAY 92					CHANNEL 1 DAY 200					CHANNEL 3 DAY 201				
	ρ_{MAX}	SNR	BLOCK COR. ΔC	BLOCK COR. ΔL	PAR. EST. COR.	ρ_{MAX}	SNR	BLOCK COR. ΔC	BLOCK COR. ΔL	PAR. EST. COR.	ρ_{MAX}	SNR	BLOCK COR. ΔC	BLOCK COR. ΔL	PAR. EST. COR.
CHANNEL 1 DAY 200	0.15	0.02	0.22	-0.46											
CHANNEL 3 DAY 201	0.15	0.02	-0.17	0.25		0.93	6.40	-0.09	-0.01						
CHANNEL 4 DAY 236	0.30	0.10	-0.02	0.11		0.30	0.10	0.17	-0.10		0.29	0.09	0.24	0.07	

ORIGINAL PAGE IS
OF POOR QUALITY

Table 8-2. (Continued)

RUN: 81064002

	CHANNEL 2 DAY 64					CHANNEL 3 DAY 172					CHANNEL 1 DAY 190				
	ρ_{MAX}	SNR	BLOCK COR. ΔC	BLOCK COR. ΔL	PAR. EST. COR.	ρ_{MAX}	SNR	BLOCK COR. ΔC	BLOCK COR. ΔL	PAR. EST. COR.	ρ_{MAX}	SNR	BLOCK COR. ΔC	BLOCK COR. ΔL	PAR. EST. COR.
CHANNEL 3 DAY 172	0.17	0.03	0.11	0.24		—				—	—				—
CHANNEL 1 DAY 190	0.22	0.05	-0.19	-0.23		0.22	0.05	0.04	0.09		—				—
CHANNEL 4 DAY 226	0.16	0.03	—	—		0.15	0.02	0.11	-0.34		0.29	0.09	0.03	0.15	

ORIGINAL PAGE IS
OF POOR QUALITY

Table 8-2. (Continued)

RUN: 81079001

	CHANNEL 1 DAY 79					CHANNEL 2 DAY 115					CHANNEL 3 DAY 151				
	ρ_{MAX}	SNR	BLOCK COR. ΔC	BLOCK COR. ΔL	PAR. EST. COR.	ρ_{MAX}	SNR	BLOCK COR. ΔC	BLOCK COR. ΔL	PAR. EST. COR.	ρ_{MAX}	SNR	BLOCK COR. ΔC	BLOCK COR. ΔL	PAR. EST. COR.
CHANNEL 2 DAY 115	0.64	0.69	0.07	-0.07											
CHANNEL 3 DAY 151	0.60	0.56	0.03	-0.02		0.74	1.21	-0.03	0.05						
CHANNEL 4 DAY 187	0.26	0.07	0.33	-0.04		0.29	0.09	-0.10	-0.11		0.33	0.12	32.0	0.67	

ORIGINAL PAGE IS
OF POOR QUALITY

Table 8-2. (Continued)

RUN: 81092001

	Channel 2 Day 92					Channel 3 Day 191					Channel 1 Day 200				
	ρ_{MAX}	SNR	Block Cor.		Par. Est. Cor.	ρ_{MAX}	SNR	Block Cor.		Par. Est. Cor.	ρ_{MAX}	SNR	Block Cor.		Par. Est. Cor.
			ΔC	ΔL				ΔC	ΔL				ΔC	ΔL	
Channel 3 Day 191	0.17	0.03	-0.29	0.52											
Channel 1 Day 200	0.19	0.04	0.09	-0.20		0.25	0.07	0.08	0.79						
Channel 4 Day 218	0.16	0.03	0.15	0.05		0.07	0.00	-4.93	-3.84		0.21	0.05	-0.14	-0.13	

ORIGINAL PAGE IS
OF POOR QUALITY

Table 8-2. (Concluded.)

RUN: 81092002

	CHANNEL 2 DAY 92					CHANNEL 1 DAY 200					CHANNEL 3 DAY 201				
	ρ_{MAX}	SNR	BLOCK COR. ΔC	BLOCK COR. ΔL	PAR. EST. COR.	ρ_{MAX}	SNR	BLOCK COR. ΔC	BLOCK COR. ΔL	PAR. EST. COR.	ρ_{MAX}	SNR	BLOCK COR. ΔC	BLOCK COR. ΔL	PAR. EST. COR.
CHANNEL 1 DAY 200	0.40	0.19	0.07	-0.04											
CHANNEL 3 DAY 201	0.40	0.19	0.00	-0.03		0.93	6.40	0.06	-0.08						
CHANNEL 4 DAY 218	0.11	0.01	6.64	-1.05		0.15	0.02	5.96	-1.29		0.15	0.02	6.03	-1.23	

ORIGINAL PAGE IS
OF POOR QUALITY

revealed in the linear theory and is the cause of faulty image registration results. A good distribution of accurate points is required for good uniform image registration and failures in correlation can cause poor results even though the theory may have predicted good overall results.

The correlator due to Chan, called the parameter estimation method cited above, was investigated as a potentially more robust algorithm since, in effect, it predicts the weighting function rather than assumes it, as most other methods do. The theoretical development of the algorithm is outlined in the Appendix. A one-dimensional version was implemented and tested on the segment data. Results are not encouraging, as the algorithm failed on all scene pairs having correlations below .5. This could have been due to its being one-dimensional and shifts existing in the orthogonal direction could be causing a drop in correlation below what would allow the algorithm to operate. Further investigation of this and other novel schemes was not pursued in this study to enable efforts to be focused on unique, new approaches to scene matching which would take into account scene spatial and temporal structure. These efforts are discussed next.

Image Analysis Methods for Registration

A majority of the image registration methods available today use classical correlation as the basis for determining misregistration between image pairs. In these methods, no consideration is made of scene structure and temporal variation characteristics other than to assume probability density and spatial correlation functions. In the approach investigated here, temporally invariant known features are attempted to be located in an image. Locating these features in an image pair will provide matching control points which can then be used to register the images.

The type of imagery of greatest interest in this study is agricultural land which is predominantly composed of rectangular fields distributed throughout a rectangular grid of roads. In some parts of the world, fields are nonrectangular and the road pattern random, but for major production areas, the rectangularity is a valid assumption. Also, misregistration is generally small enough or can be made small by locating one unique feature, such as a bend in a river or a small urban area, so that matching roads can be paired unambiguously. Thus the approach tested here is location of roads and road intersections in Landsat imagery of nominally mile-square grid agricultural terrain.

The operation basic to detection of roads, edges, or any linear feature is edge detection. There are two basic approaches to edge detection: One clusters image pixels into homogeneous groups (Kettig, 1976) and defines edges at the boundaries of these groups (conjunctive approach). The second uses differential or template edge operators (Abdou, 1979) to detect step jumps in image gray level as an indication of an edge.

A third method, called disjunctive, starts with an entire image and subdivides given blocks if they are found to be dissimilar (Robertson, 1973), but the method has not been widely discussed in the literature. The

differential/template method is by far the most widely used as it is simple, low-cost, local, and produces very good results.

The reason for the clustering approach is that it produces closed boundaries which are required for classification of the set of points within the boundary as is desired in Kettig's work. Here we only seek a good edge detection to allow fitting of road models to the possibly noisy discontinuous edges.

Edge-detection methods were investigated by LARS in previous Supporting Research (Anuta, 1982). Of the several differential and template operators, the Sobel 3 by 3 operator appeared to perform generally the best. This is verified by Abdou and other authors. Nonetheless the Hueckel edge operator is of interest because it gives an edge detection decision and the orientation of the edge in a window (Hueckel, 1973). It uses a set of eight basis functions which it fits to an image disk and bases its decision on the results of the mask products with the image disk. Figure 8-4 shows the basis functions and image disk. Figure 8-5 shows the output parameters of the algorithm. It provides edge height (t), width (r), orientation (α), and left and right base levels (b-,b+). For our purposes here, we need only α and the position of the edge in the disk. This algorithm was applied to test imagery from Webster County, Iowa. The algorithm was first applied to the original imagery with very poor results. In a second test, it was applied to edge detected imagery produced by the Sobel operator. Generation of the Sobel edge image is discussed next.

The Sobel operator consists of a vertical and horizontal 3 by 3 mask defined as:

$$H_1 = \begin{bmatrix} 1 & 0 & -1 \\ 2 & 0 & -2 \\ 1 & 0 & -1 \end{bmatrix} \qquad H_2 = \begin{bmatrix} -1 & -2 & -1 \\ 0 & 0 & 0 \\ 1 & 2 & 1 \end{bmatrix}$$

The operator value for the pixel at the center of the mask is obtained by multiplying each mask value by the underlying pixel value and summing the products to get H_1 and H_2. Then the output value is:

$$G = \sqrt{H_1^2 + H_2^2}$$

The edge is defined for the center pixel if G is above a threshold.

$$\text{Define edge if } G \geq T$$

A gray-scale image of the test site is shown in Figure 8-6 for MSS Band 5 (.6-.7μm) and the Sobel edge image for the area is shown in Figure 8-7. The threshold T is set based on the a priori probability of an edge for a

ORIGINAL PAGE IS
OF POOR QUALITY

- FITS A SET OF BASIS FUNCTIONS TO AN IMAGE DISK

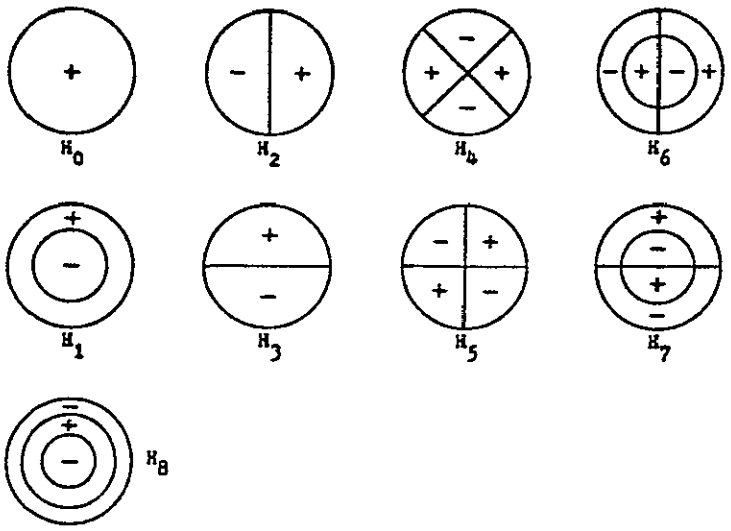

- IMAGE DISK OF 69 PIXELS USED:

		1	2	3	4	5		
	12	11	10	9	8	7	6	
13	14	15	16	17	18	19	20	21
30	29	28	27	26	25	24	23	22
31	32	33	34	35	36	37	38	39
48	47	46	45	44	43	42	41	40
49	50	51	52	53	54	55	56	57
	64	63	62	61	60	59	58	
		65	66	67	68	69		

Figure 8-4. Basis function and image disk of Hueckel line- and edge-finding algorithm.

ORIGINAL PAGE IS
OF POOR QUALITY

- OUTPUT IS SUCCESS/FAIL DECISION AND THE EQUATION OF THE LINE/EDGE FOR SUCCESSFUL FITS PLUS EDGE PARAMETERS:

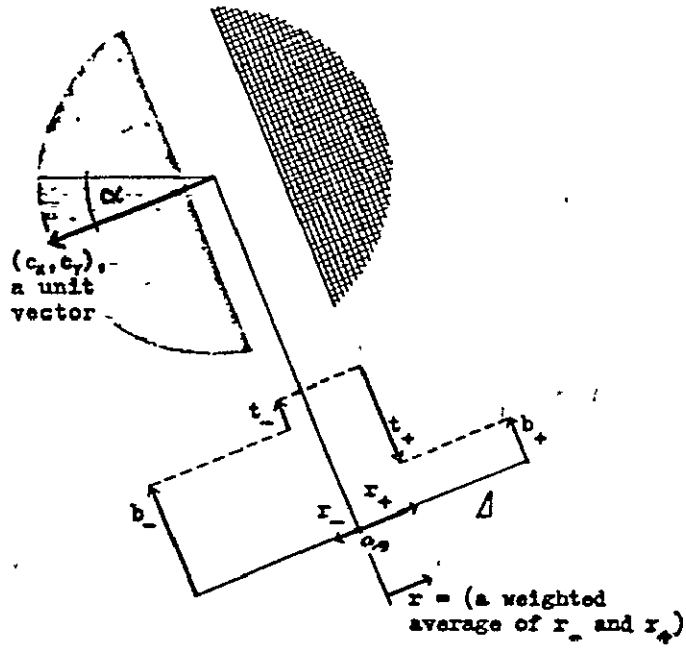

- OUTPUT EQUATION IS:

$$X \cos \alpha + Y \sin \alpha = R$$

Figure 8-5. Output parameters of Hueckel line/edge-finding algorithm.

ORIGINAL PAGE IS
OF POOR QUALITY

particular image. For the images of the type considered here, generally 15% of the pixels are edge pixels; thus T was set so that 15% of the gradient pixels are classed as edges based on the histogram of the entire G image. The question of edge classification is discussed in more detail in a following section.

A second step in preparation for road detection was to visually define road intersection in the image and compute the parameters of a line along each road. A straight line is defined by two parameters and when the parameters are R and θ for the equation is of the form:

$$X \cos\theta + Y \sin\theta = R$$

The R,θ representation is commonly called the Hough transform of the line (Duda, 1972). The Hough transform for major roads in Segment 893 in the coordinates of the digital image is given in Table 8-3. A plot of the coordinates in R,θ space is presented in Figure 8-8.

A second method for road detection was also investigated. In this case, a straight line is fit to the edge points inside a window enclosing the expected position of a road. A least-squares fit criterion is used. The classical least-squares equations have a singularity at a slope angle of 90° so a method called the eigenvector fit is used which does not have this problem. This method can be described by the following matrix equations:

Given N data points X_i, Y_i $\quad i = 1 \ldots N$

Compute the scatter matrix:

$$\underline{S} = (\underline{X} - \underline{M}^t)(\underline{X} - \underline{M})$$

$$\underline{X}^t = \begin{matrix} x_1 & x_2 & & x_n \\ & \cdots & & \\ y_1 & y_2 & & y_n \end{matrix} \qquad \underline{M} = \text{mean vector of } \underline{X}$$

Compute the eigenvalues of S from:

$$\underline{S} - \lambda I = 0$$

Find λ_1, λ_2. Select the largest λ (λ_L).

ORIGINAL PAGE IS
OF POOR QUALITY

Figure 8-6. Gray-scale image of Webster County, Iowa test site.

ORIGINAL PAGE IS
OF POOR QUALITY

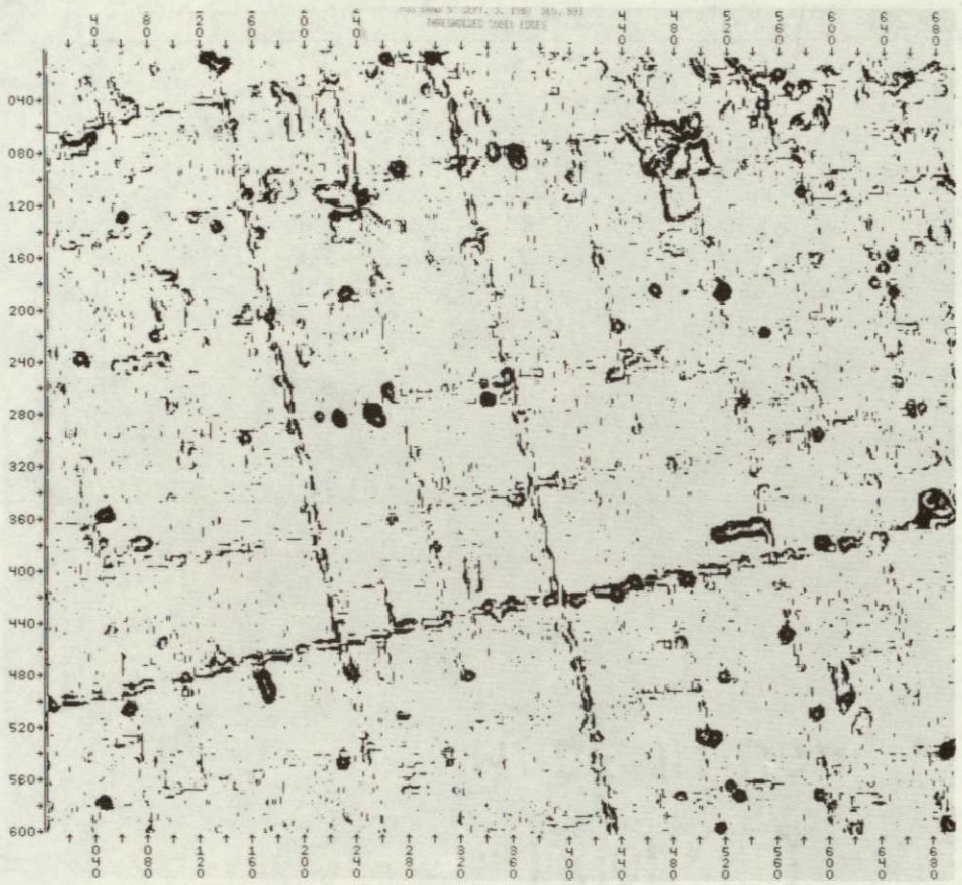

Figure 8-7. Sobel edge image of Webster County, Iowa test site.

Table 8-3. Hough transform for major roads in coordinates of the digital image for Webster County, Iowa site (Run 80002400, Band 5, September 3, 1980).

Point 1		Point 2			
Line	Col.	Line	Col.	ρ	θ
34	65	174	95	56.4	12.1
48	126	160	150	113.1	12.1
86	192	178	210	171.9	11.1
109	252	190	273	216.6	14.5
73	15	185	40	0	12.6
28	93	137	116	85.2	11.9
34	65	22	120	47.1	-77.7
61	70	48	126	75.2	-76.9
117	82	86	192	134.8	-74.3
145	88	109	252	160.5	-77.6
173	95	138	260	190.3	-77.7
198	101	165	264	214.1	-78.5

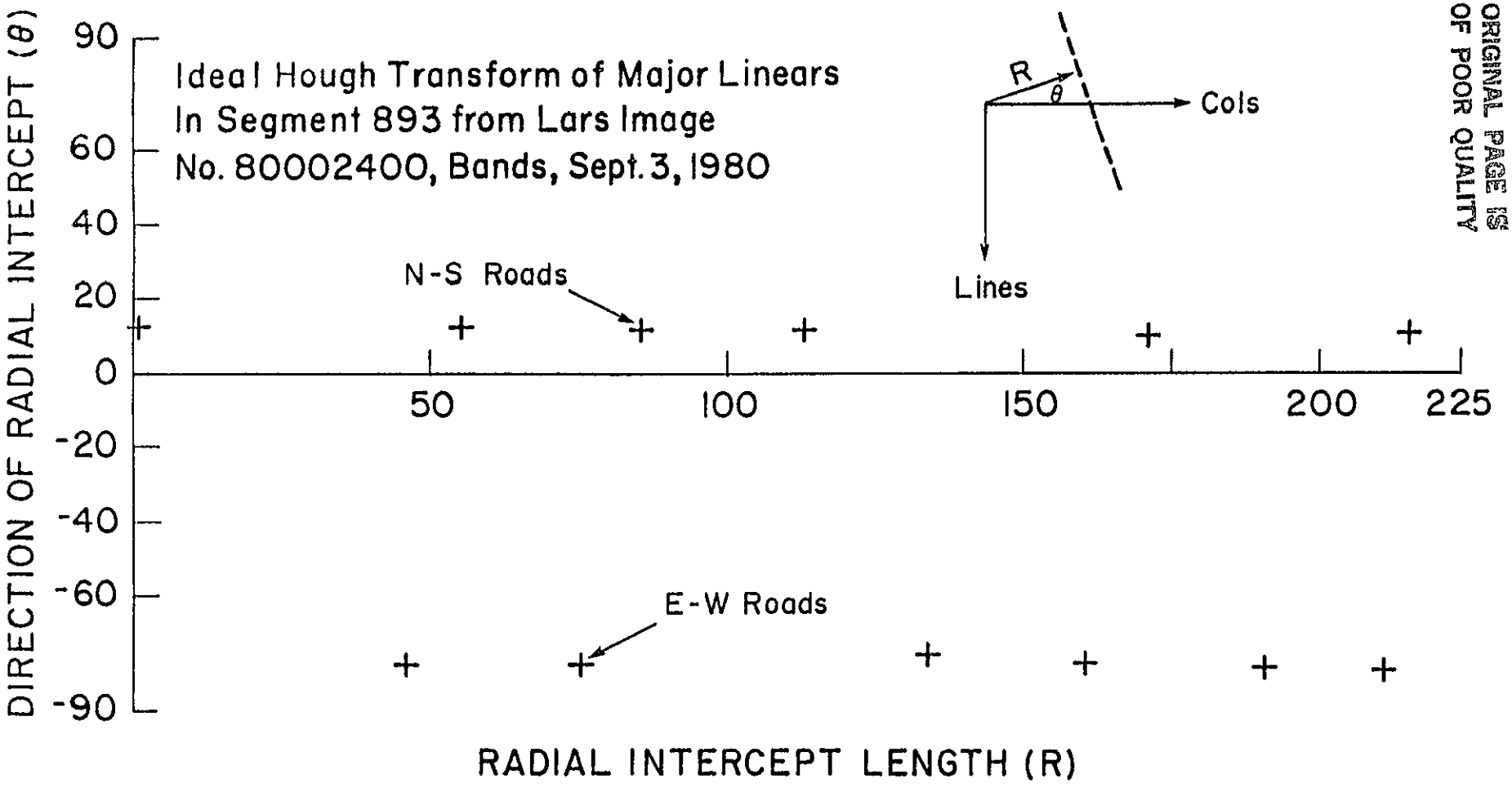

Figure 8-8. Plot of coordinates for major roads. Webster County, Iowa test site (see Table 8-1).

Compute the eigenvector for λ_L: $\underline{X}_L$

$$\left[\underline{S} - \lambda_L I\right] \underline{X} = 0$$

Least-squares line passes through M and has direction of $\underline{X}_L$. This method avoids singularities in classical least-squares fit.

The Hueckel and eigenvector methods were applied to the edge image for the Webster County, Iowa site. The eigenvector method requires that a window be defined for each road so that only edge pixels which are for the particular road are fitted. Figure 8-9 contains the window logic implemented for this test. A width of ±10 pixels was defined for the road window and this corresponds to a registration uncertainty of ±10 pixels or 570m for Landsat MSS data.

The Hueckel algorithm was applied to the edge image in Figure 8-7 and the results were again unsatisfactory. Figure 8-10 contains results for eight tests using 69 pixel disks positioned over clear road edges. The eigenvector method was also applied to each disk. The 100s represent edges and the 0s represent no-edge. The expected angles are nominally 12.1° and -77.6° for the N-S and E-W roads and the results are scattered widely around these numbers. The eigenvecteor fit tended to perform better than the Hueckel but the scatter of Hough coordinates was large. Figure 8-11 contains a plot of the Hough coordinates for results over a particular road showing the scatter. It was concluded that the pixel disk being tested was too small and the road edges too noisy to permit good clustering of road coordinates and further work should be conducted on the small disk or window approach.

The large-window approach was tested next using the eigenvector fit. Rectangular windows were positioned over the 12 significant roads in Segment 893 and the position coordinates for each were obtained from eigenvector fits of the edge image. Table 8-4 contains the coordinate of the mean and the angle of the eigenvector and the Hough coordinates for the 12 test roads. This method is intended to find control points; thus the road estimates were used to solve for intersection of all pairs of N-S and E-W roads. This was done for the true and estimated roads and these results are in Table 8-5. The error between estimated and ideal intersections was computed and listed in Table 8-6. This table is an evaluation of the end product that we are attempting to obtain from this process. Clearly, the accuracy of the position of the points will decrease with distance from the mean point and we believe this is evident in the large errors for E-W and N-S Road 6 and to a certain extent the No. 1 roads. The error means are subpixel but the standard deviations reflect the large errors for certain of the roads.

Work is continuing on this approach to finding control points with the goal of finding a method which is more stable for widely time-separate registration image pairs. The conclusion at this time is that the method looks promising but further "cleaning" operations are needed to remove

ORIGINAL PAGE IS
OF POOR QUALITY

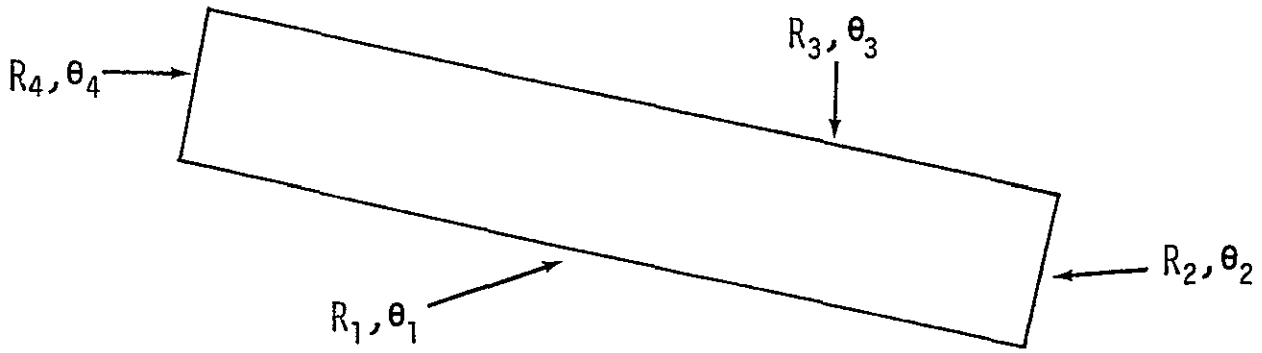

FOR A GIVEN LINE, COLUMN:

$$\text{COL. } 1 = \left(R_1 + \text{LINE} \cdot \sin(\theta_1)\right) / \cos(\theta_1)$$
$$\text{COL. } 2 = \left(R_2 + \text{LINE} \cdot \sin(\theta_2)\right) / \cos(\theta_2)$$
$$\text{COL. } 3 = \left(R_3 + \text{LINE} \cdot \sin(\theta_3)\right) / \cos(\theta_3)$$
$$\text{COL. } 4 = \left(R_4 + \text{LINE} \cdot \sin(\theta_4)\right) / \cos(\theta_4)$$

IF (COL .GT. COL1 .AND. COL .LT. COL2 .AND. COL .LT. COL3 .AND. COL .GT. COL4) THEN PIXEL IS IN RECTANGLE.

Figure 8-9. Window logic implemented for Webster County, Iowa test site by Hueckel and eigenvector methods.

ORIGINAL PAGE IS
OF POOR QUALITY

RUN 80002451 SEG. 893 BAND 5
DISK RADIUS 4.7

LINE 5 COL. 10 E-W ROAD
HUECKEL ANGLE -51.4 R = .09
EIGENVECTOR ANGLE -50.1 R = .3

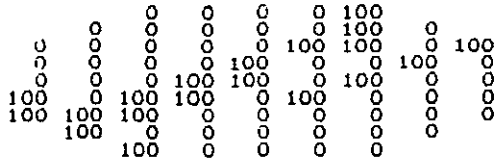

LINE 105 COL. 85 N-S ROAD
HUECKEL θ = 12.3 R = -.04
EIGEN θ = 14.0 R = -.07

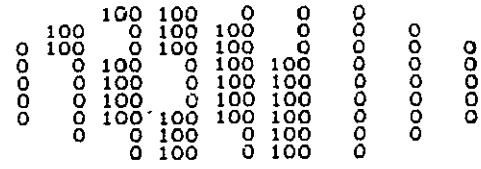

LINE 95 COL. 140 N-S ROAD
HUECKEL θ = 10.8 R = -.6
EIGEN θ = 15.5 R = .2

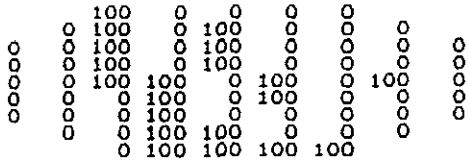

LINE 110 COL. 85 N-S ROAD
HUECKEL θ = 7.2° R = .06
EIGEN θ = 8.7° R = .3

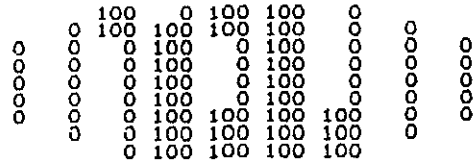

LINE 160 COL. 95 N-S ROAD
HUECKEL θ = 18.9 R = .46
EIGEN θ = 16.3 R = -.63

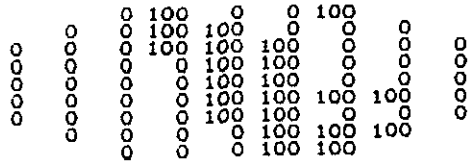

LINE 140 COL. 90 N-S ROAD
HUECKEL θ = 15.8 R = 4.4
EIGEN θ = 12.7 R = 1.3

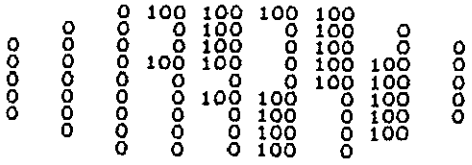

LINE 145 COL. 90 N-S ROAD
HUECKEL FAILED
EIGEN θ = 13.7 R = 1.23

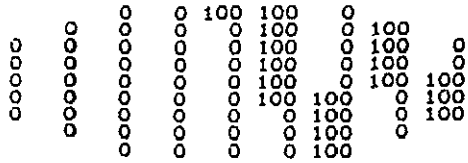

LINE 165 COL. 115 E-W ROAD
HUECKEL θ = -86.4 R = -.4
EIGEN θ = -83.9 R = -.2

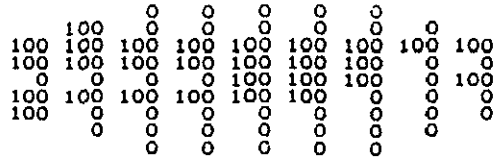

Figure 8-10. Results of eight tests using 69 pixel disks positioned over clear road edges. Hueckel algorithm was applied to the edge image and the eigenvector method was applied to each disk.

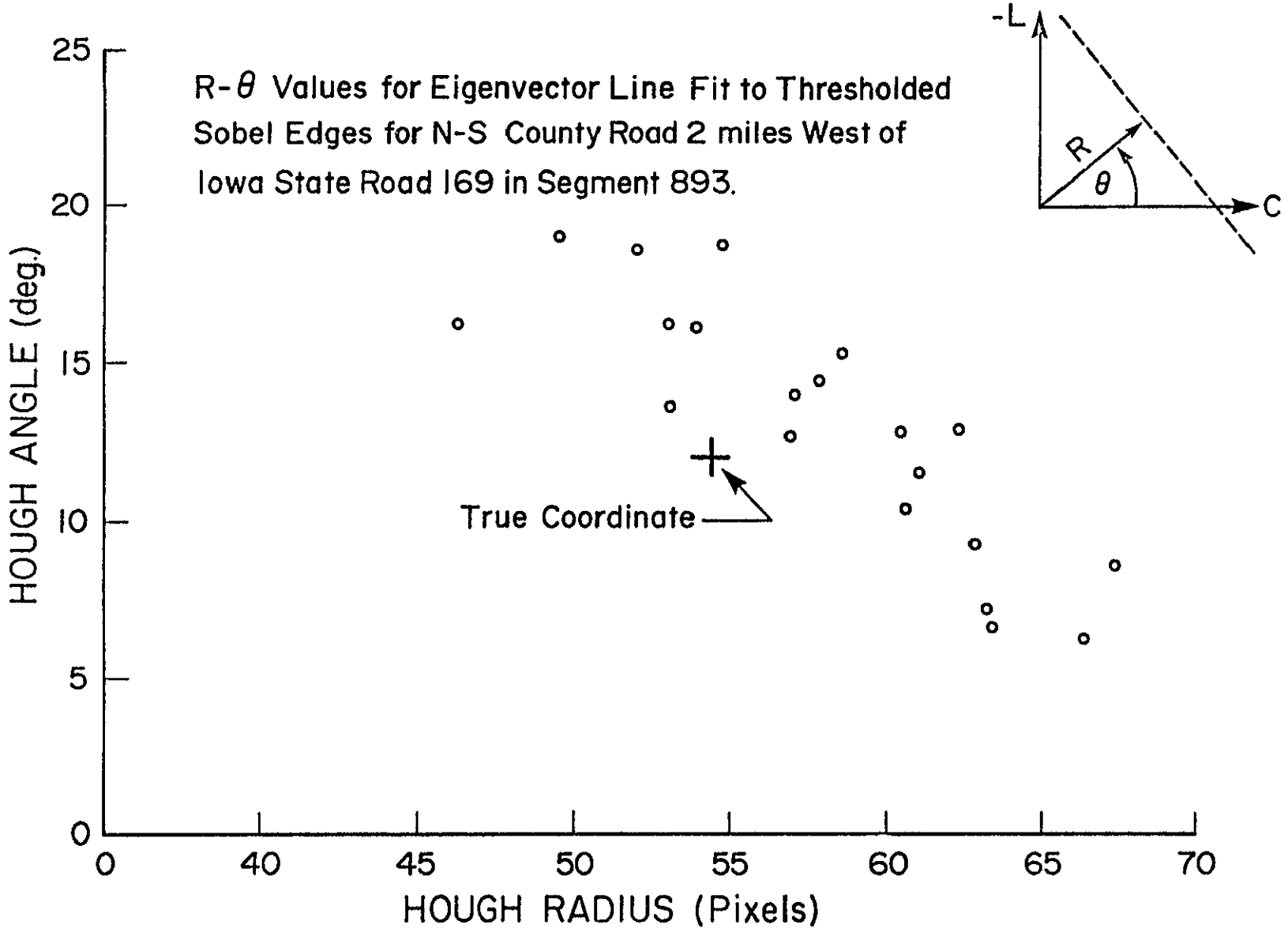

Figure 8-11. Scatter over a particular road shown by Hough coordinates.

ORIGINAL PAGE IS
OF POOR QUALITY

Table 8-4. Rectangular window line-finding algorithm results for segment 893.

WINDOW	NPIX	NEDGE	LINE MEAN	COL. MEAN	ANGLE	Hough Coordinates R	Hough Coordinates θ
1	3694	656	92.00	78.00	77.50	0.0	-12.6
2	4030	666	83.00	104.00	77.68	56.4	-12.1
3	3909	679	90.00	136.00	77.70	85.2	-11.9
4	3662	794	72.00	189.00	77.78	113.1	-12.1
5	3472	602	72.00	235.00	78.16	171.9	-11.1
6	3936	546	108.00	23.00	77.50	216.6	-14.5
7	4283	1123	22.00	121.00	-10.66	47.1	77.7
8	4640	1149	47.00	134.00	-11.92	75.2	76.9
9	4887	619	109.00	123.00	-12.02	134.8	74.3
10	4997	571	137.00	114.00	-11.92	160.5	77.6
11	5124	1118	166.00	122.00	-13.02	190.3	77.7
12	5220	537	192.00	120.00	-11.69	214.1	78.5

Table 8-5. Control-point solutions from ideal and estimated road locations.

IDEAL INTERSECTIONS

N-S Road	1		2		3		4		5		6	
E-W Road	Line	Col.	Line	Col.	Line	Col.	Line	Col.	Line	Col.	Line	Col.
1	46.0	10.3	34.0	65.0	27.9	93.0	22.0	120.4	9.6	177.1	- .5	223.6
2	73.4	16.4	60.8	70.7	54.3	98.5	47.9	125.9	34.9	182.0	23.7	229.9
3	131.7	29.4	116.8	82.7	109.1	110.1	101.4	137.4	86.0	192.1	71.9	242.3
4	156.6	35.0	144.8	88.7	138.8	116.3	132.6	144.1	120.6	198.8	108.9	251.9
5	185.7	41.5	174.1	95.0	168.1	122.5	162.0	150.4	150.2	204.6	138.2	259.5
6	209.0	46.7	198.1	100.2	192.5	127.6	186.8	155.7	175.8	209.7	164.3	266.2

ESTIMATED INTERSECTIONS

N-S Road	1		2		3		4		5		6	
E-W Road	Line	Col.	Line	Col.	Line	Col.	Line	Col.	Line	Col.	Line	Col.
1	42.8	10.4	32.6	64.8	27.5	91.9	22.0	121.2	11.6	176.0	3.3	220.6
2	71.7	16.8	60.3	71.0	54.6	97.8	48.5	127.0	37.0	181.5	27.6	225.7
3	128.9	29.5	117.4	83.6	111.7	110.3	105.5	139.4	93.9	193.7	84.6	237.6
4	153.1	34.9	141.6	89.0	136.0	115.6	129.9	144.7	118.4	199.0	109.2	242.8
5	184.4	41.8	172.0	95.7	165.9	122.1	159.2	151.1	146.7	205.0	136.6	248.6
6	207.1	46.9	195.9	101.0	190.5	127.5	184.4	156.6	173.2	210.7	164.2	254.3

ORIGINAL PAGE IS
OF POOR QUALITY

Table 8-6. Errors in road intersection coordinates for segment 893 (estimated - ideal).

	N-S Road											
	1		2		3		4		5		6	
E-W Road	ΔL	ΔC	ΔL	ΔC	ΔL	ΔC	ΔL	ΔC	ΔL	ΔC	ΔL	ΔC
1	-3.2	.1	-1.4	-.2	- .4	-1.1	0	.8	2.0	-1.1	3.8	-3.0
2	-1.7	.4	- .5	.3	.3	- .7	.6	1.1	2.1	- .5	3.9	-4.2
3	-2.8	.1	.6	.9	2.6	.2	4.1	2.0	7.9	1.6	12.7	-4.7
4	-3.5	-.1	-3.2	.3	-2.8	- .7	-2.7	.6	-2.2	.2	.3	-9.1
5	-1.3	.3	-2.1	.7	-2.2	- .4	-2.8	.7	-3.5	.4	-1.6	-10.9
6	-1.9	.2	-2.2	.8	-2.0	- .1	-2.4	.9	-2.6	1.0	- .1	-11.9

	Line	Column
Mean	-.23	.97
Std. Dev.	3.37	3.77

ORIGINAL PAGE IS
OF POOR QUALITY

along-road artifacts, such as homesteads and bright fields, which may be shifting the R and from the true value.

References

1. Abdou, I.E., and W.K. Pratt. 1979. Quantitative design and evaluation of enhancement/thresholding edge detectors. Proc. IEEE, 67(5):753-763.

2. Anuta, P.E., and C. Pomalaza. 1982. Comparison of edge detection methods and Landsat imagery, in M.E. Bauer and Staff, "Remote Sensing of Agricultural Crops and Soils," Annual Technical Summary and Final Report, Contract NAS9-15466, Laboratory for Applications of Remote Sensing, Purdue University, West Lafayette, IN 47906-1399. LARS Contract Report 113081, pp. 143-150.

3. Chan, Y.T., R.V. Hattin, and J.B. Plant. 1978. The least squares estimation of time delay and its use in signal detection, IEEE Trans. on Acoustics, Speech and Signal Processing. 26:217-222.

4. Duda, R.O., and P.E. Hart. 1972. Use of the Hough transform to detect lines and curves in pictures. ACM Commission 15:11-15.

5. Hueckel, M.H. 1973. A local visual operator which recognizes edges and lines. J. Assoc. for Computing Machinery, 20(4):634-647.

6. Kettig, R.L., and D.A. Landgrebe. 1976. Classification of multispectral image data by extraction and classification of homogeneous objects. IEEE Trans. on Geoscience Electronics 14(1):19-25.

7. Knapp, C.H., and C. Carter. 1976. The generalized correlation method for estimation of time delay. IEEE Trans. on Acoustics, Speech and Signal Processing 29:320-327.

8. Robertson, T.V. 1973. Extraction and classification of objects in multispectral images. Proc. Symp. on Machine Processing of Remotely Sensed Data, Purdue University, West Lafayette, IN, Oct. 16-18, 1973, pp. 3B/27-34.

9. Svedlow, M.E., C.D. McGillem, and P.E. Anuta. 1976. Analytical and experimental design and analysis of an optimal processor for image registration. LARS Technical Report 090776, Laboratory for Applications of Remote Sensing, Purdue University, West Lafayette, IN 47906-1399.

Appendix

PARAMETER ESTIMATION CORRELATION METHOD

METHOD IS BASED ON ASSUMPTION THAT CONTINUOUS IMAGE CAN BE REPRESENTED USING THE SINC FUNCTION (I.E., BAND LIMITED TO 1/2D). EVALUATION IS IN 1-DIMENSION. THE REFERENCE IS:

$$R(X) = \sum_{I=-\infty}^{\infty} S(ID)\ \mathrm{SINC}(X-ID)$$

THE MISREGISTERED SENSED IMAGE CAN THEN BE REPRESENTED AS:

$$s(X) = s(X + (L+F)\cdot D) = \sum_{I=-\infty}^{\infty} S(ID)\ \mathrm{SINC}(X+L+F-ID)$$

WHERE: D IS THE SAMPLE SPACING
L IS THE INTEGER SHIFT
F IS THE FRACTIONAL SHIFT

FOR CONVENIENCE, LET D=1 AND DEFINE K-I=N AND EVALUATE S AT INTEGER LOCATIONS:

$$s(K) = \sum_{K-N=-\infty}^{\infty} R(K-N)\ \mathrm{SINC}(N+L+F)$$

SINCE K IS FINITE, THE INDEX CAN BE IN TERMS OF N ONLY.

DEFINE: $\zeta_N = \text{SINC}(N+L+F)$

THEN THE RELATION BETWEEN S AND R BECOMES A CONVOLUTION OF S WITH A FILTER ζ:

$$S(K) = \sum_{N=-\infty} \zeta_N \, R(K-N)$$

THE ζ_N ARE SAMPLES OF THE FUNCTION SINC(X+L+F) WITH THE MAXIMUM AT X+L+F = 0.

IT CAN BE SHOWN THAT THE DESIRED SHIFT IS:

$$\Delta = L+F = -J + \frac{\zeta_{J-1}}{\zeta_J + \zeta_{J-1}}$$

WHERE: J IS THE INDEX OF THE MAXIMUM VALUE OF ζ_N

ORIGINAL PAGE IS
OF POOR QUALITY

A SIGNAL PLUS NOISE MODEL IS ASSUMED:

$$(x) = R(x) + \theta(x)$$

$$W(x) = S(x) + \Psi(x)$$

THE ζ_N IS TRUNCATED TO -P TO P AND BECOMES AN FIR FILTER.

THE PROBLEM BECOMES ONE OF ESTIMATING 2P+1 PARAMETERS ASSUMING N+1 DATA POINTS AVAILABLE. A LEAST SQUARES SOLUTION WAS IMPLEMENTED:

$$\hat{\underline{\zeta}} = (\underline{Z}^T \underline{Z})^{-1} \underline{Z}^T \underline{W}$$

WHERE:

$$\underline{W} = \begin{bmatrix} W_P \\ W_{P+1} \\ \vdots \\ W_{P+N} \end{bmatrix} \qquad \underline{Z} = \begin{bmatrix} Z_{2P} & Z_{2P-1} & \cdots & Z_0 \\ Z_{2P+1} & & & \\ \vdots & & & \\ Z_{2P+N} & \cdots & & Z_N \end{bmatrix} \qquad \underline{\zeta} = \begin{bmatrix} \zeta_{-P} \\ \vdots \\ \zeta_P \end{bmatrix}$$

ORIGINAL PAGE IS
OF POOR QUALITY

THIS SOLUTION CAN BE SHOWN TO BE EQUIVALENT TO THE ROTH PROCESSOR[2] WHICH COMPUTES THE CORRELATION FUNCTION AS:

$$H(X) = \int_{-\infty}^{\infty} \frac{G_{ZW}(\omega)}{G_{ZZ}(\omega)} E^{J\omega X_{DW}}$$

WHERE: $G_{ZW}(\omega)$ IS THE CROSS SPECTRAL DENSITY BETWEEN THE NOISE ADDED REFERENCE AND RECEIVED SIGNALS.

$G_{ZZ}(\omega)$ IS THE SPECTRAL DENSITY OF THE NOISY REFERENCE.

- THE ROTH PROCESSOR IS A SUB-OPTIMUM FILTER WHICH GIVES LESS WEIGHT TO FREQUENCIES WHERE THE NOISE IS LARGE.

- THE PERFORMANCE OF THE PARAMETER ESTIMATION CORRELATOR WAS EVALUATED ANALYTICALLY AND EXPERIMENTALLY. THE VARIANCE EXPRESSION IS:

$$VAR[\hat{D}] = \frac{2\Pi \int_{-\infty}^{\infty} |\psi(\omega)|^2 \omega^2 [G_{ZZ}(\omega) G_{WW}(\omega) - |G_{ZW}(\omega)|^2 DW}{L\left[\int_{-\infty}^{\infty} 2\psi(\omega) |G_{ZW}(\omega)| DW\right]^2}$$

WHERE: $\psi(\omega) = 1$ FOR NO PREPROCESSING

$\psi(\omega) \quad \frac{1}{G_{ZZ}(\omega)}$ FOR THE ROTH PROCESSOR

DISTRIBUTION

NASA Johnson Space Center
SA2: R. MacDonald
SC1: J. Erickson
SC2: I. Browne (6)
SC3: F. Hall
G. Badhwar
K. Henderson
G. Houston
D. Pitts
SC4: J. Dragg
R. Heydorn
D. Thompson
SC5: R. Hill
SC6: R. Musgrove
BB63: Carol Homan
JM6: Technical Library (4)
AT3: Technology Utilization Office
AP: Public Affairs Office

NASA Headquarters
EL4: H. Hogg

NASA Goddard Space Flight Center
920: V. Salomonson
923: R. Murphy

NASA Ames Research Center
D. Peterson

NASA Earth Resources Lab.
S. Wu

Jet Propulsion Laboratory
J. Paris

USDA/Agricultural Research Service
G. Boatwright
H. Gausman
J. Hatfield
R. Jackson
C. Wiegand
J. Musick

USDA Soil Conservation Service
R. Gilbert

Environmental Research Inst. Mich.
G. Suits

ASTER Consulting
N. Goel

Univ. California - Santa Barbara
D. Botkin
K. Woods

Kansas State University
E. Kanemasu
G. Asrar

Pan American University
J. Chance
E. LeMaster

Oregon State University
B. Schrumpf
M. Hall

University of Kansas
F. Ulaby

Texas A & M University
J. Heilman

South Dakota State University
C. Harland

University of Nebraska
B. Blad
J. Norman

CIMMYT
P. Hobbs

Canada Centre for Remote Sensing
P. Teillet

Purdue University
M. Baumgardner
T. Phillips
M. Phillips
B. Baumgardt
D. Landgrebe